

University of Windsor

Scholarship at UWindor

Electronic Theses and Dissertations

Theses, Dissertations, and Major Papers

2005

Investigation of total gaseous mercury in the atmosphere of the Great Lakes and St. Lawrence River basin.

Hongyu You
University of Windsor

Follow this and additional works at: <https://scholar.uwindsor.ca/etd>

Recommended Citation

You, Hongyu, "Investigation of total gaseous mercury in the atmosphere of the Great Lakes and St. Lawrence River basin." (2005). *Electronic Theses and Dissertations*. 2512.
<https://scholar.uwindsor.ca/etd/2512>

This online database contains the full-text of PhD dissertations and Masters' theses of University of Windsor students from 1954 forward. These documents are made available for personal study and research purposes only, in accordance with the Canadian Copyright Act and the Creative Commons license—CC BY-NC-ND (Attribution, Non-Commercial, No Derivative Works). Under this license, works must always be attributed to the copyright holder (original author), cannot be used for any commercial purposes, and may not be altered. Any other use would require the permission of the copyright holder. Students may inquire about withdrawing their dissertation and/or thesis from this database. For additional inquiries, please contact the repository administrator via email (scholarship@uwindsor.ca) or by telephone at 519-253-3000ext. 3208.

INVESTIGATION OF TOTAL GASEOUS MERCURY IN THE ATMOSPHERE OF
THE GREAT LAKES AND ST. LAWRENCE RIVER BASIN

BY

HONGYU YOU

A Thesis

Submitted to the Faculty of Graduate Studies and Research
Through the Department of Civil and Environmental Engineering
in Partial Fulfillment of the Requirements for
the Degree of Master of Applied Science at the
University of Windsor

Windsor, Ontario, Canada

2005



Library and
Archives Canada

Bibliothèque et
Archives Canada

Published Heritage
Branch

Direction du
Patrimoine de l'édition

395 Wellington Street
Ottawa ON K1A 0N4
Canada

395, rue Wellington
Ottawa ON K1A 0N4
Canada

Your file *Votre référence*
ISBN: 0-494-04970-7
Our file *Notre référence*
ISBN: 0-494-04970-7

NOTICE:

The author has granted a non-exclusive license allowing Library and Archives Canada to reproduce, publish, archive, preserve, conserve, communicate to the public by telecommunication or on the Internet, loan, distribute and sell theses worldwide, for commercial or non-commercial purposes, in microform, paper, electronic and/or any other formats.

The author retains copyright ownership and moral rights in this thesis. Neither the thesis nor substantial extracts from it may be printed or otherwise reproduced without the author's permission.

AVIS:

L'auteur a accordé une licence non exclusive permettant à la Bibliothèque et Archives Canada de reproduire, publier, archiver, sauvegarder, conserver, transmettre au public par télécommunication ou par l'Internet, prêter, distribuer et vendre des thèses partout dans le monde, à des fins commerciales ou autres, sur support microforme, papier, électronique et/ou autres formats.

L'auteur conserve la propriété du droit d'auteur et des droits moraux qui protègent cette thèse. Ni la thèse ni des extraits substantiels de celle-ci ne doivent être imprimés ou autrement reproduits sans son autorisation.

In compliance with the Canadian Privacy Act some supporting forms may have been removed from this thesis.

Conformément à la loi canadienne sur la protection de la vie privée, quelques formulaires secondaires ont été enlevés de cette thèse.

While these forms may be included in the document page count, their removal does not represent any loss of content from the thesis.

Bien que ces formulaires aient inclus dans la pagination, il n'y aura aucun contenu manquant.


Canada

1020908

Copyright © HONGYU YOU

All Rights Reserved, 2005

ABSTRACT

Mercury (Hg) is a highly toxic pollutant, and it can undergo long-range transport in the atmosphere. Hg is a pollutant of concern because of its tendency to accumulate and concentrate in biota. In this study, a statistical analysis of total gaseous mercury (TGM) was carried out using seven years of measurements at three Canadian Atmospheric Mercury Measurement Network (CAMNet) sites in the Great Lakes basin and three years measurements at two CAMNet sites in the St. Lawrence River basin. The average TGM concentrations ranged from 1.59 ± 0.24 to 1.84 ± 0.39 ng m⁻³ at the five sites. Two of the sites, Point Petre and St. Anicet, have significantly higher ($p < 0.05$) TGM concentrations in the Great Lake basin and St. Lawrence River basin, respectively. Large Hg evasion from Lake Ontario is a primary contributor for Point Petre, while nearby industrial and metropolitan areas may contribute more anthropogenic inputs to St. Anicet. Seasonal variability was detected at all five sites with a similar winter high pattern. Higher TGM concentrations were observed at Point Petre in summer, whereas lower TGM values were observed during summertime at the other four sites. In terms of diurnal pattern, minimum TGM concentrations occur before early morning and reach maximum near noon at most sites except for St. Anicet with night peak. The diurnal pattern in summer is more prominent than in other seasons.

TGM concentrations had a positive correlation with ambient temperature in all seasons at the three Ontario sites. Insignificantly weak correlation between TGM concentration and total Hg in precipitation was detected at Egbert and Point Petre, while a significantly negative correlation ($r = -0.32, p < 0.05$) was observed at Burnt Island. A digital filtering technique was used to analyze long-term trend of TGM concentrations at

the three Ontario sites. No clear trend of TGM concentration was observed at Egbert and Point Petre. At Burnt Island, there was a slight decrease of TGM concentration from 1998 to 2001, and then an 11% increase occurred in 2002, followed by a decrease in 2003.

A hybrid single-particle Lagrangian integrated trajectory (HYSPLIT) model and a box model were used to simulate a high TGM concentration episode at Point Petre. The result suggested that Hg emission from Lake Ontario has significant effects on high TGM concentration at Point Petre.

DEDICATION

To my wife Jingfang and my son Boyang

ACKNOWLEDGEMENTS

I would like to thank many people who made this project possible. In particular, I am deeply grateful to my advisor, Dr. XiaoHong Xu, for her encouragement, trust, and support. I would also like to sincerely acknowledge my other advisor, Dr. Ram Balachandar who provided valuable discussions and suggestions. Helpful suggestions and comments by committee members, Drs. Rajesh Seth and Karen Fung, have been well appreciated.

I would like to thank Drs. Hayley Hung and Pierrette Blanchard (Environment Canada) for sharing their knowledge and sparing their valuable time to discuss. Thanks should also go to research scientists in Environment Canada: Dr. Cathy Banic, Mr. Frank Froude, Dr. Laurier Poissant and Ms. Celine Audette for providing the CAMNet data.

I would also like to thank my colleagues: Abir Basu, Ripon Banik, Lillian Zhang, and Cosmas Taabazuing for their support and insightful comments. Finally, I would like to acknowledge the support from my lovely wife, Jingfang Song, my son, Boyang You, and other family members. This project is funded by the Natural Sciences and Engineering Research Council of Canada.

TABLE OF CONTENTS

ABSTRACT.....	iv
DEDICATION.....	vi
ACKNOWLEDGEMENTS.....	vii
LIST OF FIGURES	xi
LIST OF TABLES.....	xv
CHAPTER 1 INTRODUCTION	1
1.1 Background	1
1.2 Purpose of This Study	2
CHAPTER 2 LITERATURE REVIEW.....	3
2.1 Atmospheric Mercury	3
2.1.1 Physical/Chemical Properties, Toxicity, and Source of Atmospheric Mercury.....	3
2.1.2 Atmospheric Transport and Transformation of Mercury	7
2.1.3 Deposition and Re-emission of Mercury	9
2.2 Air Quality Monitoring Networks.....	11
2.3 Atmospheric Mercury Monitoring Networks.....	15
2.4 Canadian Atmospheric Mercury Measurement Network (CAMNet).....	21
2.5 Statistical Analysis of Air Quality Data.....	26
2.5.1 Descriptive Statistics	26
2.5.2 Normality Test and Selection of Parametric and Non-parametric Methods	27
2.5.3 Methods of Comparison	28
2.5.4 Correlation Analysis	30
2.5.5 Trend Analysis.....	32

2.6 Investigation of Source-Receptor Relationship	35
2.6.1 Backward Trajectory Model	35
2.6.2 Box Model	37
CHAPTER 3 METHODOLOGY	39
3.1 Data Collection.....	39
3.1.1 Monitoring Sites	39
3.1.2 TGM, Hg Wet Deposition, and Meteorological Data.....	40
3.2 Software	42
3.3 Data Compilation	42
3.4 Statistical Analysis.....	43
3.4.1 Descriptive Statistics	43
3.4.2 Normality Test and Selection of Parametric and Non-parametric Methods	46
3.4.3 Comparisons of Means	47
3.4.4 Correlation Analysis.....	47
3.4.5 Trend Analysis.....	48
3.5 Identification of High TGM Concentration Episode(s)	49
3.6 Investigation of Source-Receptor Relationship	50
CHAPTER 4 RESULTS AND DISCUSSION.....	53
4.1 Descriptive Statistics.....	53
4.1.1 Ontario Sites	53
4.1.2 Quebec Sites	59
4.1.3 Spatial Comparison of the Five CAMNet Sites.....	62
4.2 Seasonal Variability of TGM Concentrations.....	63
4.2.1 Winter High/Summer Low Pattern.....	64
4.2.2 Winter High/Summer High Pattern	66

4.3 Diurnal Variability of TGM Concentration	69
4.3.1 Ontario Sites	69
4.3.2 Quebec Sites	74
4.4 Correlation Analysis.....	78
4.4.1 TGM vs. Meteorological Parameters.....	78
4.4.2 TGM vs. Hg Wet Deposition.....	82
4.5 Trend Analysis	82
4.5.1 Six-year Trend of TGM for Burnt Island	83
4.5.2 Seven-year Trends of TGM for Egbert and Point Petre	90
4.6 Investigation of Source-Receptor Relationship	92
4.6.1 High TGM Concentration Episodes	92
4.6.2 HYSPLIT Trajectory and Box Model Application	93
CHAPTER 5 CONCLUSIONS AND RECOMMENDATION	98
5.1 Conclusions	98
5.2 Recommendations	100
APPENDIX A DERIVATION OF BOX MODEL EQUATION 3.1	102
REFERENCE.....	103
VITA AUCTORIS	111

LIST OF FIGURES

Figure 2.1 Overview of atmospheric cycling of mercury (Source: Carpi, 1997)	7
Figure 2.2 Sites map of mercury deposition network (Source: MDN, 2003).....	18
Figure 2.3 Total mercury deposition of 1999 in MDN. The arrows indicate decreasing trends from west to east and from south to north (Source: McDonald, 2003).....	20
Figure 2.4 Seasonal Hg concentrations and deposition in MDN sites of Pennsylvania in 2001 (Source: Lynch et al., 2003).....	20
Figure 2.5 Sites map of CAMNet	22
Figure 2.6 Diurnal cycle of TGM concentrations at CAMNet sites based on annual average concentrations for each hour (Source: Kellerhals et al., 2003)	25
Figure 2.7 Four-year trend of TGM observed at Point Petre site, Ontario (Source: Blanchard et al., 2002)	34
Figure 2.8 TGM concentrations at Lake Ontario buoy, Egbert and Point Petre during the October 2000 episode (Source: Blanchard et al., 2002)	37
Figure 2.9 The illustration of box model	38
Figure 3.1 Flowchart of statistical analysis in this study	45
Figure 3.2 An example of a series of 14 boxes along the trajectory. Five-pointed star indicates the end point	52
Figure 4.1 Histogram of TGM concentrations at (a) Burnt Island; (b) Egbert; (c) Point Petre. TGM concentrations greater than 10 ng m^{-3} (N=13, max.= 25.82 ng m^{-3}) at Egbert have been excluded.	55

Figure 4.2 Wind rose and TGM-rose for the three Ontario CAMNet sites. (a)-(c), wind rose, radius axis indicates frequency; (d)-(f) TGM-rose, radius axis indicates average TGM concentration in the direction.....	58
Figure 4.3 Histogram of TGM concentration at (a) St. Anicet; (b) Mingan. TGM concentrations greater than 10 ng m ⁻³ in St. Anicet (N=15, max.=53.08 ng m ⁻³) have been excluded.....	61
Figure 4.4 Box-whisker plot of TGM concentration at the five CAMNet sites during 1998 to 1999 when TGM data are available in all five sites..	62
Figure 4.5 Monthly mean of TGM concentrations observed at the three Ontario sites from May, 1998 to December, 2003. (a) Burnt Island, (b) Egbert, and (c) Point Petre. The solid circle indicates the monthly mean and the vertical bars indicate 95% confidence interval (CI) of mean.	65
Figure 4.6 Monthly mean of TGM concentrations observed at the two Quebec sites from January, 1997 to December, 1999. (a) Mingan and (b) St. Anicet. The solid circle indicates the monthly mean and the vertical bars indicate 95% CI of mean.	66
Figure 4.7 Seasonally divided wind rose and TGM-rose at Point Petre during 1998 to 2003. (a)-(d) wind rose, (e)-(h) TGM-rose. The shadow indicates onshore wind direction.	68
Figure 4.8 Diurnal variability of hourly TGM concentration at Burnt Island. (a) Overall; (b) Spring; (c) Summer; (d) Fall; (e) Winter. Solid circle indicate the mean and the vertical bars indicate 95% CI of mean.	71

Figure 4.9 Diurnal variability of hourly TGM concentration at Egbert. (a) Overall; (b) Spring; (c) Summer; (d) Fall; (e) Winter. Solid circle indicate the mean and the vertical bars indicate 95% CI of mean.....	72
Figure 4.10 Diurnal variability of hourly TGM concentration at Point Petre. (a) Overall; (b) Spring; (c) Summer; (d) Fall; (e) Winter. Solid circles indicate the mean and the vertical bars indicate 95% CI of mean.....	73
Figure 4.11 Diurnal variability of hourly TGM concentration at Mingan. (a) Overall; (b) Spring; (c) Summer; (d) Fall; (e) Winter. Solid circles indicate the mean and the vertical bars indicate 95% CI of mean.....	76
Figure 4.12 Diurnal variability of hourly TGM concentration at St. Anicet. (a) Overall; (b) Spring; (c) Summer; (d) Fall; (e) Winter. Solid circles indicate the mean and the vertical bars indicate 95% CI of mean.....	77
Figure 4.13 Time series of TGM concentration, solar radiation and wind speed (August 1~2) at Egbert (a) August 1~2, 2002 (b) June 19~20, 2002. <i>r</i> is the correlation coefficient between TGM and solar radiation, cut-off of 50 W m ⁻² for solar radiation.....	81
Figure 4.14 Trends and seasonal cycles of TGM concentrations for Burnt Island from May 1998 to December 2003.....	83
Figure 4.15 Monthly TGM concentrations at Burnt Island.....	85
Figure 4.16 Monthly precipitation (a) and temperature (b) at Burnt Island between 2001 and 2003.....	86
Figure 4.17 Wind rose and TGM rose at Burnt Island in 2001 to 2003. (a)-(c) Wind rose in 2001, 2002, and 2003. (d)-(f) TGM-rose in 2001, 2002, and 2003.....	88

Figure 4.18 Wind rose and TGM rose at Burnt Island during April-September period of 2001 to 2003. (a)-(c) Wind rose, (d)-(f) TGM rose.	89
Figure 4.19 Wind rose and TGM rose at Burnt Island during October-December period in 2001 to 2003. (a)-(c) wind rose, (d)-(f) TGM rose.	89
Figure 4.20 Trends and seasonal cycles of TGM concentrations for Egbert from January 1997 to December 2003	91
Figure 4.21 Trends and seasonal cycles of TGM concentrations for Point Petre from January 1997 to December 2003.....	91
Figure 4.22 Twenty-four-hour backward trajectories at Point Petre calculated by HYSPLIT model. (a) 8:00 am, August 7, 1999; (b) 4:00 pm, August 7, 1999.....	95
Figure 4.23 Modeled and measured TGM concentrations, along with trajectory travel time over Lake Ontario at Point Petre during the high TGM concentration episode on August 7, 1999. Estimated fluxes adopted from literatures (Table 3.3)	95

LIST OF TABLES

Table 2.1 Physical and chemical properties of selected Hg compounds.....	4
Table 2.2 Mercury emission flux measurements over soil, water, and vegetation surface, negative value indicates deposition flux.	11
Table 2.3 Some air quality networks in the USA and Canada (Source: NSTC, 1999)	14
Table 2.4 Location and site classification for the 11 CAMNet sites (Source: Kellerhals et al., 2003)	23
Table 2.5 Standard equations of descriptive statistics	27
Table 3.1 Information of the five CAMNet monitoring stations used in this study	40
Table 3.2 The parametric and non-parametric methods used in this study	46
Table 3.3 Estimated Hg emission rates used in this study	52
Table 4.1 Statistical summary of TGM concentrations (ng m^{-3}) during May 1998 to December 2003 when TGM data are available at the three Ontario sites	54
Table 4.2 Results of Anderson-Darling Normality test of TGM at the three Ontario sites (all p values < 0.05)	56
Table 4.3 Statistical summary of TGM concentrations (ng m^{-3}) during January 1997 to December 1999 when TGM data are available in the two Quebec sites	60
Table 4.4 Results of correlation between TGM concentrations and meteorological parameters at the three Ontario sites. Solar radiation less than 50 W m^{-2} have been excluded.	80
Table 4.5 Results of correlation between TGM concentrations and total Hg in precipitation and wet deposition rate of Hg at the three Ontario sites in 2002.....	82
Table 4.6 High TGM concentration episodes identified by statistical methods.	93
Table 4.7 The number of high TGM concentration episodes identified by the digital filter (Curvefit).....	93

CHAPTER 1

INTRODUCTION

1.1 Background

Mercury (Hg) is a highly toxic chemical that occurs naturally in the environment. Hg is released into the atmosphere by natural source such as volcanic eruption and anthropogenic sources such as coal combustion and waste incineration. Atmospheric mercury is removed by both wet and dry deposition. Uniquely, Hg will re-emit from the surfaces such as water, soil, and vegetation to the atmosphere and go through the emission-deposition cycle continuously.

Concerns about Hg pollution have been taken seriously by many communities. In order to reduce the anthropogenic Hg release, Canada has issued the Canada-wide Standard for different sectors including coal-fired electric power generation, waste incinerators and base metal smelters, mercury-containing lamps, and dental amalgam waste (CCME, 2003).

Hg concentrations in the ambient air are usually low and do not have direct adverse effect on human health. However, once Hg is deposited to water, it can be transformed to methyl-mercury (MeHg) by biological processes. Anthropogenic emissions of Hg to the atmosphere have been implicated for causing the increased MeHg concentration found in fish (USEPA, 1997).

MeHg is the most harmful Hg species. It is able to bio-accumulate into living organisms which form various parts of the food chain. For humans, the dominating

pathway for exposure to MeHg is fish consumption. Federal, provincial, and territorial governments in Canada have placed fish consumption advisories on various fish species in various lakes in order to prevent high levels of MeHg exposure to people (EC, 2003).

Measurements of total gaseous mercury (TGM) concentrations have been conducted by Canadian Atmospheric Mercury Network (CAMNet) since 1997. Monitoring TGM in the atmosphere is very important in providing a better understanding of mercury trends and processes in the environment, as well as information on the occurrence, pathways, behaviours, and fate of mercury emitted into the atmosphere from both natural and anthropogenic sources (EC, 2004).

1.2 Purpose of This Study

In this study, statistical analysis was carried out using seven-year TGM measurements at three CAMNet sites in the Great Lakes basin and three-year TGM measurements at two CAMNet sites in the St. Lawrence River basin. The overall objectives of this study are to improve our understanding of spatial and temporal variation of TGM in the Great Lakes and St. Lawrence River Basin, with an emphasis on source-receptor relationship of atmospheric mercury. The following are specific aspects:

(1) To identify seasonal and diurnal variability of TGM concentrations at all five sites, as well as long-term trend of TGM at the three Ontario sites.

(2) To analyze the correlation between TGM and Hg wet deposition, as well as the correlation between TGM and meteorological parameters including temperature, solar radiation, atmospheric pressure, wind speed, and wind direction at the three Ontario sites.

(3) To identify high TGM concentration episodes and investigate source-receptor relationship using both backward trajectory model and box model.

CHAPTER 2

LITERATURE REVIEW

2.1 Atmospheric Mercury

2.1.1 Physical/Chemical Properties, Toxicity, and Source of Atmospheric Mercury

Mercury occurs naturally in the environment as part of the earth's crust. Mercury exists in several forms that can be classified into three categories: elemental mercury (Hg^0), inorganic mercury, and organic mercury. Table 2.1 lists physical and chemical properties of elemental mercury and selected organic/inorganic mercury species.

Elemental mercury is a pure form of mercury and a silver-white metal in liquid phase at standard temperature and pressure. At room temperature, the vapor pressure of Hg^0 is relatively high and mercury vapor is odorless and colorless. Mercury is relatively inert and is able to rapidly combine with noble metals such as Au, Ag, Pt, and Pd to form amalgams (Schroeder and Munthe, 1998). Once mercury combines with other elements such as chlorine, sulfur, or oxygen, inorganic mercury compounds (mercury salts) occur. When mercury combines with carbon, organic mercury compounds are formed. Potentially a large number of organic mercury compounds can occur. However, by far the organic mercury compound of most concern in the environment is MeHg due to its toxic and bio-accumulative properties

Table 2.1 Physical and chemical properties of selected Hg compounds

Property	Hg ⁰	HgCl ₂	HgO	HgS	CH ₃ HgCl	(CH ₃) ₂ Hg
Melting Point (°C)	-39	277	decompose @ 500°C	584 (sublimation)	167 (sublimation)	-
Boiling Point (°C) @ 1 atm	357	303	-	-	-	96
Water Solubility (g l ⁻¹)	49.6×10 ⁻⁶ @20°C	66 @20°C	5.3×10 ⁻² @25°C	~2×10 ⁻²⁴ @25°C	~5-6 @25°C	2.95 @24°C
Vapor Pressure (Pa)	0.18 @20°C	8.99×10 ⁻³ @20°C	9.2×10 ⁻¹² @25°C	n.d.	1.76 @25°C	8.3×10 ⁻³ @25°C
Henry's Law constant (Pa m ³ mol ⁻¹)	793@25°C 729@20°C 416@5°C	3.69×10 ⁻⁵ @20°C	3.76×10 ⁻¹¹ @20°C	n.d.	3.83×10 ⁻² @15°C and PH=5.2	646@25°C 341@0°C
Octanol-water partition coefficient (dimensionless)	4.2	0.5	-	n.d.	2.5	180

Source: Schroeder et al., (1991) and references cited therein.

Hg is capable of existing in three oxidation states: 0, +1, and +2. Elemental mercury (oxidation state 0) is the predominant (~97%) form of mercury in the atmosphere (Fitzgerald, 1986, 1989). Hg in the oxidation state of (+1) is unstable and is small in quantity, if it exists at all (Schroeder and Munthe, 1998). Divalent Hg (oxidation state +2, expressed as Hg²⁺) has high solubility and can be readily removed from the atmosphere by wet and dry deposition.

Mercury in the atmosphere consists of Hg⁰, Hg²⁺, and particulate mercury (Hg(p)). Hg(p) consists of Hg bounds or strongly adsorbed to atmospheric particulate matters (PM). Several different components are possible to form Hg(p). Hg⁰ and Hg²⁺ species may adsorb to the particle surface, and Hg²⁺ species may also chemically

integrate into the particle itself (Brosset, 1987). The sum of Hg^0 and Hg^{2+} is also called total gaseous mercury (TGM). Approximately 97 % of TGM is Hg^0 , and the other 3% is Hg^{2+} (Fitzgerald, 1986, 1989). The residence time of Hg^0 in the atmosphere is in the order of one year due to its inertness and low solubility (Slemr et al., 1985; Lindqvist and Rodhe, 1985). This residence time is quite long compare to other metals which are primarily associated with airborne PM. Therefore, Hg is capable of travelling long distance with air mass thus making Hg a regional/global pollutant.

Gaseous Hg^{2+} is also called reactive gaseous mercury (RGM) due to its high reactivity. RGM is water-soluble Hg species with sufficiently high vapor pressure to exist in the gaseous phase (Munthe et al., 2001). The residence time of Hg^{2+} and $\text{Hg}(\text{p})$ are short compare to Hg^0 due to the higher solubility and the higher velocity of dry deposition, only in the order of days (Schroeder and Munthe, 1998).

The concentration of mercury in the atmosphere (97% is Hg^0) is actually very low and not directly harmful to human beings. Yet Hg^0 in the atmosphere can be transported over a long distance, and then deposited into water bodies, vegetation, and soil by dry and wet deposition. Once deposited to a water body, Hg^0 can be transformed into MeHg, the most toxic form of Hg.

Human beings are most commonly exposed to mercury from consuming fish that have been contaminated by MeHg through the food chain. MeHg is the most harmful Hg species and can cause serious damage for nerve, reproductive, digestive, and sensory systems. MeHg concentrations in fish stock have been reported as dramatically increasing during the 1980s, particularly in freshwater fish of the Northern Hemispheres (Lindqvist et al. 1991; Watras and Huckabee 1994). In 1989, the State of Michigan issued a health

advisory that pregnant or nursing women and children less than 15 years old were advised not to consume several kinds of fish caught in all of Michigan's inland lakes (Michigan Department of Public Health, 1989).

Another pathway of human exposure to mercury is inhalation of mercury vapors. Mercury vapor also has adverse effects on human health. According to Gossel and Bricker (1990), 25~50 $\mu\text{g m}^{-3}$ of mercury vapor in air and 40 $\mu\text{g L}^{-1}$ of MeHg in blood are associated with an increased risk of damage to the central nervous system. Major potential source of human exposure to mercury vapors is the dental amalgam in fillings. Studies showed that population with dental restorations had significantly higher mercury level in exhale breath as well as in urine than that in the population without dental amalgam (Jokstad et al., 1992; Patterson et al., 1985). In addition, dentists and dental staff, house painters, and individuals involved in disposal or recycling of mercury-contaminated wastes are also at risk of occupational exposure to mercury (U.S. DHHS, 1999).

Mercury is released to the atmosphere by a variety of natural and anthropogenic sources. Natural sources include volcanic eruptions, forest fires, normal breakdown of minerals, and Hg evasions from the surfaces such as soil, water, and vegetation. For example, recent studies conducted by National Center for Atmospheric Research, USA, showed that all samples of coniferous and deciduous collected from seven forests across the continental United States contained mercury at 14~71 ng g^{-1} of dry weight that has been absorbed from either soil or the atmosphere. When the samples were burnt, about 95% of the mercury contained in the samples was released to the atmosphere and 5%

remained in the ash (Friedli and Radke, 2001). In addition, the intense heat created during forest fire enhances Hg in the forest soil emitting to the atmosphere.

About 50% to 75% of total Hg releases are associated with human activities (Fitzgerald, 1995). The two primary anthropogenic sources of mercury emission are fossil fuel (particularly coal) combustion and solid waste incineration. Other anthropogenic sources include the chlorine-alkali industry, metal smelting, refining and manufacturing. In addition, mercury is commonly used in thermometers, barometers, dental fillings, batteries, switches and fluorescent lamps. Portion of mercury contained in these items will be released when they are disposed or broken during use (USEPA, 1997).

2.1.2 Atmospheric Transport and Transformation of Mercury

Once released into the atmosphere, mercury will experience a number of physical and chemical processes such as transport, transformation, and removal. The conceptual structure of atmospheric cycling of mercury is shown in Figure 2.1.

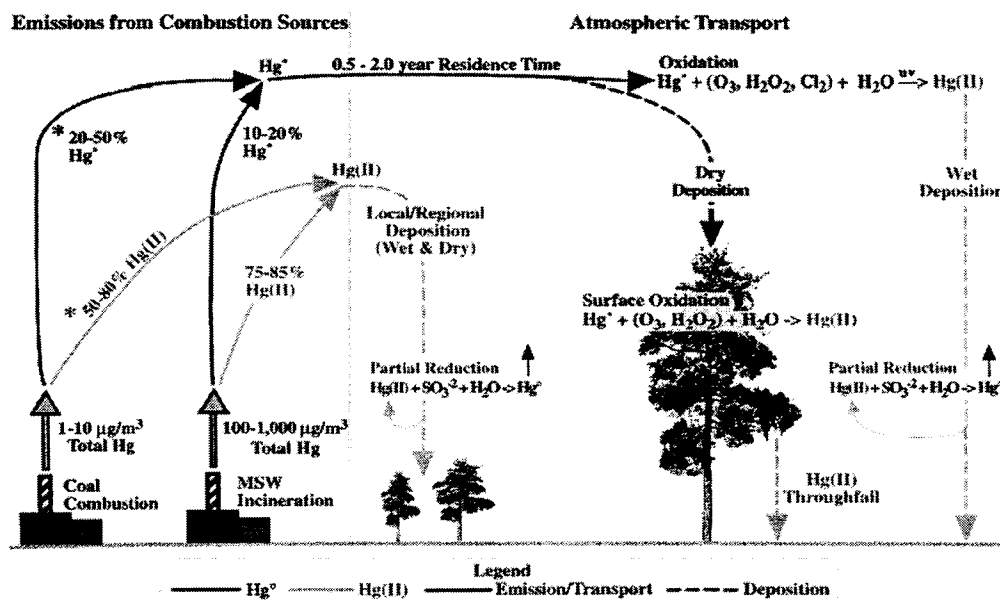
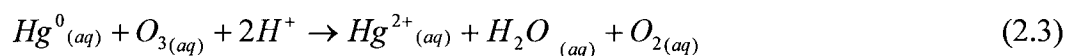


Figure 2.1 Overview of atmospheric cycling of mercury (Source: Carpi, 1997)

During the 1980s, it was recognized that Hg could be transported long distances in the atmosphere, and then might be deposited within 1000 to 2000 km from source areas. In other words, relatively remote areas with no local sources of Hg pollution could have been contaminated (Lindqvist, 1994). The regional transport of Hg has been investigated in several studies, such as in Europe by Iverfeldt (1991) and in U.S. by Glass et al. (1991). The results of their studies showed that high TGM values were associated with the air masses which had passed polluted areas within the last three days or so, as opposed to background values observed in other wind directions. There are several indications that the mercury load in the atmosphere is increasing globally. Slemr and Langer (1992) compared atmospheric Hg concentrations measured over the Atlantic Ocean during late 1970, 1980, and 1990. Their results indicated a yearly increase of 1% in the Southern Hemisphere, and slightly more in the Northern Hemisphere. This suggested that anthropogenic sources constitute a greater proportion to atmospheric mercury in the Northern Hemisphere than in the Southern Hemisphere.

Several investigations of atmospheric reactions of mercury in both gaseous-phase and aqueous-phase have been carried out in laboratory and field. The oxidation pathways of mercury are important for understanding the atmospheric cycling of mercury. The major oxidation processes are Hg^0 with ozone (O_3) (Munthe, 1992; Hall, 1995):



In a field study at Egbert, Ontario, Schroeder and Markes (1994) have observed the existence of a negative correlation between daily TGM concentrations and O_3

concentrations in ambient air, it suggested that O₃ and TGM might have chemical reactions in the atmosphere. In contrast, Poissant (1997) reported that no straightforward correlation between TGM and O₃ concentrations was observed in a study in South Quebec. His study also suggested that the oxidation reaction of Hg⁰ with O₃ in air was slow and the overall reactions of oxidation by ozone were complex.

2.1.3 Deposition and Re-emission of Mercury

Mercury is removed from the atmosphere by both wet and dry deposition of Hg⁰, Hg²⁺ and Hg(p). Hg²⁺ and Hg(p) are deposited more rapidly. Hg⁰ is largely insoluble, and has relatively low deposition velocity compare to Hg²⁺ and Hg(p). Most Hg⁰ is deposited indirectly after transformation to Hg²⁺ through oxidation reaction in rainwater or cloud droplet. Hg⁰ is also deposited after it being adsorbed onto particles to form Hg(p) (Lindqvist, 1994).

Generally, wet and dry deposition of Hg²⁺ and Hg(p) are considered to be uni-directional processes, which transfer Hg from the atmosphere to the earth's surfaces including soil, water, and vegetation (Schroeder and Munthe, 1998). However, air-surface exchange of Hg⁰ is able to occur bi-directionally, i.e. Hg⁰ also can re-emit from the surfaces to the atmosphere.

Hg air-water exchange is governed by Henry's Law. Several studies have found that concentrations of dissolved gaseous mercury (DGM) in ocean or inland water are supersaturated relative to the equilibrium values predicted by Henry's Law. Therefore Hg⁰ emission indeed occurs over water bodies. For instance, Poissant et al. (2000) reported that the degree of saturation of DGM in Lake Ontario and the St. Lawrence River ranged from 476% to 2163%. Water and ambient temperature affect Hg air-water

exchange. Poissant and Casimir (1998) reported that Hg flux over water body had a positive correlation with both water and ambient temperature. Solar radiation also plays an important role in Hg air-water exchange. Gardfeldt et al. (2001) concluded that solar radiation enhanced the formation of DGM in water bodies, especially in summer. Consequently, high DGM super-saturation led to high Hg emission from water bodies during summertime. In addition, a study by Boudala et al. (2000) indicated that air-water Hg emission flux positively correlated with wind speed suggesting enhanced Hg emission flux due to increased vertical mixing of Hg within the water column, which is driven by higher wind speed.

The air-soil Hg exchange can be considered as a surface physicochemical process consisting of adsorption/desorption of Hg^0 and Hg^{2+} to/from the soil surfaces (Zhang et al., 2001; Johnson et al., 2003). Several factors affect the air-soil Hg exchange. They are soil Hg content, soil water content, soil and air temperature, solar radiation, wind speed, and ambient TGM concentration. Studies indicated that air-soil exchange of Hg has strongly positive correlation with solar radiation and soil temperature in summer (Poissant and Casimir, 1998; Zhang et al., 2001).

The air-vegetation Hg exchange is important to the Hg cycling in the terrestrial ecosystem. Hg^0 , Hg^{2+} , and $\text{Hg}(\text{p})$ can be deposited on foliages of vegetation by wet and dry deposition. Hg can also be removed from foliages by both litterfall and throughfall. Several factors affect Hg air vegetation exchange and they are vegetation type, Hg concentration in vegetation and in ambient air, water content in soil, wetness of foliage surface, solar radiation, wind speed, and air temperature (Xu et al., 1999). Air-vegetation Hg exchange also exhibits seasonal variations. A study by Lindberg et al (2002) reported

that summer daily Hg flux over cattail was two times of that in winter. It suggested that lower temperature in winter diminished the supply of Hg⁰ in the rooting zone through decreased DGM production in soil. Table 2.2 lists some studies of measured Hg emission fluxes over water, soil, and vegetation.

Table 2.2 Mercury emission flux measurements over soil, water, and vegetation surface, negative value indicates deposition flux.

Location	Exchange type	Hg Flux (ng m ⁻² h ⁻¹)	Measurement period	Reference
Ontario and Quebec, Canada	Air-water	2.88 (median)	July, 1998	Poissant et al., 2000
Sweden	Air-water	11.1 ± 12.0	August, 1999	Gardfeldt et al., 2001
Quebec, Canada	Air-soil	2.95±2.15	Summer, 1995	Poissant and Casimir, 1998
Tennessee, US	Air-soil (forest soil)	7.5±7.0	May-Nov, 1993	Kim et al., 1995
Tennessee, US	Air-vegetation	-4.7 ~ 49	1996 - 1998	Lindberg et al., 2002

2.2 Air Quality Monitoring Networks

Air pollution has become a significant concern all over the world in past decades. The adverse effects of air pollution on human health and the ecosystems have been well known. Air quality measurements are an important data source for researches and management of air pollution control. In order to monitor air quality in different scales, governments, non-profit organizations and private sectors have established air quality-monitoring networks to continuously measure air pollution in the atmosphere. The ultimate purpose of air quality monitoring is not only to collect data, but also to provide information to scientists and policymakers on the nature of pollutants. It also provides insights into the transport and removal processes of pollutants as well as source-receptor

relationship. Moreover, based on the air quality data collected at the monitoring stations, air pollution levels at places where measurements are not available can be inferred.

Long-term variation in air quality and atmospheric deposition may be masked by the different time-scale (day-to-day, season-to-season, and year-to-year) variations of meteorological factors such as wind, temperature, and precipitation. These variations will affect dispersion, transport, and deposition of pollutants (NSTC, 1999). Therefore, it is necessary to monitor both air quality and meteorological data continuously using consistent procedures as well as quality-controlled practices.

Air quality monitoring networks have been established in many areas of the world on various purposes and scales. In the United State, federal government, state governments and private organizations have set up several air quality-monitoring networks. Some air quality networks measure major air pollutants such as SO₂, NO_x, PM, and O₃, as well as meteorological condition. Some networks are established to monitor a particular pollutant such as mercury in CAMNet. Table 2.3 lists some air quality monitoring networks in US and Canada, as well as chemical constituents and atmospheric deposition they monitor.

The key in the design stage of air quality-monitoring networks is site selection. It mainly depends on the objectives of air quality networks. Some monitoring sites may be located near known point sources of pollutants (such as coal-fire power plant) to monitor local impacts (Nychka et al., 1998). Some sites may be remotely placed to measure the background concentration of pollutants, e.g. CAMNet sites (EC, 2003).

Quality assurance and control (QA/QC) is an essential part of any air quality networks. It is a program of activities to ensure that measurements meet defined and

appropriate standards of quality, with a stated level of confidence. The overall objectives of QA/QC in air quality monitoring networks include providing accurate and consistent measurements, comparable and traceable results, and optimizing resources (Nychka et al. 1998). During network operation, an audit of field operations should be carried out within certain time interval by senior administration or a third party. For example, USEPA has the Office of Air Quality Planning and Standards Quality Assurance Team (OAQPS/QA) that is established to ensure the quality of measured data meet or exceed the requirement for informed environmental decision-making (USEPA, 1997).

Data validation is an important process in the operation of air quality networks. Data with significant variation from expected measurement results should be identified. Causes for unexpected data trends may be due to instruments malfunctioning, for example, measurements during the instrument power failure, or due to the occurrence of special environmental events. Filtering the unexpected data caused by instrument malfunctioning can ensure the consistency of data, while analyzing the unexpected data caused by environment events could particularly identify certain characteristics of atmospheric processes (Fuentes, 1995).

Table 2.3 Some air quality networks in the USA and Canada (Source: NSTC, 1999)

Air quality Networks	Abbreviation	Chemical constituents measured	Atmospheric deposition and other measurements
Interagency Monitoring of Protected Visual Environments	IMPROVE	PM	Visibility
State and local air monitoring stations and National Air Monitoring Stations	SLAMS/NAMS	Nitrogen species, Sulfur species, Pb, PM, CO, Ozone and Ozone precursors	
Mercury Deposition Network	MDN	Hg concentration in precipitation and precipitation amount	Wet deposition of mercury
Clean Air Status and Trends Network	CASTNet	Nitrogen species, Sulfur species, PM, Ozone and Ozone precursors	Visibility, dry & wet deposition
Atmospheric Integrated Research Monitoring Network	AIRMoN	Nitrogen species, Sulfur species in precipitation.	Dry and wet deposition
Gaseous Pollutant Monitoring Program	GPMP	Ambient Sulfur species, Ozone and Ozone precursors	
National Air Pollution Surveillance Network	NAPS	SO ₂ , O ₃ , CO, PM, VOC and total suspended particulates (TSP)	
Integrated Atmospheric Deposition Network	IADN	PCBs, PAHs, Pb, DDT, etc.	Dry and wet deposition
Canadian Atmospheric Mercury Network	CAMNet	Total gaseous mercury (TGM)	Wet deposition

2.3 Atmospheric Mercury Monitoring Networks

Atmospheric mercury is considered as a significant contributor of Hg pollution in the ecosystems. Anthropogenic mercury is released to air, water, and soil. According to U.S. DHHS (1999), approximately 80% of total anthropogenic mercury is released to the atmosphere. Thus, establishing the atmospheric mercury monitoring network is the first step in understanding and controlling the atmospheric mercury input to the aquatic and terrestrial ecosystems.

Several countries have established networks to monitor Hg in the atmosphere as well as in the aquatic and the terrestrial ecosystems in local and regional scales. According to the definition made by the Expert Panel on Atmospheric Process, local scale generally refers to 100 km radius of a source and regional scale generally refers to 100 - 2000 km radius of a source (MPPTF, 1996). Mercury Deposition Network (MDN) in National Atmospheric Deposition Program (NADP) in the United States and CAMNet in Canada are two primary nationwide atmospheric Hg monitoring networks in North America (MDN, 2003; CAMNet, 2003). More details about these two networks are to follow.

In Europe, although none of the air quality-monitoring networks covers the whole continent, some countries such as Sweden and German, have their national air quality monitoring and precipitation networks to monitor atmospheric mercury. Other European countries also measure atmospheric mercury at a few air quality monitoring sites. In 2001, a group of scientists proposed that European Union should establish mandatory monitoring networks for TGM in ambient air and mercury in precipitation (wet deposition) over their Member States (European Communities, 2001). Several studies have been completed in Europe based on the data obtained from these networks. For

example, Wangberg et al. (2001) observed concentrations of TGM, total particulate mercury (TPM), and RGM in the Mediterranean region were higher than in Northwest Europe during simultaneous measurements at ten sites in Northwest Europe and in the Mediterranean region in four seasons.

Schmolke et al. (1999) reported the spatial distribution and temporal variability of TGM using simultaneous measurements of TGM concentration at four sites in Central Europe. In their study, a prominent diurnal variation in summer was observed, which had a distinct maximum TGM concentration in early morning before sunrise, and decreasing of TGM values were observed afterward. The elevated TGM concentrations in morning hours were likely due to low wind speed and low air mixing height leading to the TGM concentrations building up near the surfaces. The decrease of TGM concentration after sunrise was likely due to strong atmospheric mixing processes diluting the TGM.

In Asia, China and Korea have established some local scale atmospheric mercury monitoring networks. Liu et al. (2002) measured TGM concentrations in both urban and suburban sites in Beijing, China. Different diurnal patterns of TGM concentrations were observed in winter and summer. The seasonal pattern at both urban and suburban sites was higher TGM concentrations in summer and lower in winter. Their observed seasonal pattern is opposed to the winter high/summer low pattern observed by studies in Europe and North America.

In Seoul, Korea, diurnal and seasonal patterns of atmospheric mercury were observed in urban areas by Kim and Kim (2001). They found that the maximum TGM concentration occurred at night and this pattern was more prominent in winter than that in other seasons. The seasonal pattern was that high TGM concentrations occurred in winter

and summer, compared to that in spring and fall. The results of correlation analysis showed that TGM concentrations exhibited strong positive correlations with other pollutants such as PM, SO₂, and NO. The authors concluded that if SO₂ was considered as an indicator of coal combustion, the winter-time TGM was most likely to come from the anthropogenic sources such as household heating systems from late fall to early spring.

In North America, MDN was established in 1996 following a year of field-testing in United States (Vermette et al., 1995). The objective was to develop a regional database on the weekly concentrations of total mercury in precipitation and the seasonal and annual flux of total mercury in wet deposition. The measurements are employed to develop information on spatial and temporal variations in mercury deposited toward surface waters, forested watersheds, and other sensitive receptors (NSTC, 1999).

MDN initially began with 26 sites, and it has currently grown to a network with over 50 sites in operation, as shown in Figure 2.2. Most monitoring sites of MDN are located in rural areas and at least 10 to 20 kilometers from major air pollution sources. Most sites are in open, grass-covered areas well away from overhanging vegetation and buildings (MDN, 2003). Weekly samples of mercury in precipitation are collected using a modified Aerochem Metric sampler. A motor-driven lid on the top of the sampler is automatically opened when precipitation events occur. The collected precipitation samples are sent to a laboratory and analyzed by the cold vapor atomic fluorescence spectroscopy (CVAFS) method (Hayward et al., 2003).

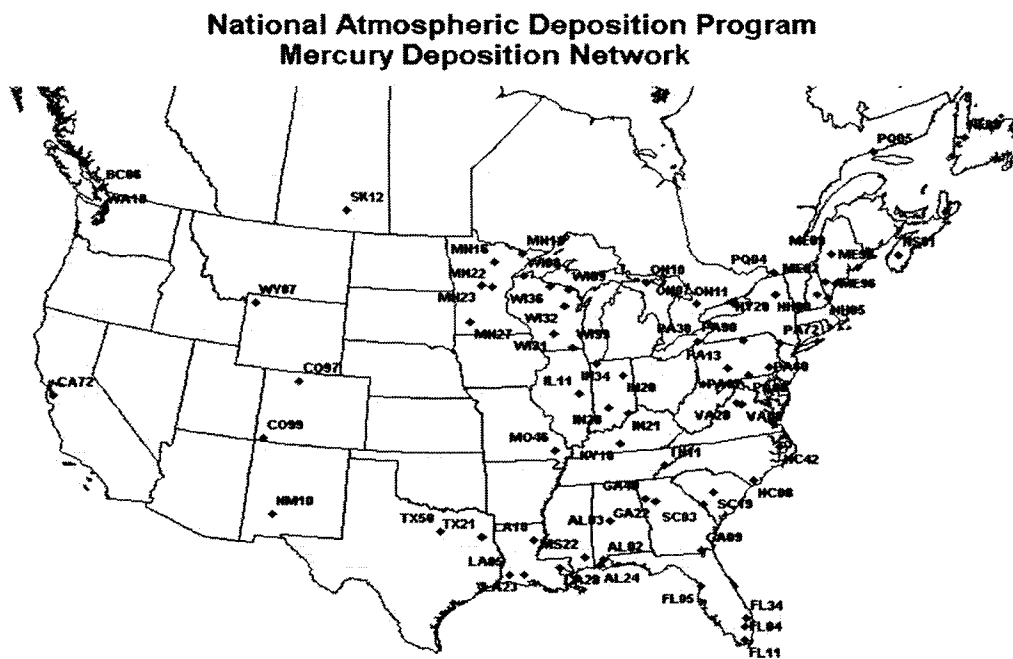


Figure 2.2 Sites map of mercury deposition network (Source: MDN, 2003)

In MDN, total Hg concentration in precipitation and Hg wet deposition not only showed seasonal variation, but also indicated decreasing trends from west inland area to east coast as well as from south to north as illustrated in Figure 2.3. Lynch et al. (2003) reported that total Hg concentrations in precipitation among the seven sites in Pennsylvania, US, ranged from 1.4 to 159 ng L⁻¹, and presented spatial and temporal variations. The average total Hg concentration in precipitation in summer (June-August) was higher than that in any other seasons, and the average concentration was about 1.5 times of that in winter (December-February). Mercury deposition rate was also higher in summer than that in any other seasons, nearly three times higher than that in winter (Figure 2.4). The seasonal pattern of total Hg in precipitation and annual Hg wet deposition observed in Pennsylvania was similar to the pattern observed in most MDN sites in the United States and Canada.

Chalmers et al. (2003) investigated total Hg concentration in wet deposition in New England area during 2002. Total Hg concentrations in wet deposition ranged from 2~20 ng L⁻¹. The median of Hg concentration varied from 7.2 to 8.8 ng L⁻¹ at the three urban sites around Boston, and median Hg concentration was observed 5.7 ng L⁻¹ at a rural area in New Hampshire. It indicated that localized urban emission sources might have significant effects on Hg concentration in precipitation in New England, and might result in variable deposition pattern on a sub-regional scale.

CAMNet is another mercury monitoring network in North America. In the following section, CAMNet will be discussed in detail.

Total Mercury Concentration, 1999

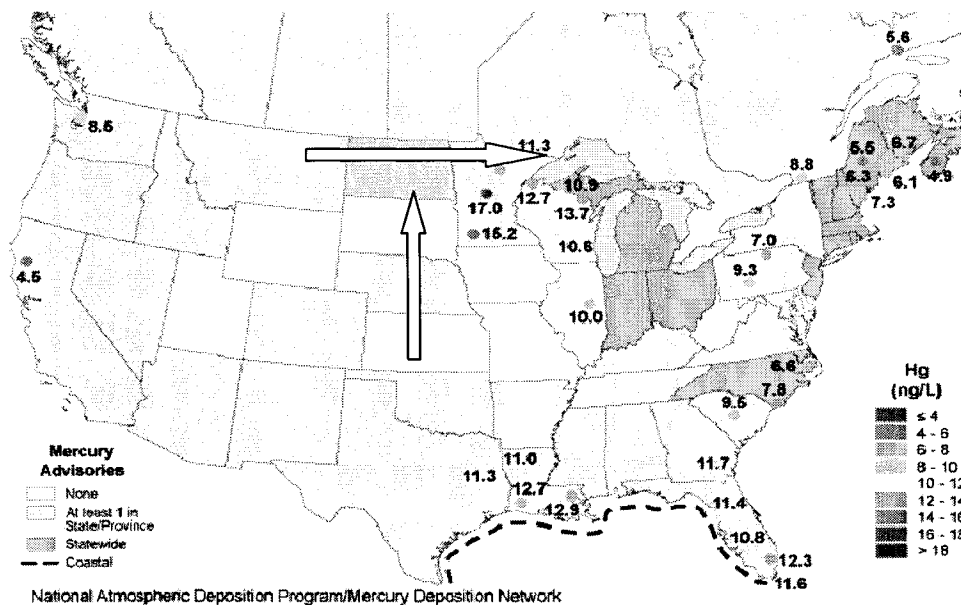


Figure 2.3 Total mercury deposition of 1999 in MDN. The arrows indicate decreasing trends from west to east and from south to north (Source: McDonald, 2003)

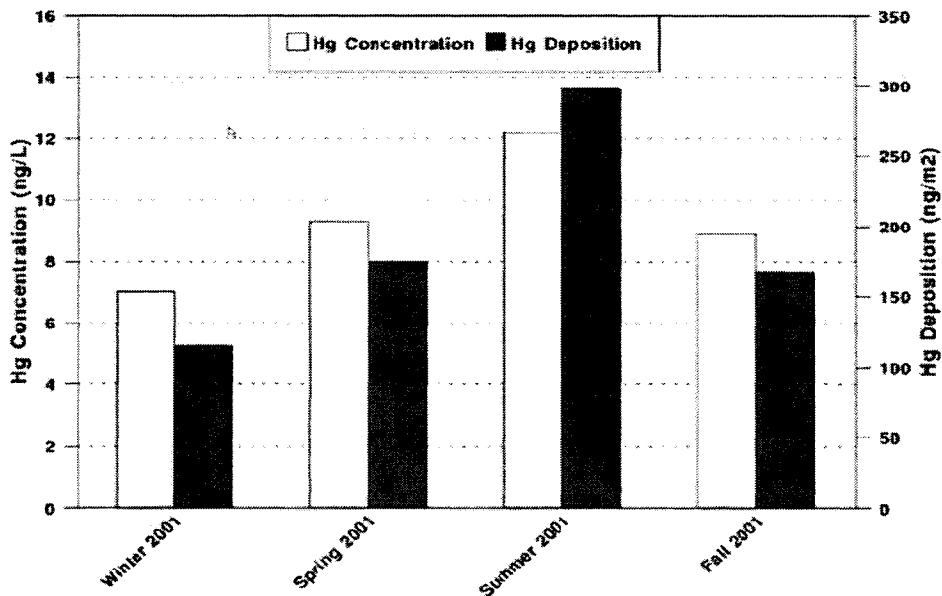


Figure 2.4 Seasonal Hg concentrations and deposition in MDN sites of Pennsylvania in 2001 (Source: Lynch et al., 2003)

2.4 Canadian Atmospheric Mercury Measurement Network (CAMNet)

In 1996, Environment Canada initiated the CAMNet to provide a better understanding of mercury trends and processes in the environment. The objectives of CAMNet are: 1) to provide a long term and accurate measurement of TGM concentrations across Canada; and 2) to assess temporal and spatial variability of atmospheric mercury, as well as sources and sinks of atmospheric mercury (EC, 2003).

There are currently 11 sites participating in this collaborative research effort with locations ranging from approximately 43° to 82° N latitude and 62° to 123° W longitude as shown in Figure 2.5. The sites are selected to represent major geographical and ecological regions of Canada. Among the 11 sites, there are seven sites (Figure 2.5) also measuring total mercury in precipitation.

According to the impact of nearby anthropogenic mercury emission, the sites are classified into two categories: rural-remote sites are considered as background sites and rural-affected sites are expected to be impacted by nearby anthropogenic Hg emissions. (Kellerhals et al., 2003). Table 2.4 lists the location and the classification of CAMNet sites. The four rural-affected sites basically are located near metropolis: St. Anicet is located 100 km southwest of Montreal; Point Petre and Egbert are located 160 km and 90 km away from Toronto, respectively; Reifel Island is located near the Great Vancouver area. The other seven CAMNet sites are rural-remote sites.

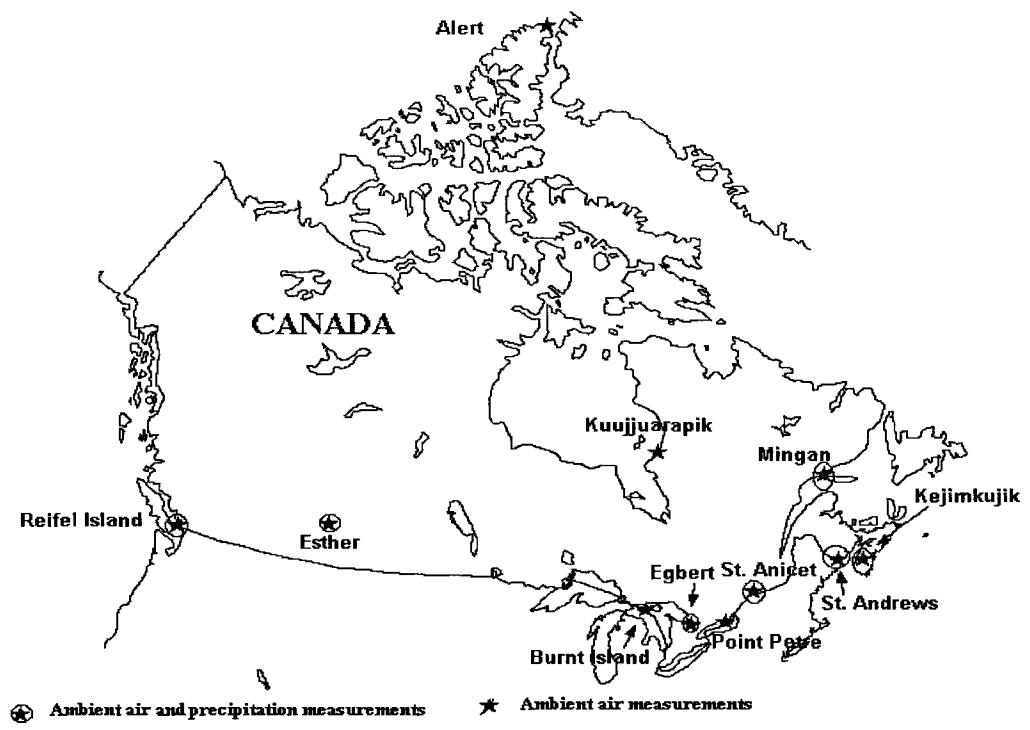


Figure 2.5 Sites map of CAMNet

Table 2.4 Location and site classification for the 11 CAMNet sites (Source: Kellerhals et al., 2003)

Site	Province	Latitude	Longitude	Classification
Alert	NU	82.50N	62.30W	Rural-Remote
Kejimkujik	NS	44.43N	65.21W	Rural-Remote
St. Andrews	NB	45.09N	67.00W	Rural-Remote
Mingan	QC	50.27N	64.23W	Rural-Remote
St. Anicet	QC	45.12N	74.28W	Rural-affected
Point Petre	ON	43.83N	77.15W	Rural-affected
Egbert	ON	44.22N	79.78W	Rural-affected
Burnt Island	ON	45.80N	82.95W	Rural-Remote
Esther	AB	51.67N	110.20W	Rural-Remote
Reifel Island	BC	49.10N	123.16W	Rural-affected
Kuujuarapik	QC	55.28N	77.75W	Rural-affected

In all CAMNet sites, the Tekran™ Model 2537A continuous ultra-trace mercury vapor analyzer (Tekran Inc., 2003) is used to measure the TGM concentration in the atmosphere. The analytical train of Model 2537A is based on the amalgamation of Hg onto a pure gold surface followed by a thermo-desorption and analyzed by CVAFS ($\lambda = 253.7$ nm). The dual cartridge design allows measuring and analyzing continuously. The analyzer is automatically calibrated on a daily basis and manually calibrated in a quarterly basis. The Research Data Management and Quality Control System (RDMQ™) (RDMQ, 2003), developed by Environment Canada, is used to quality control TGM measurements of CAMNet. Each TGM datum is assigned a validity flag based on programmed criteria. Hourly average TGM concentrations were then calculated for all hours with at least 25% data completeness (Kellerhals et al., 2003).

The seasonal variation of TGM in CAMNet has been investigated. Kellerhals et al. (2003) reported that the seasonal pattern was observed at eight of the nine mid-latitude sites of CAMNet over a two years period. The seasonal pattern presented higher TGM concentrations in winter/spring and lower TGM concentrations in summer/fall, similar to seasonal patterns observed in US and Europe (Ames et al., 1998; Slemr and Scheel, 1998). This seasonal pattern of TGM could be affected by factors including strong wet deposition during summertime and increasing coal combustion for heating purpose during wintertime. In contrast, Kim and Kim (2001) reported a different seasonal pattern that high TGM occurred not only during wintertime, but also during summertime. The elevated TGM concentration during summertime was likely due to enhanced Hg emission from the surfaces under high temperature.

The diurnal variation of TGM concentrations, shown in Figure 2.6, has been observed in all CAMNet sites during 1997 to 1999 (Kellerhals et al., 2003). The most common pattern was that maximum TGM concentration occurred near noon and minimum TGM concentration happened before sunrise. The diurnal pattern was seasonally modulated at all sites as well, reaching maximum amplitude between June and September at the mid-latitude sites. The nocturnal decreases of TGM concentration observed at most sites in summer might indicate a significant removal of mercury from the atmosphere (Kellerhals et al., 2003). Similar observation in the Great Lakes Basin was reported by Keeler et al (1994): the average of TGM concentrations in morning/noon samples during daytime (8:00 am to 2:00 pm) was 3.3 times of that in nighttime samples (8:00 pm to 8:00 am); the average of TGM concentrations in afternoon samples (2:00 pm to 8:00 pm) was 2.1 times of that in nighttime samples.

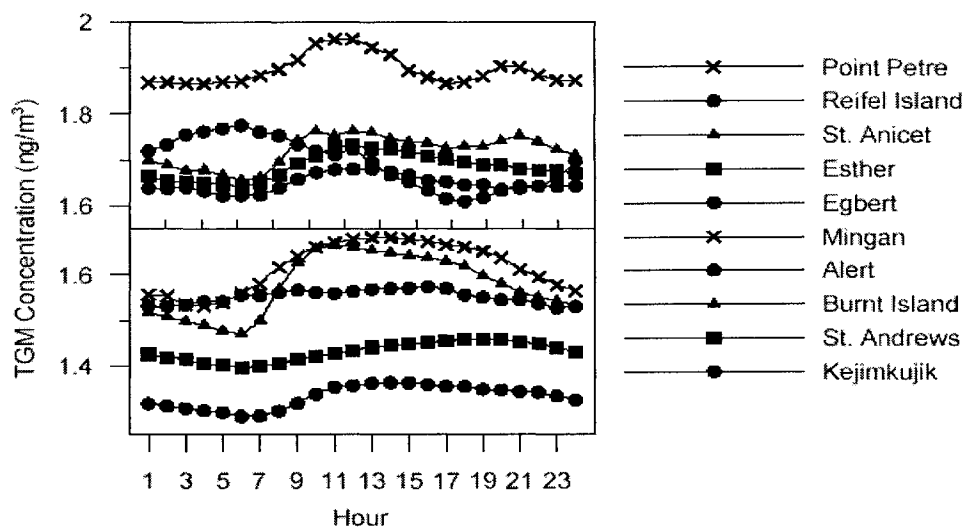


Figure 2.6 Diurnal cycle of TGM concentrations at CAMNet sites based on annual average concentrations for each hour (Source: Kellerhals et al., 2003)

At the Alert site in the Arctic, seasonal pattern of TGM is quite different from the observations in other sites. TGM concentrations reached peak values during summertime. It was speculated that this phenomenon might be due to temperature and/or sunlight-induced emission or re-emission of volatile mercury species from the Earth's surface (terrestrial and/or the aquatic ecosystems) during summertime (Schroeder et al., 1998). In spring, mercury depletion events in Arctic atmosphere were also observed. TGM concentrations dropped from 2 ng m^{-3} to 1 ng m^{-3} during three months of polar sunrise period. In recent studies, scientists discovered that gaseous elemental mercury (GEM) converted to reactive mercury species during mercury depletion events. Mercury concentrations in snow showed 20 times increases from dark to light period of the Arctic (Steffen et al., 2002). With polar sunrise, an increase in snow temperature then might stimulate the exchange of Hg from the snow pack to air throughout the day. At the Antarctic, scientists observed similar mercury depletion events after polar sunrise. Both groups discovered that mercury depletion events coincide with ozone depletion events in

the lower troposphere. The hypothesis is that bromine species are likely involved in TGM and ozone depletion events (Ebinghaus et al., 2002).

2.5 Statistical Analysis of Air Quality Data

Once air quality data have been obtained, statistical analysis is an essential method to gain better understanding of atmospheric behaviors of pollutants. Statistical analyses are often used to investigate temporal and spatial variation, long-term trend of pollutants, and correlations between pollutants and other factors such as meteorological parameters.

2.5.1 Descriptive Statistics

Descriptive statistics are often used to describe central tendency and dispersion patterns of a dataset. Together with simple graphics analysis, descriptive statistics form the basis of virtually every quantitative analysis of data. After obtaining a dataset, descriptive statistics usually will be employed to compute statistics including mean, median, standard deviation, 1st quartile (25% of the data are less than or equal to this value), 3rd quartile (75% of the data are less than or equal to this value), maximum, minimum, and skewness. Table 2.5 lists some standard equations of descriptive statistics.

The descriptive statistics can characterize the air quality data in many ways. For example, Slemr and Scheel (1998) showed the yearly variation of TGM concentration by using frequencies distribution plot. Kellerhals et al. (2003) concluded that the median of TGM concentration at rural-affected sites is significantly ($p < 0.005$) higher than that at rural-remote sites.

Table 2.5 Standard equations of descriptive statistics

Descriptive statistics	Standard equation
Mean	$\bar{x} = \frac{1}{n} \sum_{i=1}^n x_i$, n is number of measurements
Standard deviation	$s = \sqrt{\frac{\sum_{i=1}^n (x_i - \bar{x})^2}{n-1}}$
Standard error of mean	$SEM = \frac{s}{\sqrt{n}}$
95% confidence interval	$CI = \bar{x} \pm t_{(\alpha/2, n-1)} SEM$, t is student's t distribution (two tailed), $\alpha = 0.05$.
Upper limit of outlier	$Q_3 + 1.5(Q_3 - Q_1)$, Q_1 and Q_3 are 1 st and 3 rd quartile, respectively
Lower limit of outlier	$Q_1 - 1.5(Q_3 - Q_1)$, Q_1 and Q_3 are 1 st and 3 rd quartile, respectively

2.5.2 Normality Test and Selection of Parametric and Non-parametric Methods

Normality test is a common application for distribution fitting procedures when the assumptions of normality need to be verified before conducting some parametric tests. Anderson-Darling test is an often-used normality test (Comrey et al., 1989).

Parametric analysis methods are based on the assumption that the variable follows normal distribution, whereas non-parametric analysis methods are distribution-free methods. Therefore, the result of normality test is a major factor in selecting either parametric or non-parametric methods. In addition, the sample size is another factor of determination of which method to be used. Central limit theorem states that in spite of the distribution of population being skewed or irregular, the shape of the sampling

distribution of the sample mean approaches normal shape as the sample size increases (Comrey et al., 1989). Hence, if the sample size is large enough (e.g. $n > 100$), parametric methods are likely appropriate due to more statistical power (Montgomery, 1999).

2.5.3 Methods of Comparison

Two-sample *t-test* is commonly used as a parametric method to compare the difference of means between two independent groups. The non-parametric equivalent of 2-sample *t-test* is the Mann-Whitney U test.

Usually, the 95% confidence interval is selected in a two-sample *t-test*. The null hypothesis (H_0) is the difference of means between two groups equals to zero, while the alternative hypothesis (H_1) is the difference of means between two groups does not equal to zero (two-tailed) (Montgomery, 1999). Some comparisons may need to examine which group mean is greater or less than another, in that case, the alternative hypothesis (H_1) of test will be modified to the difference of means is greater or less than zero (one-tailed).

The Mann-Whitney U test is a non-parametric two-sample test. It tests two groups of samples only using ranks of data. The samples from both groups are combined and ranked, with the average rank assigned in the case of ties. The number of ties should be small relative to the total number of samples. The null hypothesis (H_0) is that the two samples have been drawn from the same population distribution (Montgomery, 1999).

The one-way analysis of variance (ANOVA) is commonly applied to test differences of means in two or more groups. For comparing the means of two independent groups, one-way ANOVA gives the same results as the two-sample *t-test* does. The null hypothesis (H_0) is no differences of means between two or more groups of samples, while the alternative hypothesis (H_1) is that means of multiple group samples

are not all being equal. H_0 is tested using an F ratio test. The F statistic compares the variability between groups to the variability within groups. A significant F ratio indicates that there is at least one pair of groups that their means are different. However, the result does not point to which pair(s) of group means are significantly different. Thus further multiple group comparison is applied to determine which groups are particularly different among the groups. Performing two-sample t -tests to compare the means of each two groups is a simple way for multiple comparisons. However, with several groups, the more two-sample t -tests (e.g. type I error of each t -test, $\alpha=0.05$) are made, the more opportunities type I error will be made ($n\alpha$, n is the number of two-sample t -test) (Comrey et al., 1989).

The Scheffe's test is one of the multiple comparison methods. It is also recommended when the sample sizes are unequal (Kleinbaum et al., 1987). The procedure of Scheffe's test is as follows. First, compute t value using following equation:

$$t_{ij} = \frac{M_i - M_j}{\sqrt{s_w^2 [(n_i + n_j) / n_i n_j]}} \quad (2.4)$$

where M_i and M_j is means for group i and j ; n_i and n_j are the size of groups; s_w^2 is the mean square for within-groups. Second, the critical t value at significance level of 0.05 was calculated by

$$t'_{0.05} = \sqrt{(k-1)F_{0.05, k-1, N-k}} \quad (2.5)$$

where k is the number of groups and N is the total sample size of groups. If the computed t value exceeds the critical t value, the difference between that pair of group means is statistically significant at level of 0.05 (Comrey et al., 1989).

Nadim et al. (2001) conducted one-way ANOVA and Scheffe's method to investigate temporal and spatial variation of atmospheric mercury in Connecticut, US. Their results showed that no significant difference of TGM concentrations were detected during three collection years. However, comparison results indicated that TGM concentrations in urban and inland areas were significantly higher than that in rural and coastal areas.

2.5.4 Correlation Analysis

Generally, the correlation coefficient is a measurement of the degree of linear relationship between two variables. Several correlation analysis approaches could be employed depending upon the situations (Cohen et al., 2003).

Pearson's correlation analysis is the most common correlation analysis method. It is a parametric method assuming the datasets follow normal distribution (Comrey et al., 1989). Pearson product-moment correlation coefficient (Pearson r) is calculated using following equation:

$$r = \frac{N \sum XY - \sum X \sum Y}{\sqrt{N \sum X^2 - (\sum X)^2} \sqrt{N \sum Y^2 - (\sum Y)^2}} \quad (2.6)$$

where X, Y are raw scores in two variables, N is the number of cases.

Outliers may have a profound influence on the value of the correlation coefficient. A single outlier is capable of considerably changing both the value and significance level of the correlation coefficient (Gibbons, 2001). Hence, outliers should be excluded before conducting correlation analysis. The significance of the sample correlation coefficient r should be tested as well. The null hypothesis (H_0) states that ρ (the population correlation

coefficient) is equal to zero, while the two-tailed alternative hypothesis (H_1) is that ρ is not equal to zero (Comrey et al., 1989).

Kim and Kim (2001) employed Pearson correlation analysis to the TGM data paired with meteorological data such as wind speed, relative humidity, and temperature and other pollutants including SO_2 , NO_x , O_3 , and PM. In their study, TGM concentrations had relatively strong positive correlation with NO_2 , SO_2 , and PM_{10} during daytime. Thus they concluded that TGM concentrations might be impacted by strong man-made sources.

Spearman's rank order correlation is an alternative correlation analysis for the dataset with non-normal or unknown distribution. It is considered as the non-parametric equivalent of Pearson's analysis. The Spearman's coefficient (ρ) is computed from the ranks of two groups of samples with the following equation:

$$\rho = \frac{n \sum r(X_i Y_i) - \sum r(X_i) \sum r(Y_i)}{\sqrt{n \sum r(X_i)^2 - [\sum r(X_i)]^2} \sqrt{n \sum r(Y_i)^2 - [\sum r(Y_i)]^2}} \quad (2.7)$$

where r is the rank of variable, the average rank is assigned in the case of ties. Therefore, unlike Pearson's method, the coefficient (ρ) does not rely on the estimation of parameters of datasets such as mean and standard deviation (Siegel and Castellan, 1988).

In the significance testing of Spearman ρ , the null hypothesis (H_0) states that no linear correlation between two variables. If the computed Spearman ρ is greater than or equal to the critical ρ that is based on the number of samples and significance level of 0.05, the H_0 is rejected (Comrey et al., 1989). This means that the correlation between two variables is different from zero.

Poissant (2000) used Spearman rank order correlation analysis for a dataset of non-normal distribution. The study identified significantly negative correlation between TGM concentration and air temperature. In a study by Poissant et al. (1996), the results of Spearman's correlation analysis suggested that O₃ had positive correlation with CO, SO₂, NO_x, and isoprene. They concluded that the pollutants such as NO_x, isoprene from urban areas significantly affected the O₃ concentration.

2.5.5 Trend Analysis

Some statistical approaches for detecting and estimating trend in air quality measurements have been developed and applied. These approaches include simple correlation and regression analysis, time-series analysis, non-parametric methods, and curve fitting method.

Kendall's test is non-parametric, rank order based, insensitive to missing values, and easy to calculate. It is a widely used statistical test for detecting monotonic trends (that is, trends that are either increasing or decreasing) in time-series (Kendall, 1938). Hirsch et al. (1982) proposed a non-parametric test for trend which is insensitive to the existence of seasonality. The test will identify whether the data are randomly ordered or have a monotone trend.

A two-sample *t*-test is often employed to examine the difference of mean between two groups of data. However, a simple approach to detect a trend is just to decide whether or not significant difference exist between the means of first half of data and the second half of data. It should be noted that this test is only valid when observations are random samples from their respective populations. If zero is not contained in the 95% confidence interval (CI) of the difference of means, one can conclude that a trend exists.

However, care should be taken that serially dependent data is not the case to use this test (Hess et al., 2001).

In addition, *t*-test can also be adjusted for incorporating seasonality by adding season and year as factors. Thus, one data point comprises the mean of samples, the effect of year and season, and residuals. Similar to two-sample *t*-test, 95% CI of the difference of means is calculated. If zero is contained in the interval, one can conclude that a trend exists (Neter et al., 1996; Hess et al., 2001).

Digital filtering is a time series analysis tool that uses curve-fitting techniques. In time series analysis, the data are considered as sum of three components including trend, seasonal cycle and residuals (Brockwell, 2002). The original data are de-trended and the seasonal cycles are removed by fitting a smooth cubic spline and Fourier components to the data. The outliers of data are identified as being greater than the 3 times standard errors away from fitting curve. They will be rejected after each iterative fit and not be used in the further analysis. The differences between fitted value and original value, i.e. residuals, are then interpolated onto an equally spaced data format. The residuals pass through the digital filter to derive inter-annual (long term trend) and intra-annual (seasonal cycle) variations. Two cutoff periods are used in DF: long term cutoff period from 12 to 24 months and short term cutoff period about 4 months (Nakazawa et al., 1997).

DF has been successfully used to determine long-term trends in atmospheric pollutants. Worthy et al. (1998) detected an increasing trend of methane concentration over seven years (1990~1996) using the DF technique at a rural site in Ontario. The DF technique was employed to determine atmospheric Polychlorinated biphenyls trends as

well as its growth/decline rates at the Arctic over five year period of time in the study by Hung et al., (2001). DF was also applied to the five years (1992~1997) dataset of organochlorine pesticides (OCs) at the Arctic and the results suggested that the concentrations of most OC pesticides declined over five years (Hung et al., 2002).

DF technique has been used to analyze the trend of TGM concentration.

Blanchard et al. (2002) employed DF to analyze the trend of TGM using four years data from two CAMNet sites (Egbert and Point Petre) in Ontario, the result of Point Petre is shown in Figure 2.7. No clear trend of TGM concentration was detected at both sites. It is probably because Canadian Hg emissions have been steady after 1995 (Blanchard et al., 2002).

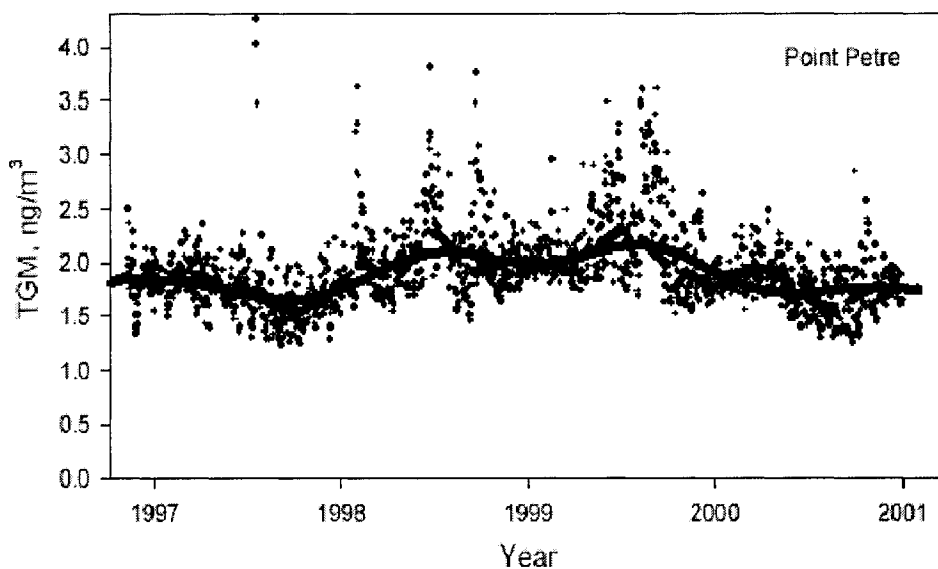


Figure 2.7 Four-year trend of TGM observed at Point Petre site, Ontario (Source: Blanchard et al., 2002)

2.6 Investigation of Source-Receptor Relationship

Air pollution models are broadly used to investigate source-receptor relationship. Many studies have shown that sources can be identified by backward trajectory models (Poissant, 1999; Lin et al., 2001; Blanchard et al., 2002). Box models are widely used in air pollution modeling as well, because of its simplicity of computation.

2.6.1 Backward Trajectory Model

Backward trajectories in meteorology are defined as the pathways where small particles of air came from. They are often used to identify possible sources of pollutant measured at receptor location (Stohl, 1998). Hybrid single-particle Lagrangian integrated trajectory (HYSPLIT) model, developed by National Oceanic and Atmospheric Administration (NOAA), is one approach to compute backward trajectories (HYSPLIT, 2004).

The HYSPLIT model is a complete system that is designed to support a wide range of simulations related to the long-distance transport, dispersion, and deposition of air pollutants. The output of HYSPLIT model can vary from simple air parcel trajectories to complex dispersion and deposition simulations (NOAA, 1999). The model calculates advection, dispersion using either puff or particle approaches under a Lagrangian framework. The trajectory is calculated by the time integration of the position of an air parcel as it is transported by the three dimensional winds (Draxler and Hess, 1997). The integration is applied backward in time to generate backward trajectories. The HYSPLIT model calculates trajectories by assuming puff with horizontal distribution and particle dispersion in the vertical direction (Draxler, 2003). The errors of trajectories are mainly caused by numerical computation and estimation of vertical wind fields. The errors could

be significant (as large as 1000 km after five days), and care should be taken in selecting the time duration of trajectories (Stohl, 1998; Lin et al., 2001).

The Long Range Transport model of Air Pollution, a backward trajectory model, has been used in some Hg studies to detect source-receptor relationship. Poissant (1999) used five-day backward trajectories in the potential source contribution function (PSCF) to investigate potential source of TGM observed at two sites along the St. Lawrence River. The results showed the potential source of TGM during wintertime stretching from the Gulf of Mexico to the southern tip of Greenland. Similarly, Lin et al. (2001) used 10-day backward trajectory generated by HYSPLIT and PSCF and identified that the sources of TGM in winter in the Arctic were from populated area in Europe, the United States and Canada.

The backward trajectories may be used to explain some episodes of high TGM concentration as well. Figure 2.8 shows a particular episode that was observed in the study of Blanchard et al (2002). The Hg analyzer (Tekran 2537A) on a buoy at Lake Ontario detected 70 to 80 ng m⁻³ of TGM concentration at October 1 - 2, 2000. At Egbert where is 97 km north of the buoy, TGM concentration reached 26 ng m⁻³ on the night of October 2nd, 2000. At Point Petre, 186 km northwest of the buoy, high value of TGM concentrations around 6 ng m⁻³ was also observed on the night of October 2. Three-day Lagrangian backward trajectories indicated that the air mass travelled over the local industrial areas to the buoy during this high TGM episode, the elevated levels of TGM observed at the buoy might originate from the local industrial areas.

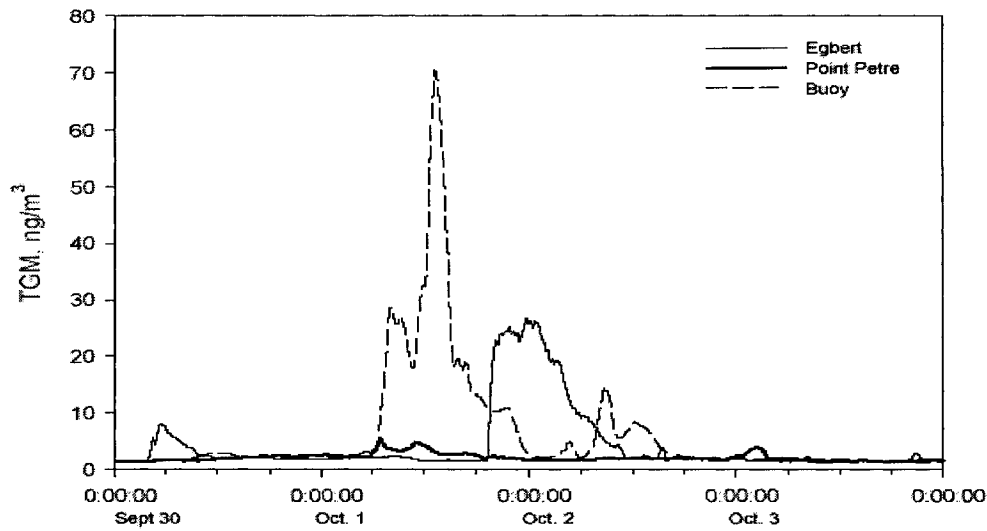


Figure 2.8 TGM concentrations at Lake Ontario buoy, Egbert and Point Petre during the October 2000 episode (Source: Blanchard et al., 2002)

2.6.2 Box Model

Box model is a simple approach to estimate the average concentration of an airshed such as a valley. The airshed of a domain is considered as a rectangle box that the mass of pollutants inside the box is fully conserved. Figure 2.9 is shown as the demonstration of a box model. Box model assumes that incoming pollution is mixed instantaneously, creating a homogeneous concentration throughout the airshed (Collett and Oduyemi, 1997). The mass conservation constraint permits the construction of a mass balance equation of the form:

$$\frac{dC}{dt} AH = FA + uC_{in}WH - uCWH \quad (2.8)$$

where A is the horizontal surface area of the box (L*W), F is the emission rate of the pollutant source in the box, C_{in} is the concentration entering in the box, C is the

concentration inside the box, W is the width of box, H is the mixing height, and u is the average wind speed normal to the box in horizontal direction.

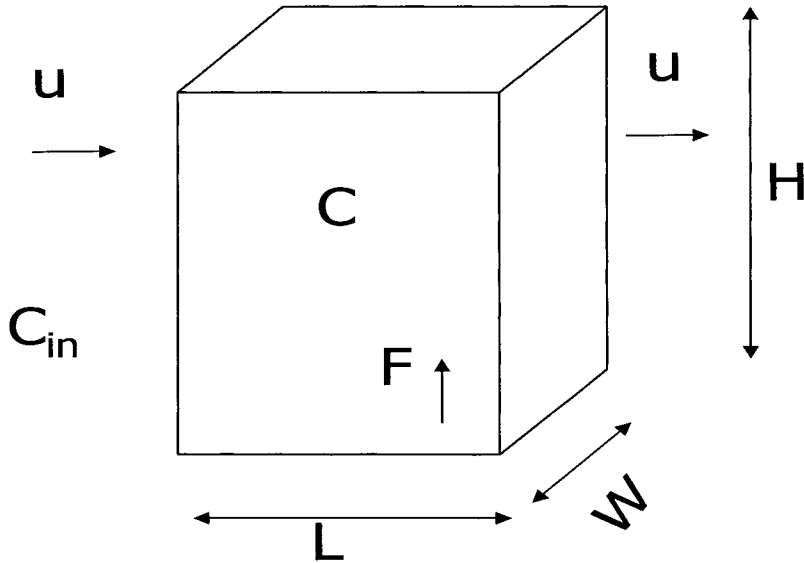


Figure 2.9 The illustration of box model

Cheng et al. (2004) has developed a three dimensional multiple-box model to predict SO_2 concentration in an urban area in China. In their study, mixing height was estimated using meteorological data. In their model, the interval between the ground and the mixing height was divided vertically into three layers, and each layer was 200 m high. Both measured and modeled SO_2 concentrations showed significant vertical profile, i.e. the ground level concentration was quite high, however, the concentration value decreased rapidly in vertical direction.

CHAPTER 3

METHODOLOGY

3.1 Data Collection

3.1.1 *Monitoring Sites*

The TGM measurements used in this study were obtained from three CAMNet sites in Ontario and two other CAMNet sites in Quebec. Map and geographical information of the five sites are shown in Figure 2.5 and Table 3.1, respectively. The brief descriptions of the five sites are as follows (Kellerhals et al., 2003):

- Burnt Island, a rural remote site, is located approximately 110 km southwest of Sudbury, Ontario and 90 km southeast of Sault Ste. Marie, Ontario. The surrounding area of the site is wooded lightly populated.
- Egbert, a rural affected site, is located near Barrie, Ontario. The surrounding area is 70 percent cleared with about 15 hectares of mixed deciduous/coniferous forest to the northwest. Toronto, Ontario (population of three million) lies about 90 km south of site.
- Point Petre, a rural affected site, is a small peninsula on the eastern end of Lake Ontario, about 160 km east of Toronto and approximately 85 km north of Rochester, NY. Highway #401 is located 40 km north of the site. The surrounding area contains mixed brush, a small wooded area, agricultural land (corn), and some summer cottages.

- St. Anicet, a rural affected site, is located along the St. Lawrence River and 100 km southwest of Montreal, Quebec (population of three million). There is a major industrial area in Valleyfield, lies 30 km northeast of the site. The site is a flat grassy area surrounded by fields and deciduous wood lots.
- Mingan, a rural remote site, is located 1 km inland on the north shore of Gulf of Saint Lawrence and is surrounded by black spruce forest. It is located north of Anticosti Island between Sept-Iles (population of 25000) and Havre-St. Pierre (population of 3500).

Table 3.1 Information of the five CAMNet monitoring stations used in this study

Station Name	Latitude	Longitude	Elevation	Data period in this study
Burnt Island	45.81	82.95	184 m	May 1998- Dec2003
Egbert	44.23	79.78	251 m	Jan 1997- Dec 2003
Point Petre	43.84	77.15	78 m	Jan 1997- Dec2003
Mingan	50.27	64.23	11 m	Jan 1997-Dec1999
St. Anicet	45.12	74.28	49 m	Jan 1997- Dec 1999 Jan 2001 – Dec 2001

3.1.2 TGM, Hg Wet Deposition, and Meteorological Data

Standard operating procedures of TGM measurements are adopted for all five sites (Steffen and Schroeder, 1999). Tekran[™] Model 2537A analyzer is employed to measure TGM concentration. It automatically performs continuous measurements and its detection limit is 0.1 ng m⁻³. The analytical train of Model 2537A is based on the amalgamation of Hg onto a pure gold surface followed by a thermo-desorption and analyzed by CVAFS ($\lambda = 253.7$ nm). The dual cartridge design allows sampling and analyzing alternately, thus achieving measurements of mercury in the air stream

continuously. The analyzer samples air at the flow rate from 0.5 to 1.5 L min⁻¹.

Particulate matters (> 0.45 µm) are removed by a 47 mm diameter Teflon™ filter (Tekran Inc., 2003). The user specified sampling interval of Model 2537A can be as short as 2.5 minutes. Fifteen minutes sampling interval is adopted at all five sites. Sampling inlet heights varied from three to six meters above ground level with 10-15 m Teflon inlet lines.

The Model 2537A has two methods of calibration: 1) injection port for manual calibration using standard gas tight syringes, and 2) internal permeation source allows automatic unattended recalibration at user specified intervals. The standard procedure of instrument calibration and audit protocol of CAMNet site has been described in detail by Steffen and Schroeder (1999) and Poissant and Casimir (1999), respectively. Briefly, the instrument is automatically calibrated in a daily basis using an internal mercury source. In addition, the permeation sources are programmed to inject a known amount of mercury into the ambient sample stream at a quarterly basis. An audit of the network takes place every two years. During the audit, a network calibration unit is used to calibrate the permeation source in each instrument and also to provide an inter-comparison of the regional calibration units.

In order to ensure that data is valid and of known precision and accuracy, a quality assurance/quality control (QA/QC) strategy has been implemented in all five sites. TGM measurements from CAMNet are quality controlled using the RDMQ system. Data may be assigned validity flags that refer to a specific data issue or problem such as "warning", "corrective action required", or "no further action required". When a condition is violated, the appropriate data point(s) are flagged. This can assure that the end-user of

the data can refer to and evaluate abnormalities in the data. The RDMQ assures that all TGM data are treated in a consistent manner. Each year of data from each site undergoes several evaluation steps before being accepted as valid (Steffen and Schroeder, 1999).

The three Ontario sites also measured weekly total Hg concentrations in precipitation and Hg wet deposition rate between 2001 and 2003. Precipitation samples were collected in a modified Aerochem Metrics model-301 collector, which is activated automatically by the occurrence of precipitation. The weekly samples were sent to the laboratory for analysis by CVAFS ($\lambda = 253.7$ nm) (MDN, 2003).

Meteorological measurements were also available in the three Ontario sites. The parameters include wind speed (m s^{-1} , by anemometer), wind direction (degree, by vane), temperature ($^{\circ}\text{C}$, by thermistor), relative humidity (% by hygistor), solar radiation (W m^{-2} , by pyranometer), and atmospheric pressure (mb, by barometer). All meteorological measurements have been hourly averaged.

3.2 Software

In this study, Minitab[®] 14 (Minitab, 2004) was used for all statistical computations and most graphics plotting. For all statistical analysis in this study, the significance level was set to 0.05. Curvefit, a DOS-based software developed by Environment Canada, was used for trend analysis. Microsoft Excel[®] (Microsoft Excel, 2002) was used to prepare the input data for Minitab and Curvefit.

3.3 Data Compilation

The TGM data provided by Environment Canada are hourly averaged from 15 min original measurements after QC, except data of years 2002 and 2003 from the three

Ontario sites, which came with original measurements in 15 min interval without QC. Those 15 min original data were hourly averaged without further manipulation.

In order to perform the statistical analysis of TGM variability using Minitab (Minitab, 2004) and Curvefit, the time (yyyy/mm/dd/hh) of TGM measurements was split to individual variables including hour, day, month, and year. The TGM measurements came with the start time and end time using Eastern Standard Time (EST), the start time was assigned to the hour variable in this study.

In addition, a season variable was assigned to each TGM measurement. The definition of season is spring from March 1 to May 31; summer from June 1 to August 31; fall from September 1 to November 30; and winter from December 1 to February 28 (or 29) of the next year. As well, all additional categorical variables are applicable with the meteorological data.

3.4 Statistical Analysis

The flowchart of basic statistical analysis procedures is shown in Figure 3.1. Firstly, descriptive statistics of TGM concentration are computed. Secondly, the sample size and the normality of data were used to determine the type of statistical analysis methods, parametric or non-parametric methods for further statistical analysis. If the distribution is not normal, the transformed (Natural logarithmic or square root) data were used for normality test.

3.4.1 Descriptive Statistics

The numerical descriptive statistics in this study included mean (with 95% confidence interval), standard deviation, median, maximum, minimum, and total number

of measurement. Histogram plots were generated to analyze the frequency distribution of TGM concentration at the five sites. Box-Whisker plots were generated to summarize the TGM data graphically with median, 1st and 3rd quartile, and upper/lower limit of outliers. In addition, descriptive statistics was calculated using seasonal grouped TGM data at each site.

Wind rose and TGM-rose plots of the three Ontario sites were drawn. Wind direction was divided into twelve 30⁰ sections. Wind frequency in each section was used to plot the wind rose, and average of TGM concentrations in each section was used to plot the TGM-rose.

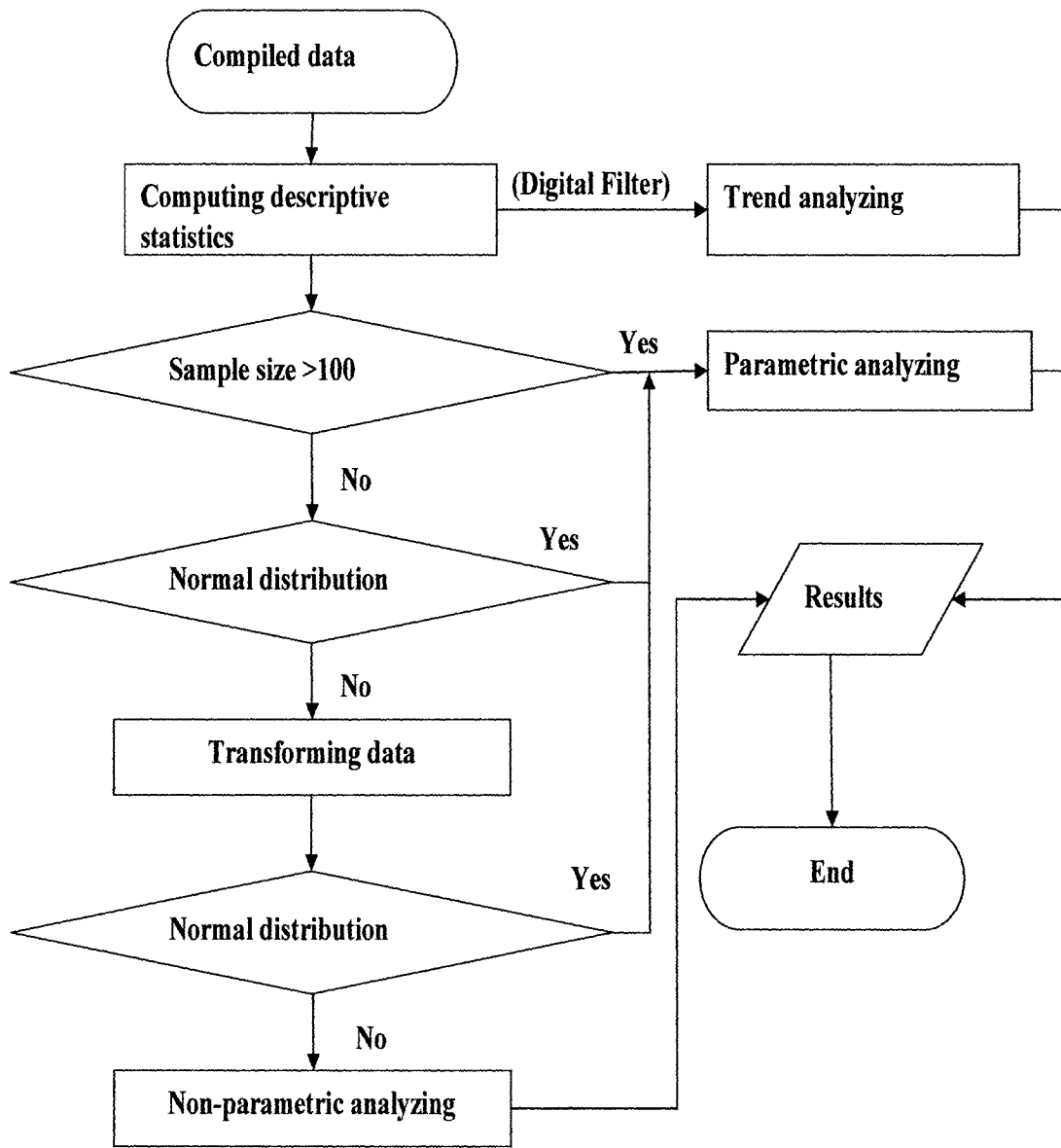


Figure 3.1 Flowchart of statistical analysis in this study

3.4.2 Normality Test and Selection of Parametric and Non-parametric Methods

Anderson-Darling test was applied to test the normality of TGM concentrations at all five sites. TGM concentrations were also transformed to natural logarithm and square root, and the normality of transformed data was also tested using Anderson-Darling method.

The result of normality test is a major factor in selecting either parametric or non-parametric methods. The sample size is another factor according to Central limit theorem. In this study, the procedure of selecting between parametric and non-parametric methods of analysis is as follows. If the sample size is greater than 100, parametric methods will be applied. If the sample size is less than 100, parametric methods will be applied to the data which follow normal distribution, while non-parametric methods will be applied to the data that do not follow normal distribution. Table 3.2 lists the parametric and non-parametric methods used in this study.

Table 3.2 The parametric and non-parametric methods used in this study

	Parametric	Non-parametric	Application
Two group comparison	Two-sample <i>t-test</i>	Mann-Whitney U test	Spatial variation of TGM.
Multiple group comparison	ANOVA and Scheffe's test	N/A	Spatial variation of TGM, comparing seasonal mean of TGM.
Correlation analysis	Pearson correlation	Spearman rank order correlation	Detect relationship between TGM and meteorological factors and Hg wet deposition

3.4.3 Comparisons of Means

Statistical comparisons were used to identify the spatial and temporal variations of TGM concentrations. Two-sample *t* test was conducted to identify the spatial variation of TGM concentration in the St. Lawrence River Basin using the data from Mingan and St. Anicet (January 1997 to December 1999). Mann-Whitney test was used to compare monthly temperature and precipitation of 2001 and 2002 in Burnt Island in order to investigate the TGM increase of the year 2002.

One-way ANOVA and Scheffe's comparison method were used as multiple-comparison approaches to investigate spatial variation of TGM concentration. In order to keep the consistency of the comparison, TGM data in the comparison were from the same period of time. One-way ANOVA and Scheffe's test were conducted to detect the spatial variations of TGM among the three Ontario sites using six-year (1998~2003) TGM data. TGM data from 1998 to 1999 were used for the multiple-comparison to analyze the spatial variation of TGM concentration in all five sites. The seasonal variation of TGM concentrations at each site was also identified using this multiple-comparison method.

3.4.4 Correlation Analysis

In the three Ontario sites, correlations analysis between TGM concentrations and meteorological data were conducted using Pearson correlation analysis due to the large sample size of TGM and meteorological data. Seasonally divided TGM and meteorological data were also used to determine the correlations between TGM concentration and meteorological parameters in each season. Meteorological parameters included ambient air temperature, wind speed, solar radiation, and atmospheric pressure. Cut-off value of 50 W m^{-2} was used for solar radiation data in the correlation analysis

with TGM. Pearson correlation analysis was also used to find correlation between TGM concentrations and natural logarithm transformation of total Hg concentration in precipitation and Hg wet deposition rate in the three Ontario sites.

Spearman rank-order correlation analysis is a non-parametric equivalent to the Pearson correlation analysis. In the three Ontario sites, Spearman's analysis was used to investigate the correlation between the averaged TGM concentration, temperature, and solar radiation for each hour. Cut-off value of 50 W m^{-2} for solar radiation data was used in this analysis. The seasonal grouped data were also used to find the correlations between diurnal TGM data and temperature as well as solar radiation in each season.

3.4.5 Trend Analysis

The long term trend analysis of TGM concentrations was conducted for the three Ontario sites using Curvefit program. The principle of DF technique can be found in Nakazawa et al. (1997).

The hourly TGM measurements with the measuring time (year, month, day, and hour) were used for the input of Curvefit. The cut-off period for long-term trend was set to 24 months. The number of harmonic for seasonal cycle was set to two. This harmonic set-up was determined by visually estimating the time series plot of monthly average TGM concentration. The cut-off period for short-term variation was set to four months.

The daily means of TGM concentrations were calculated. First, for days with missing value, Curvefit interpolated the daily mean of TGM concentrations linearly. The trend and seasonal cycle were obtained using a spline fit and a Fourier function (with harmonic number selected previously) interactively. TGM data points greater than three times standard error of fit were excluded from further analysis. The trend and seasonal

cycle were then subtracted from the original data (without outliers) to obtain residuals. These residuals still contained the long- and short-term variations of trend and seasonal cycle. Third, the residuals were smoothed with the digital filter to derive inter- and intra-annual variations. Thus the final curve fitted to the original TGM data consist of: 1) the approximate long-term trend represented by spline function, 2) the average seasonal cycle represented by the Fourier function, and 3) short- and long-term variations obtained by digital filter.

The output data include values of trend and seasonal cycle. The time interval of output values on fitted curve was set to one day. The time format of output files is the year plus fraction of Julian day in a year. For example, 1998.5 represent 1998/6/30.

3.5 Identification of High TGM Concentration Episode(s)

High TGM concentration episodes are events that TGM concentrations reach higher value in short time period, compare to adjacent data point(s). The episodes are shown as spikes in time-series plot. However, it is extremely difficult to identify these episodes visually in a time-series plot that has tens of thousands of data points. The data of large size have to be divided into subgroups with smaller sizes.

In statistics analysis, outliers have a powerful influence on the mean (center location) of a dataset. A single outlier is capable of altering significantly the mean of data, whereas the median value of data is less sensitive to outlier(s). Based on the characteristics of outliers, the following procedure was developed to identify high TGM episodes in this study.

The TGM concentrations data were grouped monthly at each site. The mean and median of TGM concentrations in each month were calculated. Then the months with

large difference between mean and median were selected. In each of these months, the hourly time-series with about 700 data points, or of shorter period if necessary, was plotted. The spikes in the time-series were then identified visually. Moreover, the outliers identified by Curvefit acted as cross-reference to identify the high TGM concentration episodes. It is noticed that both statistical method and Curvefit identified low TGM concentration episodes as well. Since this study focused on using high TGM concentration episodes to investigate source-receptor relationship, the low TGM concentration episodes will not be discussed.

3.6 Investigation of Source-Receptor Relationship

The online HYSPLIT model (<http://www.arl.noaa.gov/ready/hysplit4.html>) and a box model were applied to investigate the source-receptor relationship using a selected high TGM concentration episode. Twenty-four-hour HYSPLIT backward trajectory simulation was performed to find out the pathway of air mass for the high TGM episode. The box model was used to investigate the effects of Hg emission from the water body on the TGM concentration at the receptor quantitatively.

The archived EDAS with 80 km grid spacing, which is the finest grid data available online, was chosen as the meteorological dataset to compute trajectories using universal time (UTC). There are two options of vertical motion in HYSPLIT model: isobaric (constant pressure) and the model vertical velocity (MVV). The MVV means that the trajectory moves with the vertical velocity wind fields generated by a diagnostic or prognostic meteorological model. MMV was selected for this study since it contains contributions from all adiabatic and diabatic components, which are driving the growth and dissipation of the boundary layer (NOAA, 2004). The arrival height of trajectories

was set to 500 meters above the ground level of the end point for the HYSPLIT calculation in this study.

In this study, the fundamental assumptions of the box model application are as follows: 1) air mass picks up the uniform Hg emission from the water body along the trajectory to the end point; 2) there was no deposition and reaction along the journey of air mass; and 3) the TGM is instantaneously mixed in the box. For the end point, the backward trajectories were calculated in each hour during the period of episode. For each hour, a series of boxes were established along the trajectory of that hour over the lake as shown in Figure 3.2. The length of each box is the distance of air mass travelling one hour. Along the trajectory, the box at the end point is the last box, and the first box is at the intersection of the trajectory and the edge of lake. TGM concentration in each box was simulated using the following equation which is modified based on equation (2.8) (the details of derivation are in appendix A):

$$C = C_{in} + 0.63 \frac{F}{H} \quad (3.1)$$

where C is the estimated TGM concentration in the box (ng m^{-3}); C_{in} is the TGM concentration entering the box, i.e. the TGM concentration from the previous box; for the first box, C_{in} is the TGM concentration at the end point before the start of the episode; F is the estimated emission rate (flux) of Hg ($\text{ng m}^{-2} \text{h}^{-1}$) as shown in Table 3.3; H is the hourly mixing height (m) corresponding to that box along the trajectory, which was generated by the HYSPLIT model. The calculation of the TGM concentration of the last box, i.e. the concentration at the end point, was achieved by a series of box model applications.

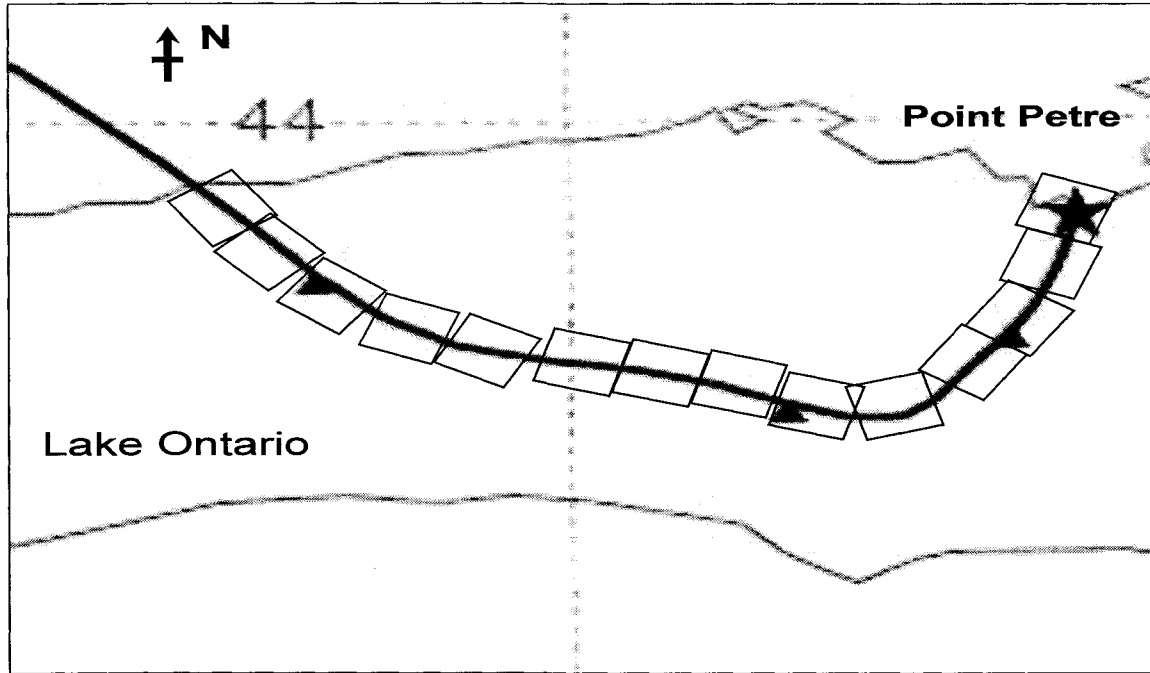


Figure 3.2 An example of a series of 14 boxes along the trajectory. Five-pointed star indicates the end point

Table 3.3 Estimated Hg emission rates used in this study

Flux ($\text{ng m}^{-2} \text{h}^{-1}$)	Location	Method	Reference
10 (maximum)	Lake Ontario	Two layer model	Poissant et al., 2000
35* (mean+2s.d.)	Sweden	Dynamic flux chamber	Gardfeldt et al., 2001
89 (maximum)	Sweden	Dynamic flux chamber	Gardfeldt et al., 2001

* Calculated based on the reported mean and standard deviation are $11 \text{ ng m}^{-2} \text{h}^{-1}$ and $12 \text{ ng m}^{-2} \text{h}^{-1}$, respectively.

CHAPTER 4

RESULTS AND DISCUSSION

4.1 Descriptive Statistics

The descriptive statistics were applied to characterize the TGM concentrations at the three Ontario sites and the two Quebec sites. The spatial comparison of TGM concentration among the five sites was also conducted using TGM data from May 1998 to December 1999 when TGM data are available at all five sites.

4.1.1 Ontario Sites

Table 4.1 shows the statistical summary of TGM concentrations at the three Ontario sites as well as in each season during May 1998 to December 2003 when TGM data are available in all three Ontario sites. The overall mean values of TGM concentrations ranged from 1.59 ng m^{-3} of Burnt Island to 1.85 ng m^{-3} of Point Petre. The maximum TGM concentration of 25 ng m^{-3} occurred at the night of October 2nd, 2000 in Egbert, the minimum TGM concentration of 0.47 ng m^{-3} occurred at the early morning of August 4th, 1999 in Burnt Island.

The histogram plots of TGM concentrations for each site are shown in Figure 4.1. The TGM concentrations at Burnt Island were nearly normal-distributed with a skewness value of 0.32. The distributions of TGM concentration were largely positive-skewed at Egbert (skewness = 25.11) due to some high TGM values. The skewness of TGM concentrations at Point Petre was 1.94. Anderson-Darling test also indicated that the

TGM concentrations did not follow normal distribution at any of the three sites, nor did natural logarithm and square root transformation of TGM concentrations (Table 4.2). The concentration of 1.40~1.70 ng m⁻³ has the highest frequency in the distribution at Burnt Island, while the concentration of 1.50~1.90 ng m⁻³ have the highest frequency at both Egbert and Point Petre.

Table 4.1 Statistical summary of TGM concentrations (ng m⁻³) during May 1998 to December 2003 when TGM data are available at the three Ontario sites

Site		Mean	St. Dev.	Median	Min.	Max.	Sample size
Burnt Island	All	1.59	0.24	1.59	0.47	4.38	46883
	Spring	1.67	0.20	1.67	0.73	3.06	11266
	Summer	1.48	0.22	1.46	0.47	4.38	12933
	Fall	1.49	0.24	1.48	0.51	3.71	11623
	Winter	1.74	0.19	1.72	1.10	3.32	11061
Egbert	All	1.71	0.42	1.68	0.76	25.82	47851
	Spring	1.81	0.30	1.77	0.93	14.35	11389
	Summer	1.61	0.25	1.56	0.82	5.05	12763
	Fall	1.60	0.65	1.53	0.76	25.82	12595
	Winter	1.83	0.25	1.77	0.93	5.93	11104
Point Petre	All	1.85	0.39	1.78	0.60	6.88	46972
	Spring	1.88	0.30	1.86	1.03	6.23	11509
	Summer	1.93	0.51	1.80	0.60	5.23	12125
	Fall	1.77	0.42	1.67	1.01	5.98	12579
	Winter	1.81	0.28	1.77	0.66	6.88	10759

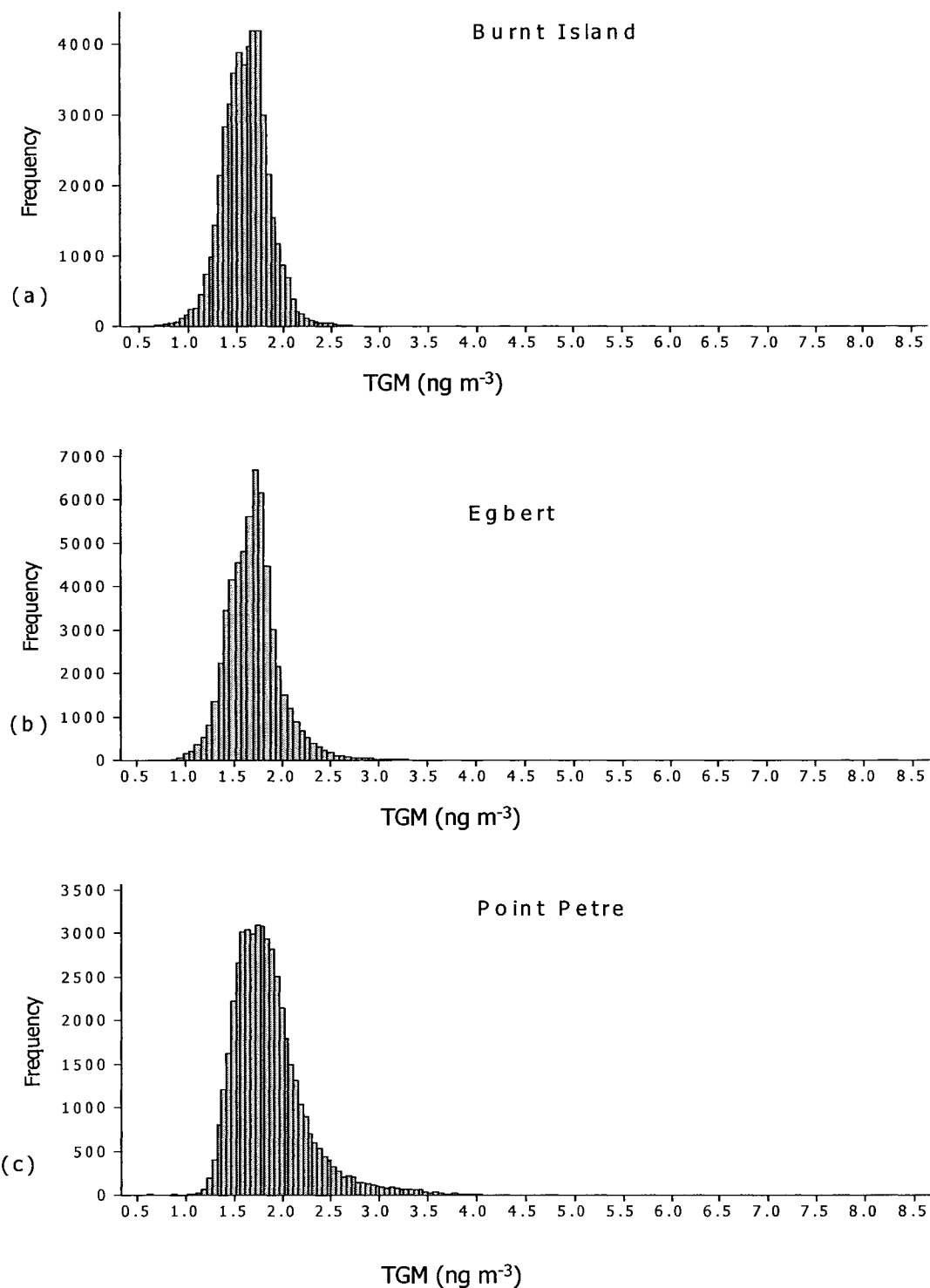


Figure 4.1 Histogram of TGM concentrations at (a) Burnt Island; (b) Egbert; (c) Point Petre. TGM concentrations greater than 10 ng m^{-3} ($N=13$, $\text{max.}=25.82 \text{ ng m}^{-3}$) at Egbert have been excluded.

Table 4.2 Results of Anderson-Darling Normality test of TGM at the three Ontario sites (all p values < 0.05)

Site	Anderson-Darling test statistic		
	TGM	Natural logarithm of TGM	Square root of TGM
Burnt Island	73.16	186.58	93.95
Egbert	2723.61	256.12	727.06
Point Petre	1115.87	327.38	648.49

One-way ANOVA and Scheffe's multiple-comparison were used to investigate spatial variation of TGM concentrations during May 1998 to December 2003 when TGM data are available in all three Ontario sites. One-way ANOVA indicated that the means of TGM concentrations were significantly different ($F = 6000$, $p < 0.05$) among the three Ontario sites. Scheffe's multiple-comparison showed that the means of TGM concentration were significantly different among the three sites ($p < 0.05$), and the order was as follows: Burnt Island (1.59 ng m^{-3}) $<$ Egbert (1.71 ng m^{-3}) $<$ Point Petre (1.85 ng m^{-3}). The spatial variation showed that the TGM concentrations of rural-affected sites (i.e. Egbert and Point Petre) were significantly higher than that of rural-remote site (i.e. Burnt Island).

The wind rose and TGM-rose for the three sites are shown in Figure 4.2. Northwesterly and southeasterly winds were the prevailing winds at Burnt Island. Northerly and southwesterly winds were the dominant winds at Egbert, and most the winds came from the west at Point Petre.

At Burnt Island, TGM-rose indicated that higher TGM concentrations were largely associated with air mass from south and southeast areas, which are known for heavy population and industrial activities. In contrast, lower TGM concentrations mainly

occurred when air mass came from Northern Ontario, which is a major forest area and lightly populated.

Background TGM concentrations of Egbert were mainly observed when winds were from north. When winds came from south, the mean TGM concentration was 1.92 ng m^{-3} , which was 23% higher than that with northerly winds (1.56 ng m^{-3}). City of Toronto, 90 km south of Egbert, is known as a heavy populated and industrialized area. The TGM rose suggested that high TGM concentrations at Egbert were likely affected by anthropogenic Hg inputs from Toronto area.

Similarly, lower TGM observations at Point Petre were associated with clean air mass from North Ontario, while high TGM concentrations were observed when the winds were from southwest to south. City of Toronto and New York State are located 160 km southwest and 80 km south of the site, respectively. Anthropogenic Hg emissions from these two areas likely contributed to high TGM values at Point Petre.

Point Petre and Egbert are both located near heavy populated and industrialized areas, yet the mean TGM concentration at Point Petre was 8% higher than that at Egbert. Poissant et al. (2000) has reported that Hg evasion fluxes were one order of magnitude greater than dry deposition fluxes at Lake Ontario which is surrounded by industrialized areas. High TGM concentrations at Point Petre were likely due to the large amount of Hg emission from water body into the boundary layer above Lake Ontario, and then picked up by on-shore winds to Point Petre.

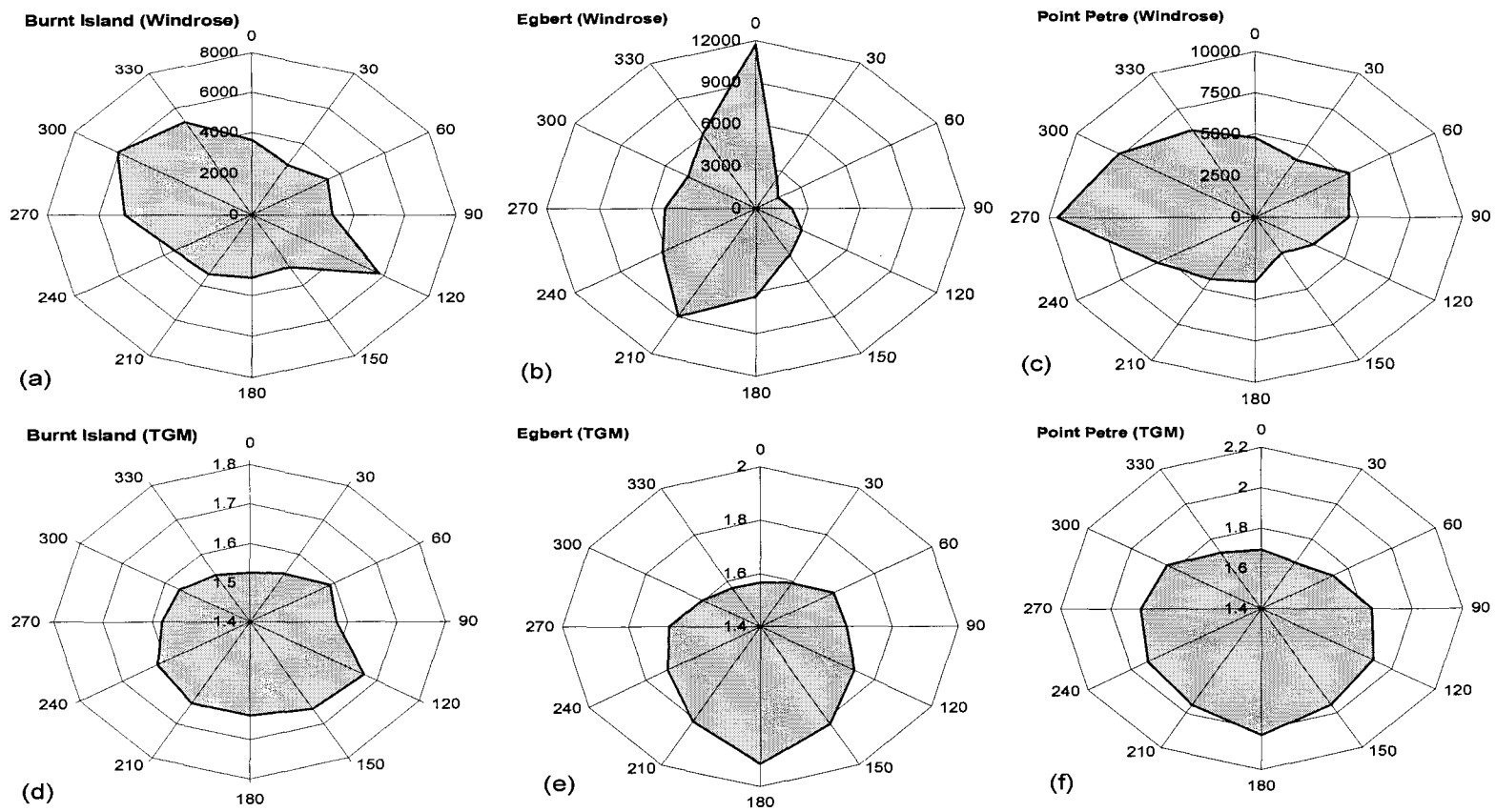


Figure 4.2 Wind rose and TGM-rose for the three Ontario CAMNet sites. (a)-(c), wind rose, radius axis indicates frequency; (d)-(f) TGM-rose, radius axis indicates average TGM concentration in the direction.

TGM concentrations observed at Burnt Island (rural-remote site) were approximately 6 to 15% lower than at the other two rural-affected Ontario sites. Less anthropogenic Hg input is a possible reason since the vicinity of this site is lightly populated with absence of major industrialized areas nearby.

4.1.2 Quebec Sites

Table 4.3 shows the statistical summary of TGM concentrations at Mingan and St. Anicet during January 1997 to December 1999 when TGM data are available in both sites. The maximum TGM concentration is 53.08 ng m⁻³ occurred at 6:00 pm February 15, 1999 in St. Anicet, the minimum TGM concentration is 0.36 ng m⁻³ occurred at midnight of May 10th, 1998 in Mingan. The median of overall TGM concentration at the two sites is the same. Histogram plots of TGM concentration are shown in Figure 4.3. The distribution of TGM concentration at St. Anicet was largely positive-skewed (skewness = 33.64) due to some extremely high TGM values. The concentration of 1.50~1.70 ng m⁻³ had the highest frequency in the distribution of TGM concentrations at St. Anicet, while the concentration of 1.60~1.80 ng m⁻³ had the highest frequency. Unlike the other four sites involved in this study, the distribution of TGM was negatively skewed (skewness = -1.22) at Mingan, and this negative skewness was observed in each season. It is because that the frequency of low TGM occurrence was higher than the other sites and the maximum value (3.07 ng m⁻³) was lower than that of other sites. Anderson-Darling normality test also indicated that the distribution of TGM concentration at the two Quebec sites did not follow normal distribution, nor did natural log and square root transformation of TGM (data not shown here). The result of *t*-test indicated that the mean

TGM concentration (1.71 ng m^{-3}) at St. Anicet is significantly higher ($t = 17, p < 0.05$) than that in Mingan (1.61 ng m^{-3}).

Table 4.3 Statistical summary of TGM concentrations (ng m^{-3}) during January 1997 to December 1999 when TGM data are available in the two Quebec sites

Site		Mean	St. Dev.	Median	Min.	Max.	Sample size
Mingan	All	1.61	0.23	1.65	0.36	3.07	23820
	Spring	1.66	0.20	1.70	0.36	2.40	5729
	Summer	1.52	0.24	1.55	0.48	3.07	5726
	Fall	1.49	0.22	1.53	0.52	2.41	6220
	Winter	1.76	0.10	1.77	1.17	2.27	6145
St. Anicet	All	1.71	0.90	1.65	0.59	53.08	25059
	Spring	1.82	0.42	1.78	0.99	7.41	6315
	Summer	1.55	0.35	1.48	0.64	5.00	6309
	Fall	1.57	0.30	1.55	0.59	9.62	6268
	Winter	1.90	1.67	1.75	1.05	53.08	6167

Higher TGM concentration at St. Anicet is likely due to anthropogenic Hg input from metropolitan of Montreal area (100 km northeast of the site) and nearby industrial areas. In particular, Valleyfield, an industrial center, is just 30 km northeast of the site. This center has cotton and synthetic textile mills, a zinc refinery, and plants making chemicals, clothing, and rubber goods. One extremely high TGM concentration episode was observed at this site. The episode started from 1:00 pm February 15, 1999, the TGM concentration increased from 1.60 ng m^{-3} to 26.10 ng m^{-3} in one hour, and then reached the maximum of 53.08 ng m^{-3} at 6:00 am February 15; afterward, the TGM concentration was back to 2.90 ng m^{-3} at 9:00 am February 16. The average of TGM concentration was 25.41 ng m^{-3} during the 21 hours period. Such high TGM concentrations were likely caused by local industrial area releasing a large amount of Hg in a short period of time.

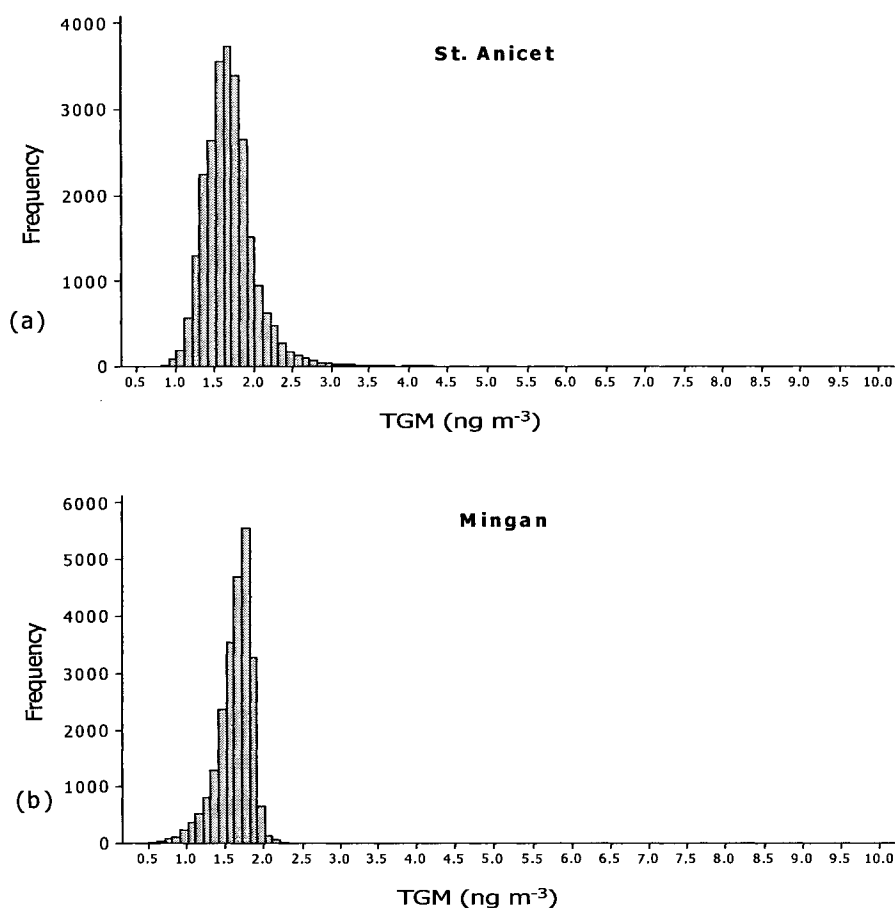


Figure 4.3 Histogram of TGM concentration at (a) St. Anicet; (b) Mingan. TGM concentrations greater than 10 ng m^{-3} in St. Anicet ($N=15$, $\text{max.}=53.08 \text{ ng m}^{-3}$) have been excluded.

The maximum TGM concentration was 3.07 ng m^{-3} at Mingan, which is only 90% higher than the mean TGM concentration of 1.61 ng m^{-3} . In contrast, the maximum of 53 ng m^{-3} is 32 times higher than the mean TGM concentration at St. Anicet. Lower TGM concentrations at Mingan are likely due to lack of nearby industrial sources and the lightly populated area surrounding. In addition, the easterly winds are prevailing winds at Mingan, thus the incoming clean marine air may lead to lower TGM values at this site.

4.1.3 Spatial Comparison of the Five CAMNet Sites

The box-whisker plot of TGM concentrations at all five sites was generated using the measurements during 1998 to 1999 when TGM data are available in all five sites (Figure 4.4). The mean TGM concentration of Point Petre was 2.11 ng m^{-3} , which was about 23~34% higher ($p < 0.05$) than that of the other four sites in this study. TGM concentrations at Point Petre also showed larger variations than that in the other four sites.

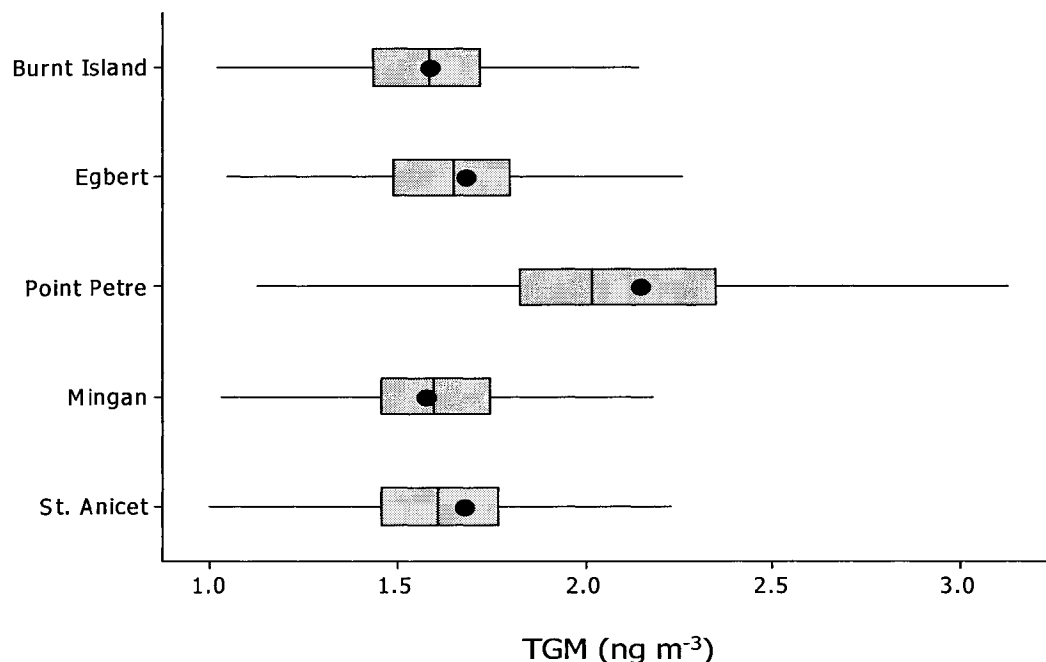


Figure 4.4 Box-whisker plot of TGM concentration at the five CAMNet sites during 1998 to 1999 when TGM data are available in all five sites. The vertical line inside the box indicates the median; the solid circle indicates the mean. The left and right boundaries of the box indicate the 25th and the 75th percentile values, respectively.

The results of ANOVA indicated that the means of TGM concentrations were significantly different ($F = 2300, p < 0.05$) among the five sites during 1998-1999 when

TGM data are available in all five sites. The Scheffe's comparison showed that the five sites could be divided into three homogeneous subsets in the following order: Burnt Island and Mingan (1.58 ng m^{-3} and 1.61 ng m^{-3}) < Egbert and St. Anicet (1.71 ng m^{-3} and 1.72 ng m^{-3}) < Point Petre (2.11 ng m^{-3}). The spatial variations of the five sites showed that TGM concentration of the rural-affected sites were significantly higher than that of the rural-remote sites, in good agreement with the site classification (Kellerhasls et al., 2003). Among the five CAMNet sites, Point Petre had the highest mean TGM concentration.

4.2 Seasonal Variability of TGM Concentrations

The results of ANOVA indicated that seasonal means of TGM concentrations were significantly different at each site ($p < 0.05$). Seasonal means of TGM concentration are listed in Tables 4.2 and 4.3. Further Scheffe's comparison showed that seasonal means of TGM concentration could be divided into homogeneous subsets as follows: summer and fall < spring < winter at Burnt Island, Egbert, Mingan, and St. Anicet, whereas fall < winter < spring < summer at Point Petre. Interval plots of monthly TGM concentration were generated to investigate the seasonal variability of TGM concentrations for the three Ontario sites (Figure 4.5) and the two Quebec sites (Figure 4.6). For the three Ontario sites, season pattern were generated using TGM data from May 1998 to December 2003 when TGM data are available for all three sites. For the two Quebec sites, TGM measurements during January 1997 to December 1999 were used to generate the seasonal pattern. Two different seasonal patterns were detected among the five sites: winter high/summer low pattern and winter high/summer high pattern as discussed below.

4.2.1 Winter High/Summer Low Pattern

The winter high/summer low seasonal pattern was detected at Burnt Island, Egbert, Mingan, and St. Anicet (Figures 4.5 and 4.6). In this seasonal pattern, the maximum TGM concentrations occurred in late winter, and then decreased gradually and reached the minimum values during late summer or early fall. A similar seasonal pattern of TGM concentrations has also been observed in German, maximum TGM concentration in March and minimum in October (Slemr and Scheel, 1998). Several factors may affect this seasonal pattern. Coal combustion for heating might be a major Hg emission source and lead to high TGM concentrations in winter (Rotty, 1987). Meteorological parameters might have effects on the seasonal variation as well. Lower air mixing height and wind speed in winter led to TGM building up near the surfaces. Low TGM concentration in summer is likely due to higher mixing layer and strong atmospheric mixing processes diluting TGM concentrations. Another cause for this summer sink modulation could be large removal from the atmosphere by strong wet deposition (Lamborg et al., 1995). More discussion on this is to follow.

Overall, Burnt Island, Egbert, Mingan, and St. Anicet have winter high/summer low seasonal pattern. However, seasonal pattern of Mingan shows a bit difference from the other three sites. A slight increase in TGM concentration occurred in June and July. Higher temperature and strong solar radiation in June and July may enhance Hg emission from the surfaces. However, the prevailing winds for this site in June and July bring clean marine air to Mingan. Thus, incoming marine air may dilute TGM concentrations, resulting in a small change in TGM concentrations

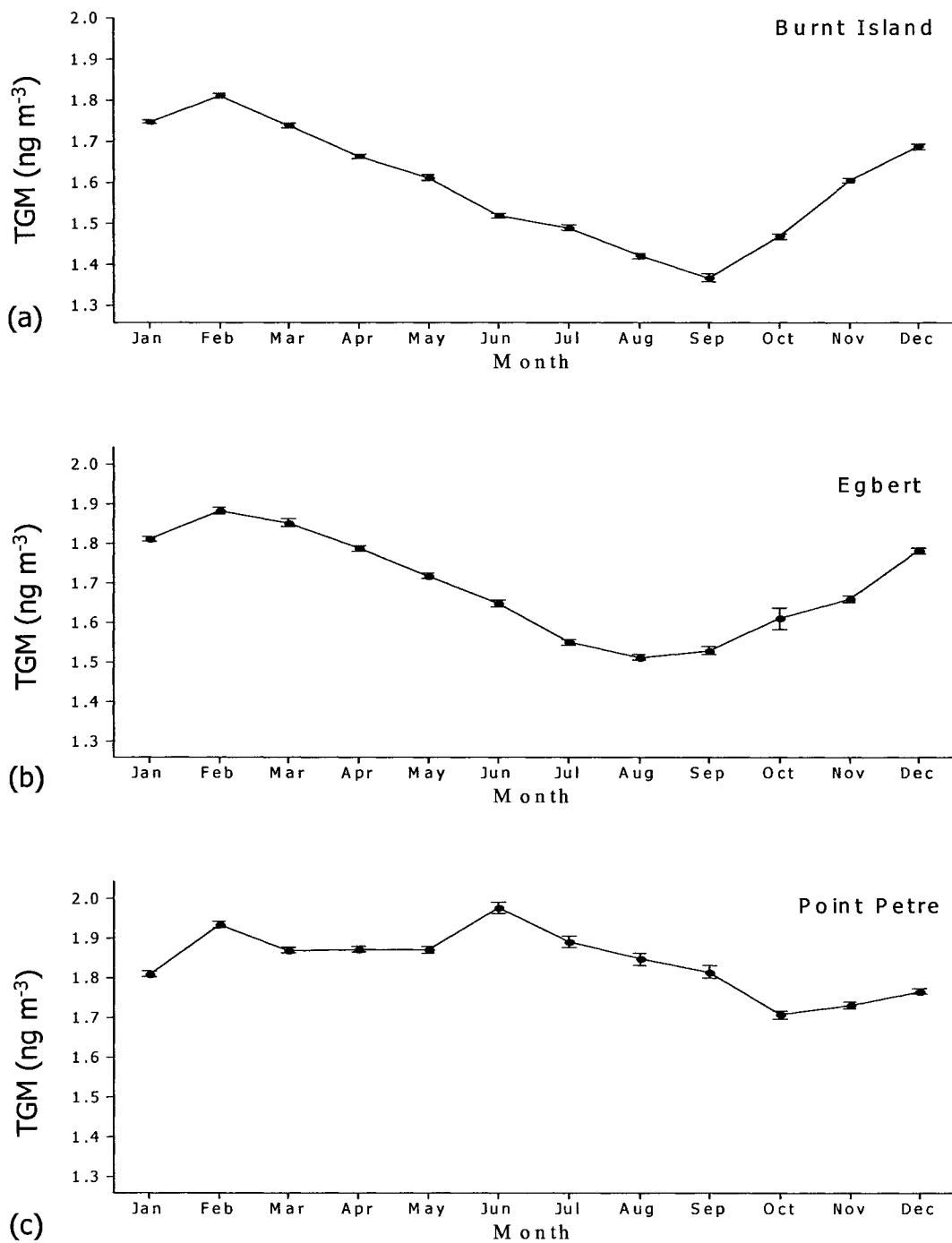


Figure 4.5 Monthly mean of TGM concentrations observed at the three Ontario sites from May, 1998 to December, 2003. (a) Burnt Island, (b) Egbert, and (c) Point Petre. The solid circle indicates the monthly mean and the vertical bars indicate 95% confidence interval (CI) of mean.

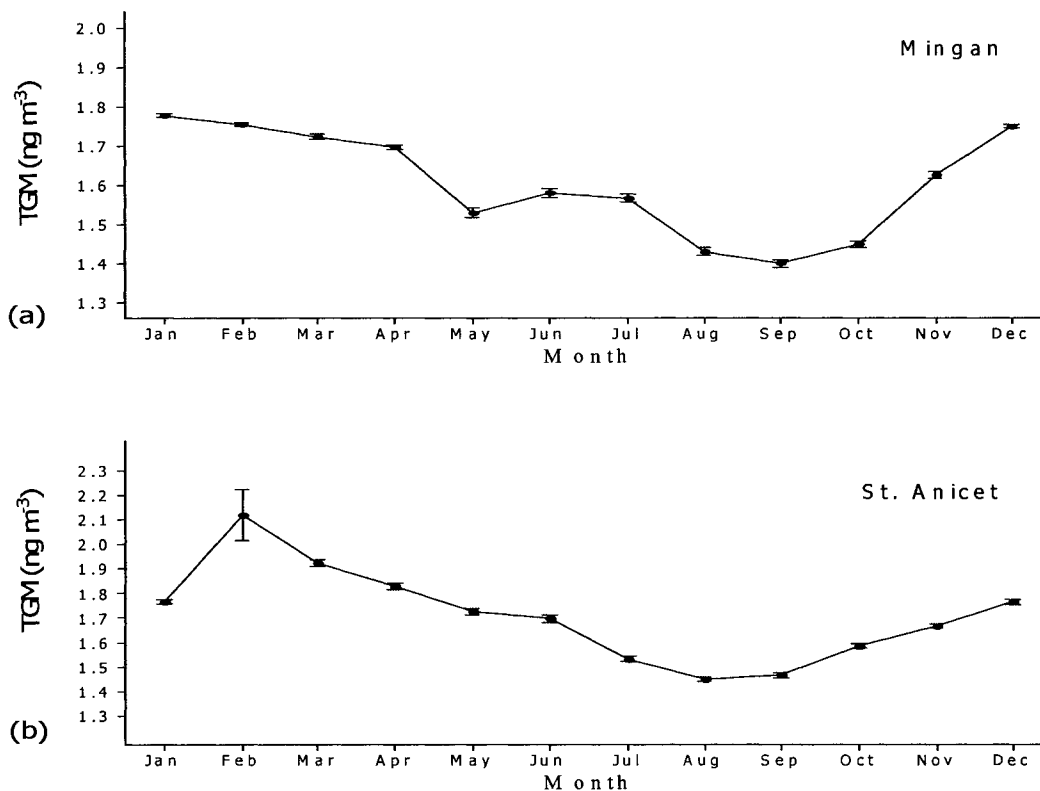


Figure 4.6 Monthly mean of TGM concentrations observed at the two Quebec sites from January, 1997 to December, 1999. (a) Mingan and (b) St. Anicet. The solid circle indicates the monthly mean and the vertical bars indicate 95% CI of mean.

4.2.2 Winter High/Summer High Pattern

The seasonal pattern of Point Petre (Figure 4.5c) was quite different from that of other four sites. High TGM concentrations were observed in late winter, and then decreased in March. However, the monthly mean of TGM remained steadily till May. The three-month nearly constant TGM concentrations led to a seasonal mean of spring to be slightly higher than that of winter. Compare to the summer low pattern observed at the other four sites, a peak occurred in June at Point Petre, and then gradually decreased and

reached the minimum TGM concentration in the middle of fall. The results of *t*-test indicated that the summer peak in TGM concentration (1.98 ng m⁻³ in June) was slightly higher than the winter peak (1.93 ng m⁻³ in February) ($t = 15, p < 0.05$). A similar seasonal pattern was observed at an urban area in Seoul, Korea by Kim and Kim (2001). They concluded that summer high pattern was likely affected by source processes such as nearby TGM emission from soil, water, and vegetation under high temperature.

Seasonally divided wind rose and TGM-rose for Point Petre are shown in Figure 4.7. Overall, westerly winds were prevailing in each season, and northwesterly winds also had high frequency in spring and winter. Seasonally divided TGM-roses in each season are similar to the overall TGM-rose (Figure 4.2f). TGM-roses in spring, fall, and winter were just proportionally reduced/amplified overall TGM-rose. In summer, significantly lower TGM concentrations were observed when air mass came from northeast of Point Petre. In each season, TGM concentrations were significantly high when onshore winds (90^o~270^o) occurred, compare to when winds came from offshore (300^o~60^o). It suggested that Hg emission from Lake Ontario had the year-round influence on the TGM concentration of Point Petre.

TGM-rose does not show that the Hg emission sources of Point Petre were seasonally varied. However, in fall and summer, TGM concentrations with onshore winds were 14% and 16% higher than that with offshore winds, respectively (Figures 4.7f and 4.7g). In spring and winter, TGM concentrations with onshore winds were about 7% higher than that with offshore winds (Figures 4.7e and 4.7h). Compare to the sink modulation observed at the four other sites in summer, high TGM concentrations reflected that source processes dominated in summer at Point Petre. In addition, it

suggested that the Hg evasion from Lake Ontario under high ambient temperature was a primary contributor to High TGM concentration at Point Petre during summertime.

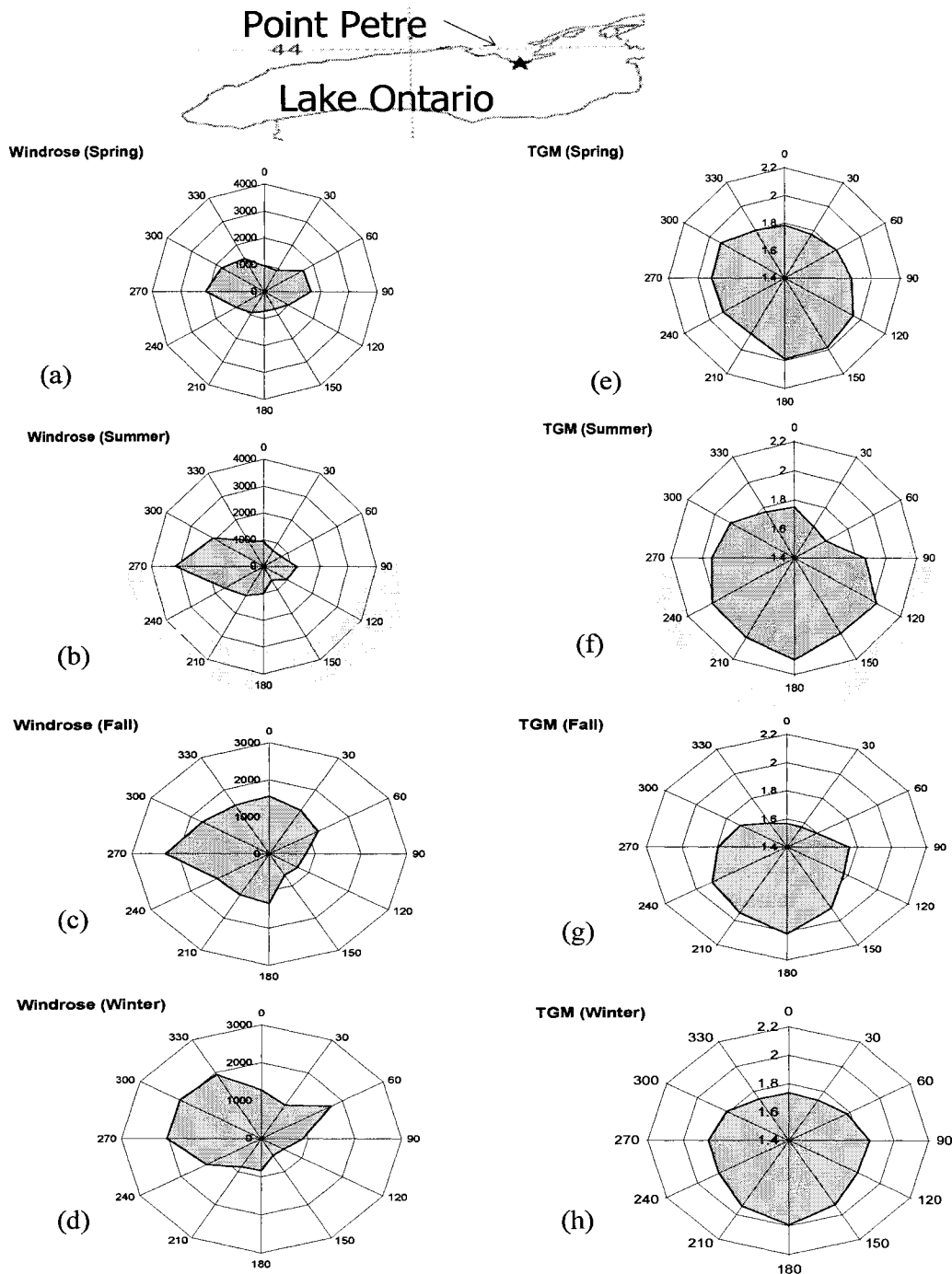


Figure 4.7 Seasonally divided wind rose and TGM-rose at Point Petre during 1998 to 2003. (a)-(d) wind rose, (e)-(h) TGM-rose. The shadow indicates onshore wind direction.

4.3 Diurnal Variability of TGM Concentration

In order to analyze diurnal variability of TGM concentrations, the means of TGM concentrations for each hour were calculated with 95% confidence interval at each site. The means of seasonal subdivided TGM concentrations were calculated for each hour as well. Similar diurnal pattern was observed throughout the five sites except for St. Anicet.

4.3.1 Ontario Sites

The diurnal distribution patterns of TGM concentrations at the three Ontario sites are shown in Figures 4.8~4.10. The minimum TGM concentration was observed during nighttime and early morning, then TGM values increased and approached the maximum near noon. This diurnal pattern appears to be quite opposite to the diurnal pattern observed in European and Asian studies (Lee et al., 1998; Kim and Kim, 2001). They observed the highest TGM concentration occurring at night, and then gradually decreasing during daytime. They concluded that the pattern was characterized as source modulation at night probably due to a shallow nocturnal mixing layer trapped TGM near the surfaces, and then the TGM concentration were diluted during daytime with higher mixing layer.

The observation in this study indicated that TGM diurnal cycle might be characterized as a sink modulation during nighttime. There are two possible reasons leading to this low TGM concentration at night. First, TGM is removed by strong dry deposition under a shallow boundary layer that was formed below inversion layer during nighttime. Second, during dew events at night, RGM may be dissolved into dew water, Hg^0 and $\text{Hg}(\text{p})$ may be deposited onto the surface of dew, and then deposited to the earth's surface (Malcolm and Keeler, 2002). After sunrise TGM concentrations increased

because the shallow boundary layer was broken down, and TGM above the boundary layer mixed down to the surfaces. In addition, Hg emission from the surfaces was enhanced under increased ambient temperature and solar radiation (Poissant and Casimir, 1998). Therefore, TGM concentrations increased during daytime.

A fairly consistent diurnal pattern was observed in each season among the three sites. Among the diurnal cycles of the three sites, TGM concentrations started increasing around 4:00 am in summer, while the increase started around 7:00 am in winter. It indicated that TGM increasing at early morning was likely due to sunrise breaking down the shallow mixing layer, and TGM depletion slowing down. Interestingly slight increases before midnight were observed at Egbert in summer and fall (Figures 4.9c and 4.9d) and at Point Petre in spring (Figure 4.10b), for unknown reasons.

It is also noted that diurnal pattern in summer is more prominent than that in other seasons at the three sites. In summer, high temperature and solar radiation enhancing Hg emission from the surfaces including soil, water, and vegetations lead to higher TGM concentration during daytime. It is a possible reason for the prominent diurnal pattern of TGM concentrations in summer. In addition, stronger diurnal variations of temperature and solar radiation and stronger diurnal cycle of mixing layer development are other possible reasons for the stronger diurnal pattern of TGM concentration in summer.

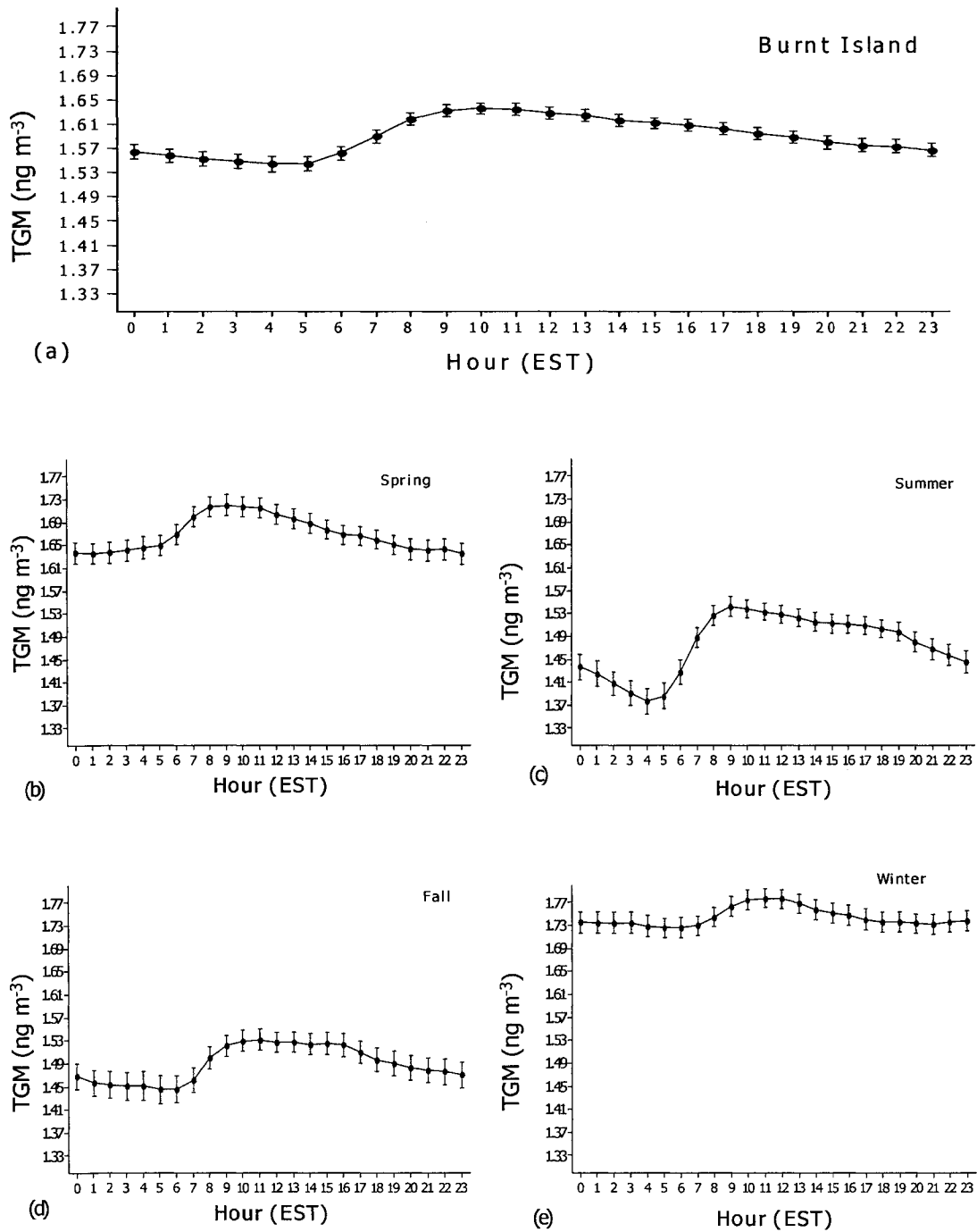


Figure 4.8 Diurnal variability of hourly TGM concentration at Burnt Island. (a) Overall; (b) Spring; (c) Summer; (d) Fall; (e) Winter. Solid circle indicate the mean and the vertical bars indicate 95% CI of mean.

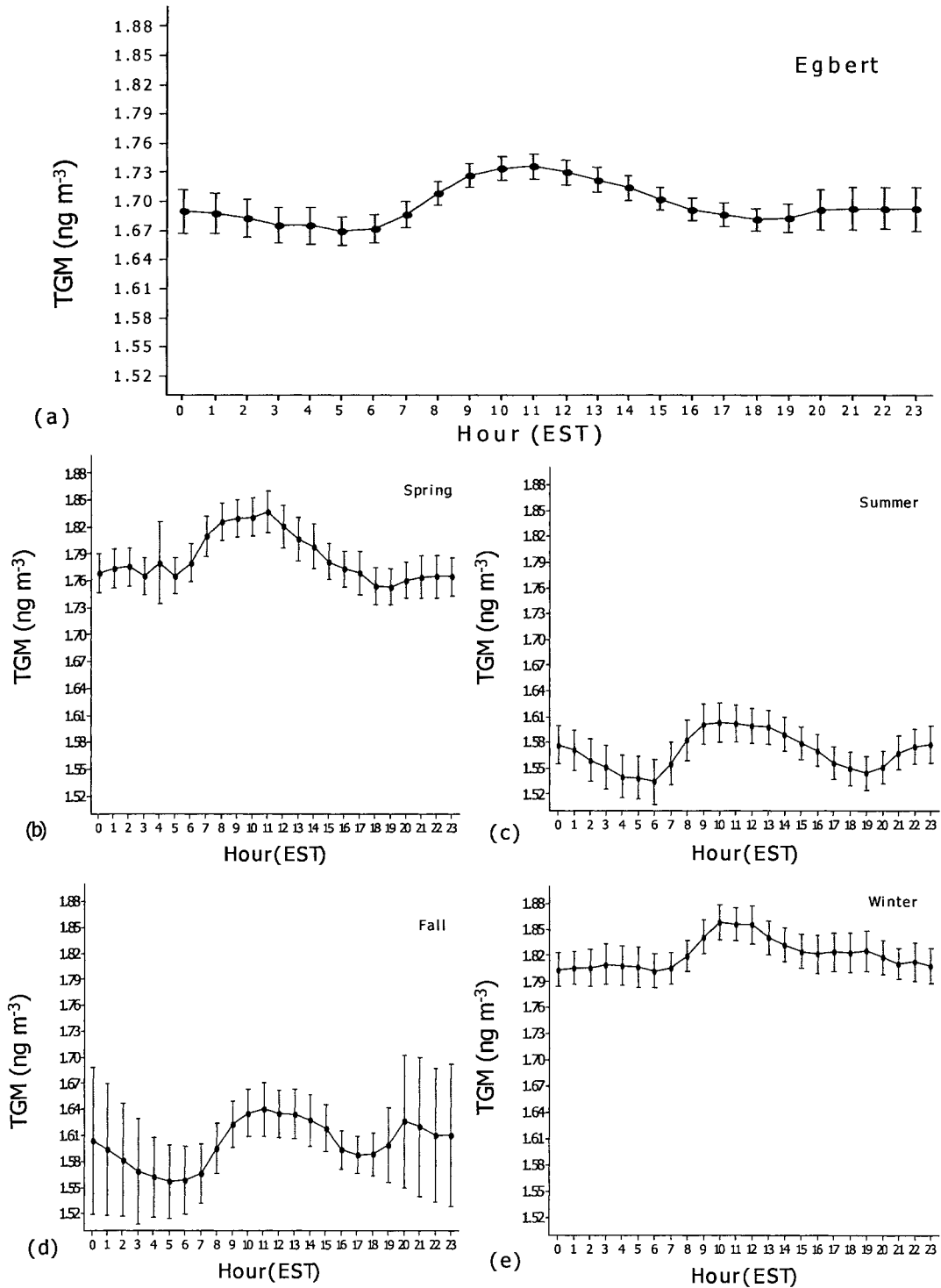


Figure 4.9 Diurnal variability of hourly TGM concentration at Egbert. (a) Overall; (b) Spring; (c) Summer; (d) Fall; (e) Winter. Solid circle indicate the mean and the vertical bars indicate 95% CI of mean.

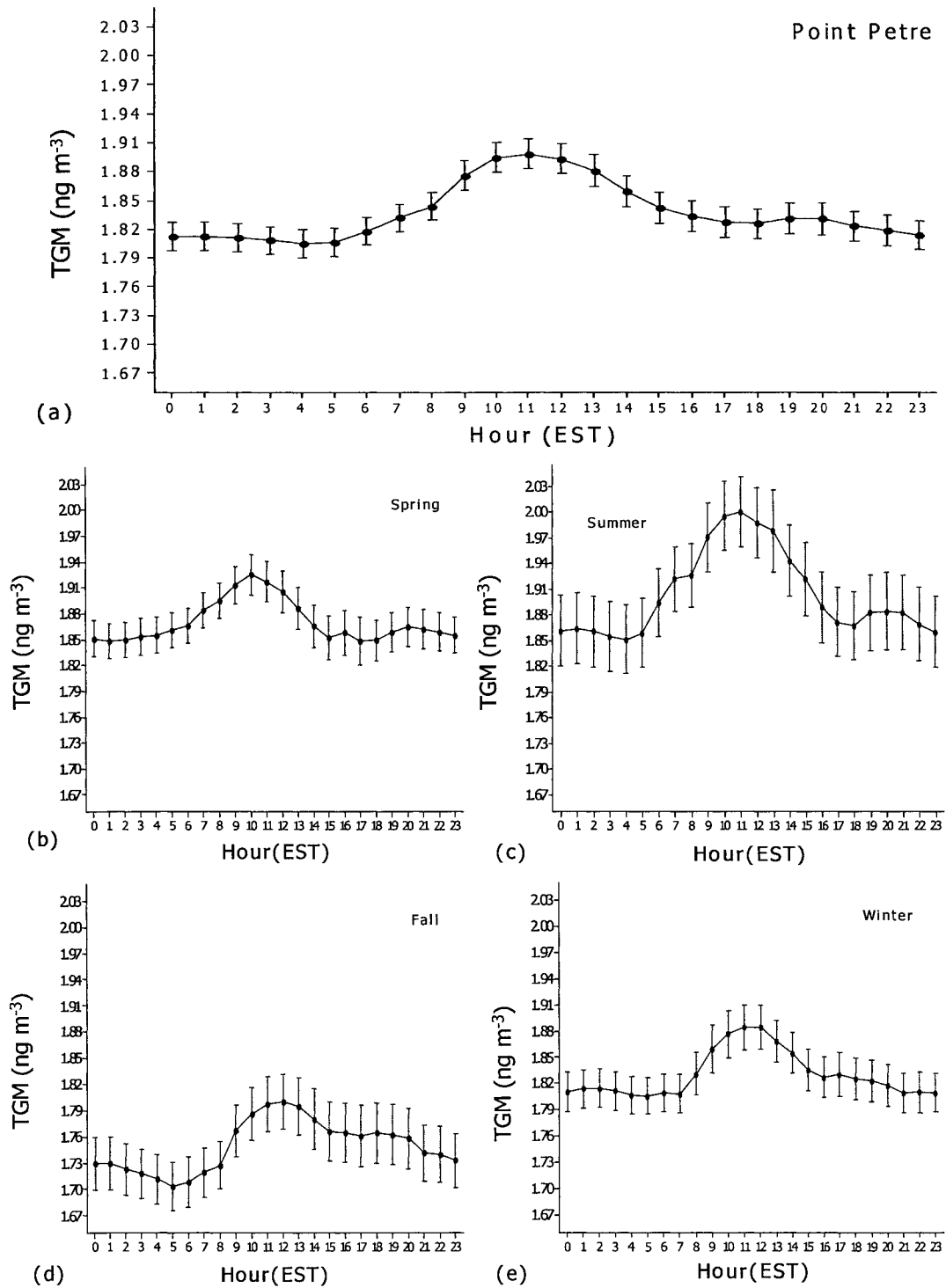


Figure 4.10 Diurnal variability of hourly TGM concentration at Point Petre. (a) Overall; (b) Spring; (c) Summer; (d) Fall; (e) Winter. Solid circles indicate the mean and the vertical bars indicate 95% CI of mean.

4.3.2 Quebec Sites

The diurnal variation of TGM concentrations at Mingan and St. Anicet are shown in Figure 4.11 and 4.12, respectively. At Mingan, the diurnal pattern was similar to the pattern of the three Ontario sites. At Mingan, however, TGM concentration increasing started around 3:00 am, about three hours earlier than that in the three Ontario sites, especially in spring and summer (Figures 4.11b and 4.11c). This earlier TGM increasing is likely because sunrise at the high latitude site (Mingan) occurred earlier than that in the other sites, thus broke down shallow mixing layer and caused the TGM increasing. It can also be seen that TGM concentrations increased much gradually during daytime in each season compare to that in the three Ontario sites, especially in winter, TGM concentrations remained almost stable about 10 hours after reaching the maximum concentration. The prevailing winds from the Gulf of St. Lawrence and marine characteristic such as lower mixing layer at Mingan may contribute to this diurnal pattern of TGM concentrations. Thus, meteorological data will be helpful to explain the diurnal pattern at Mingan.

At St. Anicet, the diurnal pattern was different from that in other four sites (Figure 4.12). The minimum TGM concentration occurred at early morning, afterward, TGM concentration increased rapidly till 9:00 am. After 9:00 am, TGM concentration kept increasing gradually and reached the maximum value around 8:00 pm. Rapid TGM increase before 9:00 am is likely due to shallow boundary layer broken down by sunrise and TGM above boundary layer mixing down to the surfaces. The maximum TGM value at night suggested that local industrial activities, especially from an industrial center 30 km from the site, might impact TGM concentration of St. Anicet. The seasonally divided diurnal patterns were not consistent at this site. In the diurnal pattern of spring (Figure

4.12b), two peaks were observed, one at 9:00 am, another one at 8:00 pm, and the values of two peaks were almost the same. In summer, TGM concentration increasing started at early morning and reached the first peak around noon. The second peak occurred at 10:00 pm, and was higher than the first peak (Figure 4.12c). In the diurnal pattern of winter (Figure 4.12e), TGM concentrations did not present clear diurnal cycle, and TGM concentration at night had large variation compare with that in daytime. Overall, meteorological data as well as more information of local Hg sources and anthropogenic activities are needed to investigate the reasons of the observed diurnal pattern at St. Anicet.

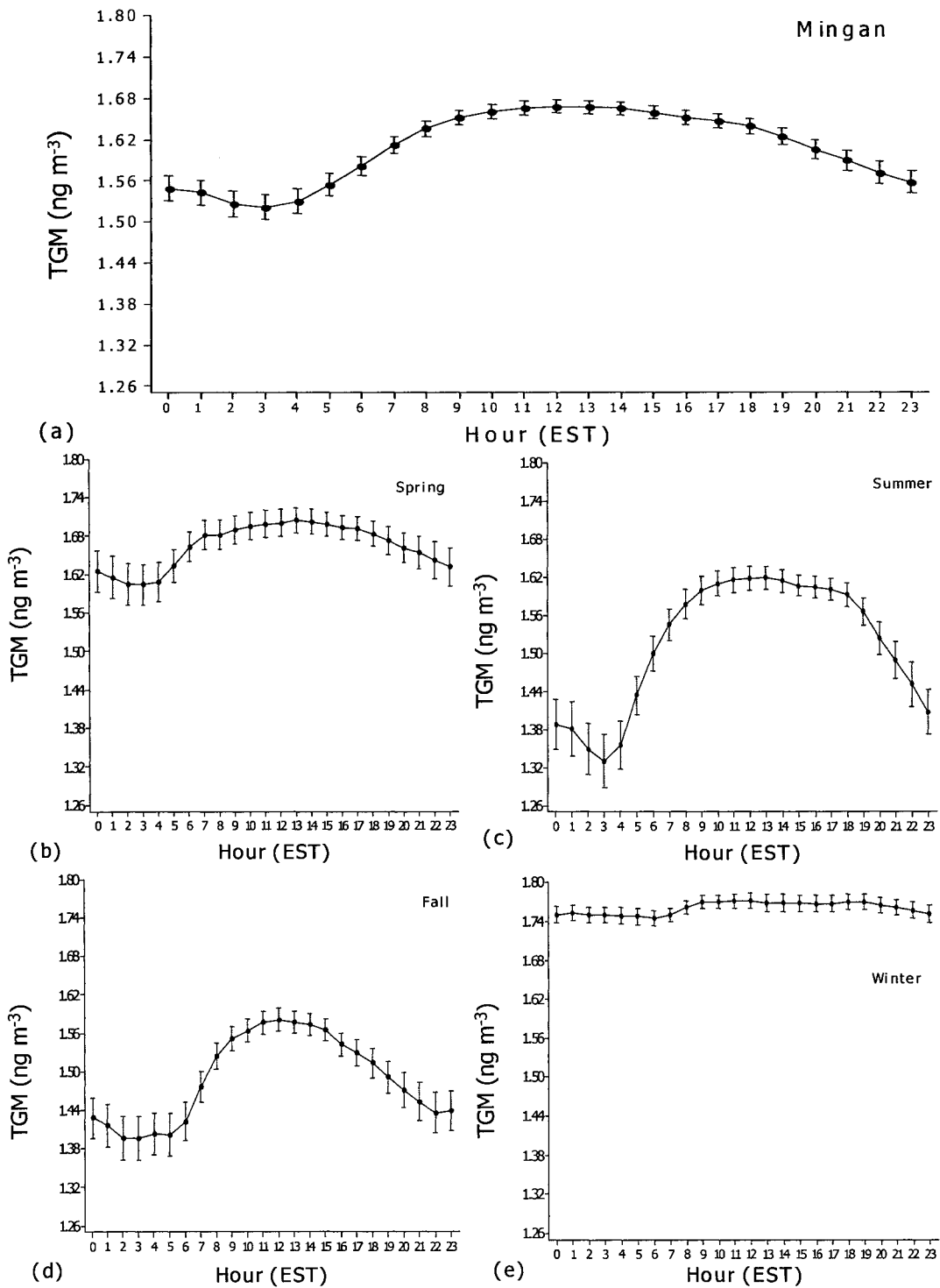


Figure 4.11 Diurnal variability of hourly TGM concentration at Mingan. (a) Overall; (b) Spring; (c) Summer; (d) Fall; (e) Winter. Solid circles indicate the mean and the vertical bars indicate 95% CI of mean.

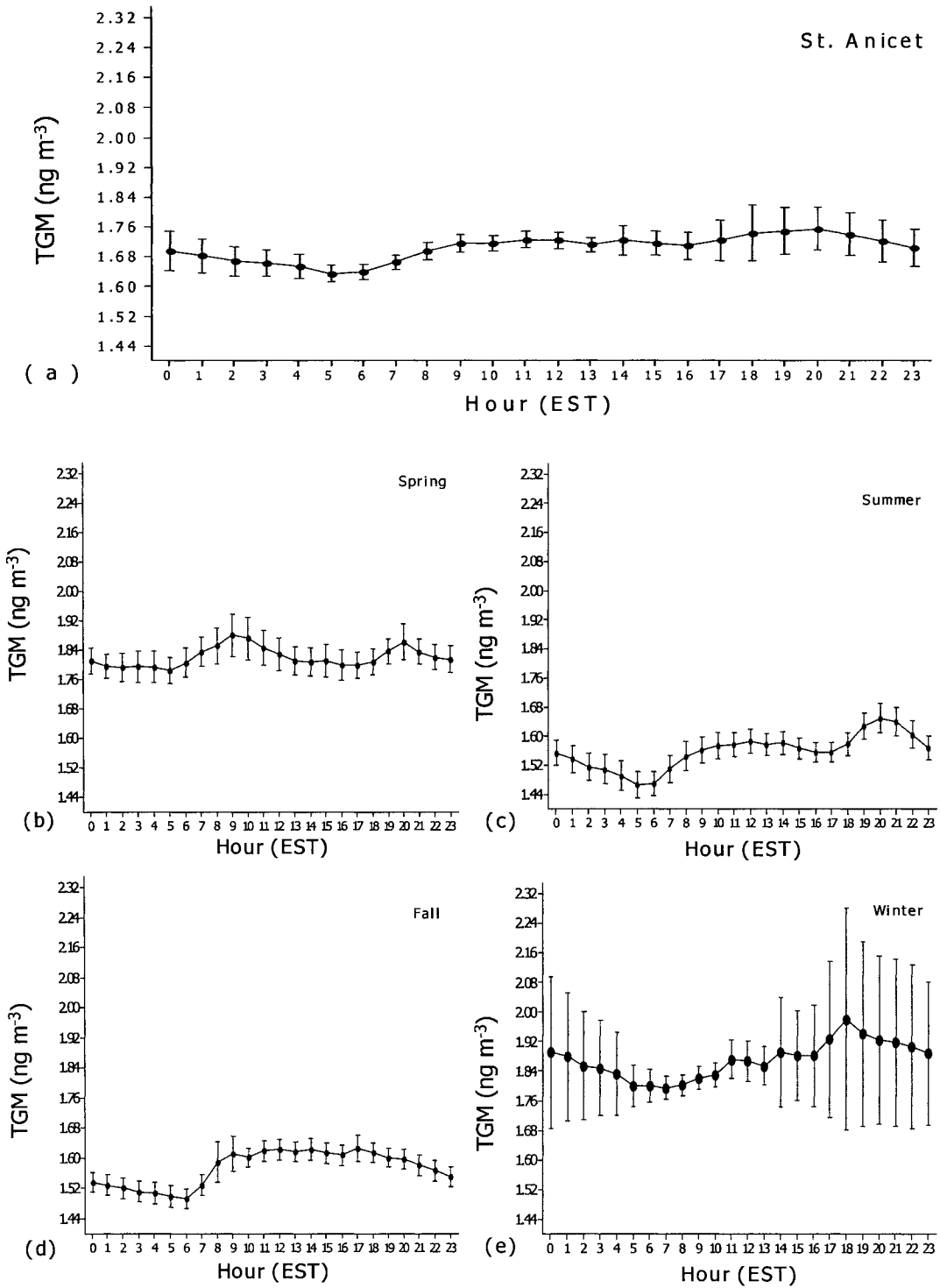


Figure 4.12 Diurnal variability of hourly TGM concentration at St. Anicet. (a) Overall; (b) Spring; (c) Summer; (d) Fall; (e) Winter. Solid circles indicate the mean and the vertical bars indicate 95% CI of mean.

4.4 Correlation Analysis

4.4.1 TGM vs. Meteorological Parameters

The results of Pearson correlation coefficients (r) are listed in Table 4.5. A significant negative correlation between TGM concentrations and ambient temperature was found at Burnt Island and Egbert, while a near-zero r -value was detected at Point Petre. Such result appears to be comparable with the TGM-temperature correlation in some other TGM studies (Poissant, 2000; Blanchard et al., 2002). It is also noticed that TGM-temperature correlations in each season and the overall correlation did not present consistency. TGM concentrations and temperature were positively correlated in most seasons at the three Ontario sites except for a small negative value at Burnt Island during springtime. In all three Ontario sites, TGM-temperature correlations in summer and winter were relatively stronger than that in spring and fall. Apparently, correlation derived from the whole data set is different from the correlations derived from the seasonally grouped data. It is likely due to the effects of non-meteorological factors such as increasing coal combustion in winter and stronger wet deposition in summer.

A positive correlation between TGM concentrations and solar radiation are expected since solar radiation enhancing Hg emissions from the surfaces (water, soil, and vegetations) and leading to TGM increase. However, weak or near-zero correlation coefficients were observed in most seasons at the three sites. Large amount of data may mask the correlation between TGM and solar radiation. In Kim and Kim (2001), weak negative but significant correlation was found between TGM and Solar radiation, although no explanation was given in their report. The size of their dataset was comparable to that in this study. Two 48-hour datasets at Egbert were also used to

investigate the correlation between TGM and solar radiation as shown in Figure 4.13. The results were quite different for the two periods. The level of solar radiation was consistent compare to the variation of TGM. During August 1~2, 2002, the correlation was negative ($r = -0.30, p < 0.1$) (Figure 4.13a). In Figure 4.13a, it can be seen that the variations of TGM and solar radiation under the shadow area led to the negative correlation. TGM concentration started increasing at 3:00 pm August 1st while solar radiation was decreasing. However, the main reason for TGM increase was rapidly decreased wind speed slowing down the atmospheric mixing. At 10:00 am August 2nd, 2002, TGM concentration started decreasing while solar radiation was increasing, and this TGM decrease was likely due to increased wind speed enhancing the atmospheric mixing. During August 1~2, 2002, TGM concentration had negative correlation with wind speed ($r = -0.50, p < 0.05$). It suggested that wind speed had significant effects on TGM concentrations during that period of time. On the other hand, during June 19~20, 2002, TGM concentrations had positive correlation ($r = 0.43, p < 0.05$) with solar radiation (Figure 4.13b). When combine the two datasets together, the correlation between TGM concentration and solar radiation decreased to 0.16 ($p < 0.23$). Overall, it suggested that solar radiation might have effects on TGM concentrations, and on some days, however, the effects of solar radiation could be masked by other factors. Thus, correlation analysis using a large dataset may not show the expected association between TGM and solar radiation.

Weak but significant negative correlations between TGM concentration and pressure were observed at most sites. Positive correlations between TGM concentrations and wind speed were observed at Burnt Island and Egbert. In summary, individual

meteorological parameter did not present strong effects on the variation of TGM concentration, and it is because that the correlation is masked by other factors. In addition, the large dataset in this study might diminish the correlation between TGM concentration and meteorological parameters.

Table 4.4 Results of correlation between TGM concentrations and meteorological parameters at the three Ontario sites. Solar radiation less than 50 W m⁻² have been excluded.

		Temperature	Wind speed	Solar radiation	Pressure
Bunrt Island	All	-0.261	0.219	-0.031	-0.165
	Spring	-0.023*	0.091	-0.021*	-0.195
	Summer	0.413	0.155	0.124	-0.224
	Fall	0.041	0.272	-0.043	-0.284
	Winter	0.244	0.071	0.03	-0.139
Egbert	All	-0.219	0.098	-0.069	-0.077
	Spring	0.129	0.001*	-0.032	0.020
	Summer	0.281	0.104	0.021	-0.147
	Fall	0.138	-0.115	0.001*	-0.137
	Winter	0.238	0.067	0.040	-0.108
Point Petre	All	0.022	-0.027	0.015	-0.120
	Spring	0.163	-0.156	-0.055	-0.150
	Summer	0.291	0.040	0.069	-0.232
	Fall	0.172	0.131	-0.002*	-0.087
	Winter	0.309	-0.072	0.02*	-0.087

* Pearson correlation is NOT significant at $\alpha < 0.05$.

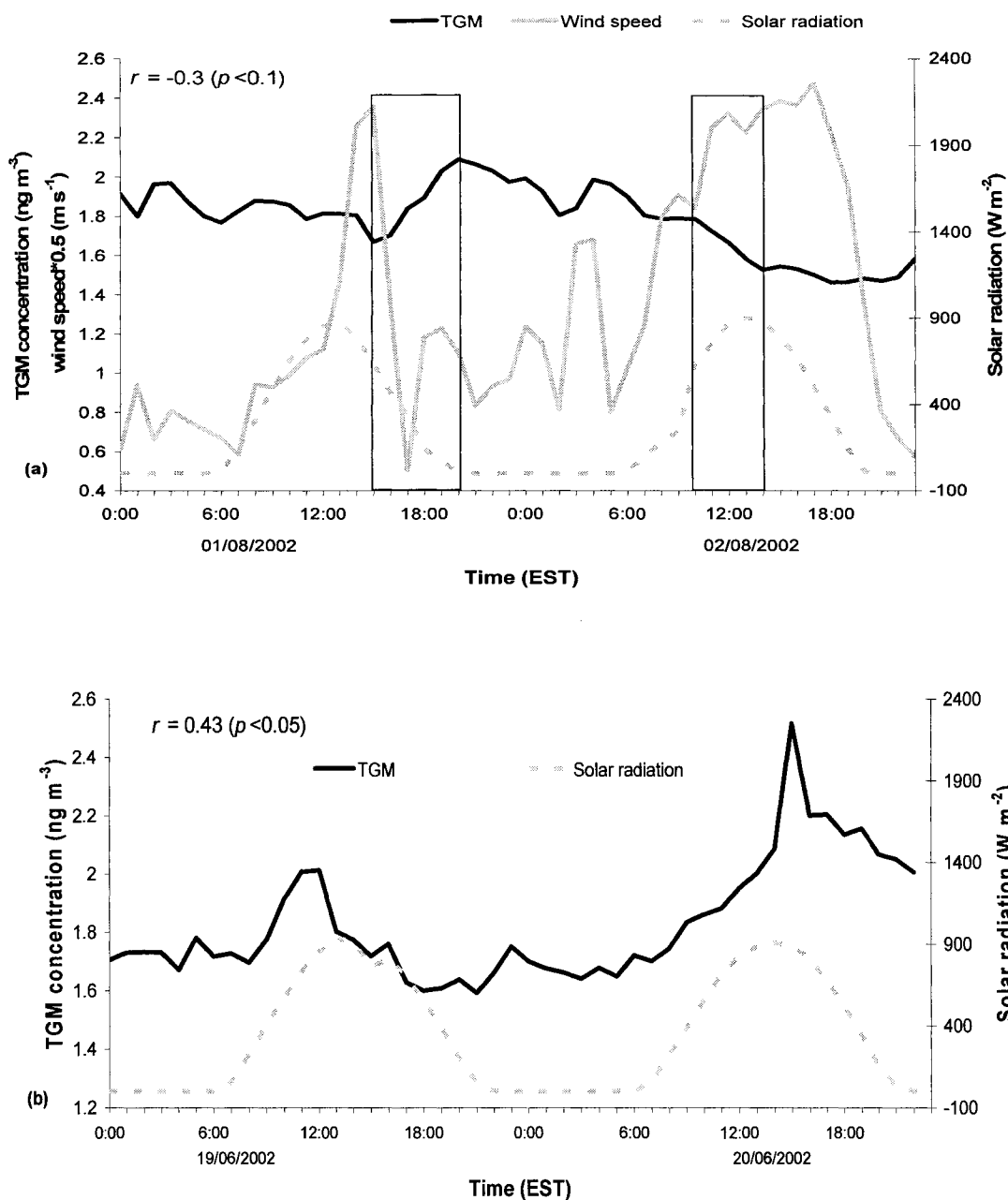


Figure 4.13 Time series of TGM concentration, solar radiation and wind speed (August 1~2) at Egbert (a) August 1~2, 2002 (b) June 19~20, 2002. r is the correlation coefficient between TGM and solar radiation, cut-off of 50 W m^{-2} for solar radiation.

4.4.2 TGM vs. Hg Wet Deposition

Correlations between weekly TGM concentration, weekly Hg concentration in precipitation, and wet deposition rate of Hg were evaluated at the three Ontario sites using measurements in 2002. The results of Pearson r are shown in Table 4.6. Only at Burnt Island, weekly TGM had weak negative correlation with Hg in precipitation at the given significance level ($p < 0.05$). Overall, the insignificant or weak correlations between TGM and wet deposition of Hg at the Ontario sites suggests that wet deposition of atmospheric Hg, primarily RGM and Hg(p), does not have significant influence to the ambient TGM level. It is likely because that RGM and Hg(p) are small portion (e.g. 3%) of TGM (Lingberg and Stratton, 1998).

Table 4.5 Results of correlation between TGM concentrations and total Hg in precipitation and wet deposition rate of Hg at the three Ontario sites in 2002.

	Weekly mean of TGM concentrations		
	Burnt Island	Egbert	Point Petre
Weekly concentration of Hg in precipitation	-0.319 (N = 44)	0.059 ^{NS} (N = 45)	-0.025 ^{NS} (N = 44)
Weekly deposition rate of Hg	-0.262 ^{NS} (N = 44)	-0.112 ^{NS} (N = 45)	-0.251 ^{NS} (N = 44)

Note: All data are natural logarithm transformed since data are log-normally distributed. (NS: Not significant at $\alpha < 0.05$)

4.5 Trend Analysis

Trend analysis of TGM concentrations was conducted for the three Ontario sites using the Curvefit. Seven years (1997 to 2003) data were used in Egbert and Point Petre, and six years (1998 to 2003) data were used in Burnt Island. The 6-year trend of TGM observed at Burnt Island and the 7-year trends observed at Egbert and Point Petre are shown in Figures 4.14, 4.19, and 4.20, respectively

4.5.1 Six-year Trend of TGM for Burnt Island

Multiple-comparison of yearly TGM concentration indicated that there was a slight decreasing trend of TGM concentrations from 1.59 ng m⁻³ of year 1998 to 1.52 ng m⁻³ of year 2001. TGM concentration of year 2002 increased significantly ($p < 0.05$) 11% relative to that of year 2001, reaching a yearly TGM concentration of 1.68 ng m⁻³. In 2003, TGM concentration decreased 6% ($p < 0.05$) from 2002. TGM concentration of year 2003 was 1.58 ng m⁻³, almost the same as in 2001.

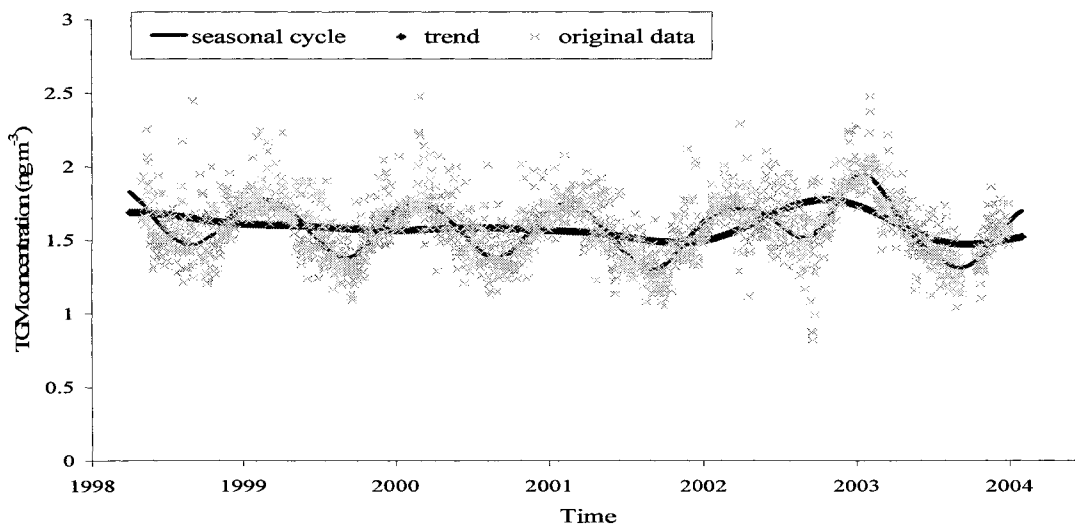


Figure 4.14 Trends and seasonal cycles of TGM concentrations for Burnt Island from May 1998 to December 2003.

In 2002, TGM concentrations presented abnormal seasonal variation compared to that in 2001 and 2003, especially in April-September period as well as in October-December period. Intra-annual variation of TGM concentration in 2001, 2002, and 2003 are shown in Figure 4.15. In 2002, TGM concentration did not decrease gradually from February as in 2001 and 2003. Instead, TGM concentrations remained steadily till July,

except for a slight decrease in April. The minimum monthly TGM concentrations were observed in September in the three years, and values were 1.24 ng m^{-3} , 1.47 ng m^{-3} , and 1.25 ng m^{-3} in year 2001, 2002, and 2003, respectively. Unlike year 2001 and 2003, monthly TGM concentration of December was the highest value in 2002.

Monthly precipitation and ambient temperature at Burnt Island in 2001, 2002, and 2003 are shown in Figure 4.16. Mann-Whitney test indicated that precipitations in August and September of year 2002 were significantly lower than in 2001 and 2003 ($p < 0.05$). It is also noticeable that monthly temperatures of August and September of year 2002 were higher than that of year 2001 and 2003 ($p < 0.05$). High temperature enhanced Hg emission from the surfaces and less precipitation indicated the absence of wet deposition. Thus, high temperature and drought condition led to higher TGM concentrations in August and September of year 2002 (1.53 and 1.47 ng m^{-3}), which were about 12~17% higher than the concentrations of these two months in 2001 and 2003. Temperature and precipitation during May to July showed the similar pattern in the three years, which could not explain why TGM concentrations remained almost constant during May to July in 2002.

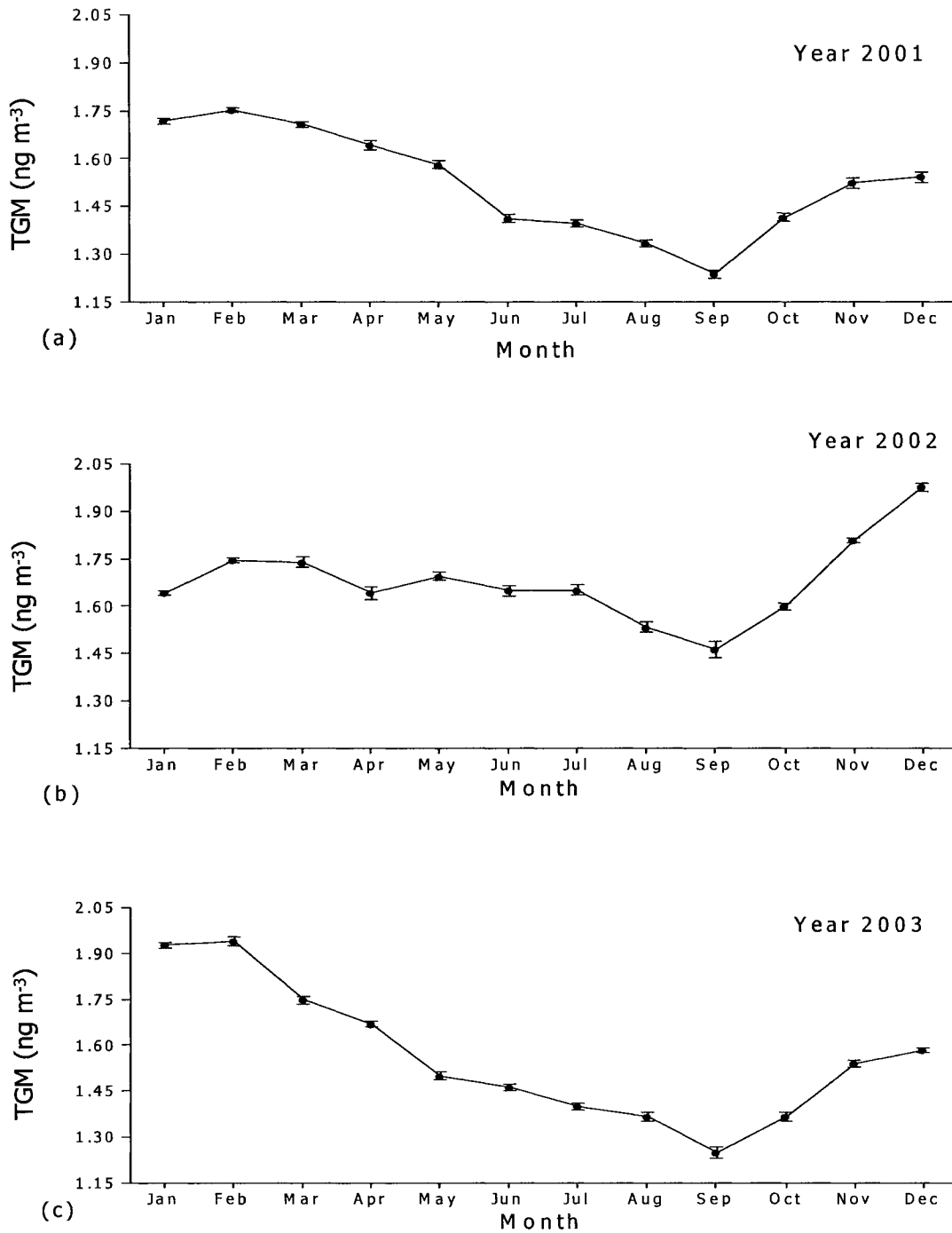


Figure 4.15 Monthly TGM concentrations at Burnt Island. (a) 2001; (b) 2002; (c) 2003

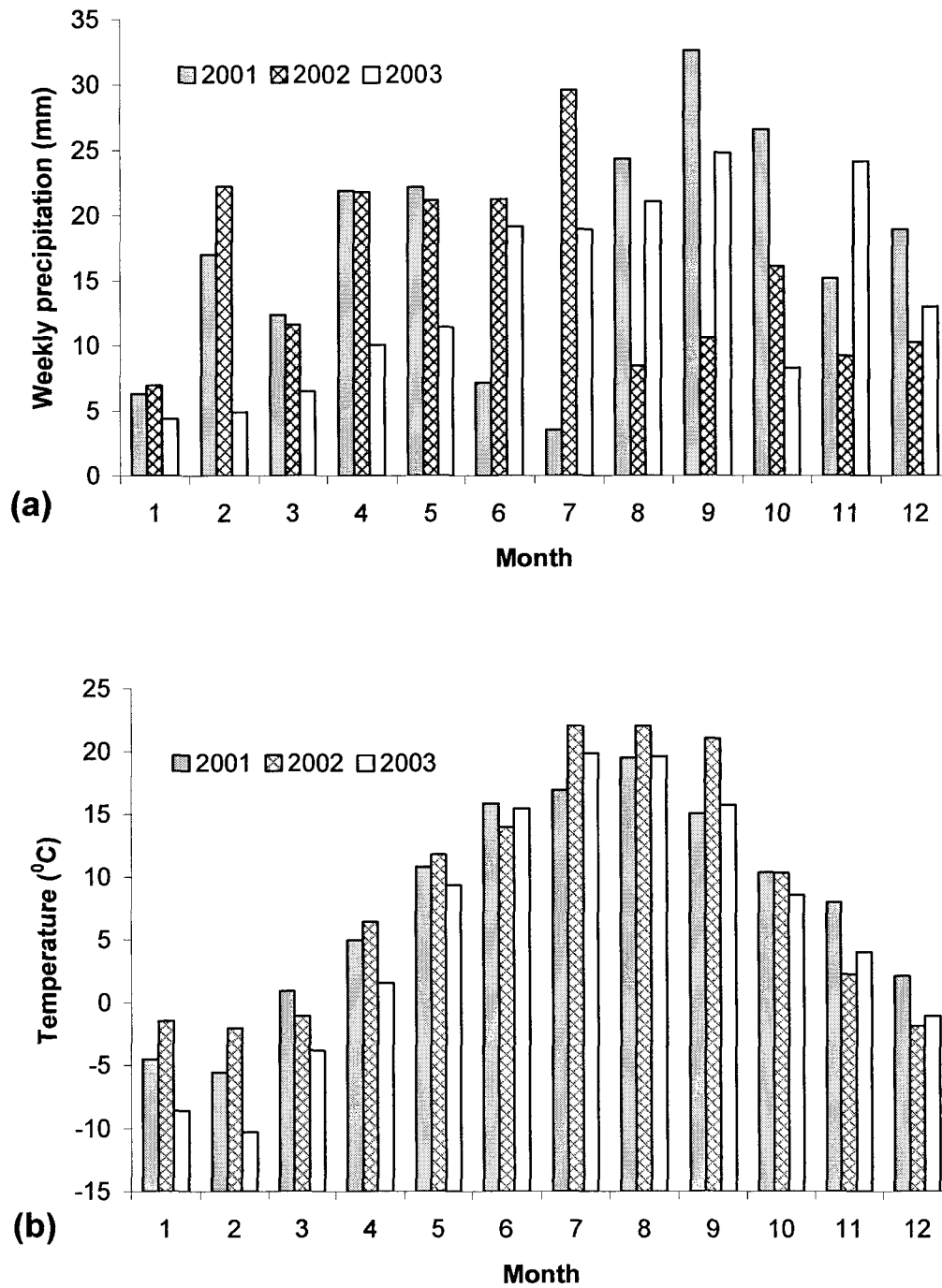


Figure 4.16 Monthly precipitation (a) and temperature (b) at Burnt Island between 2001 and 2003

According to the discussions in previous sections, the moderate-weak correlations between temperature and TGM concentration were observed in various seasons at this site. However, Mann-Whitney test indicated that there was no significant difference between monthly temperatures in 2001 and 2002 ($p < 0.88$), and temperature of year 2003 was significantly lower than that of year 2002 ($p < 0.05$). It suggested that ambient temperature was not the dominant factor for this TGM concentration increase in 2002. Thus, other factor such as nearby Hg emission should be investigated to interpret this TGM increase.

Wind rose and TGM-rose were analyzed in 2001-2003, as well as in April-September and October-December periods in the three years to investigate this variation. Northwesterly winds were prevailing winds at Burnt Island in the three years (Figure 4.17). Southeasterly winds had high frequency during April-September period in all three years (Figure 4.18), and northwesterly winds dominated during October-December period in all three years (Figure 4.19). The TGM roses of whole year, April-September period and October-December period (Figures 4.17, 4.18, and 4.19) showed similar pattern in all three years. Overall, TGM-roses did not indicate that Hg inputs from a particular direction contributed to the TGM increase in 2002.

In 2002, no elevated TGM concentrations were observed at Egbert and Point Petre, which are located 300 km and 500 km east of the site, respectively. However, at Eagle Harbor, 470 km west of Burnt Island, yearly TGM concentrations of 2 ng m^{-3} were observed in 2002, compared to $1.4\text{-}1.6 \text{ ng m}^{-3}$ TGM value in other years (Gildemeister et al., 2003). They concluded that TGM concentrations rose when atmospheric transport was from Thunder Bay, Ontario, Southern Minnesota, Northwestern Wisconsin, and from

the land on the south/southwestern shore of Lake Michigan. However, from TGM roses of Burnt Island in this study, no evidence showed any of those areas particularly contributed to the TGM increase in 2002 at Burnt Island.

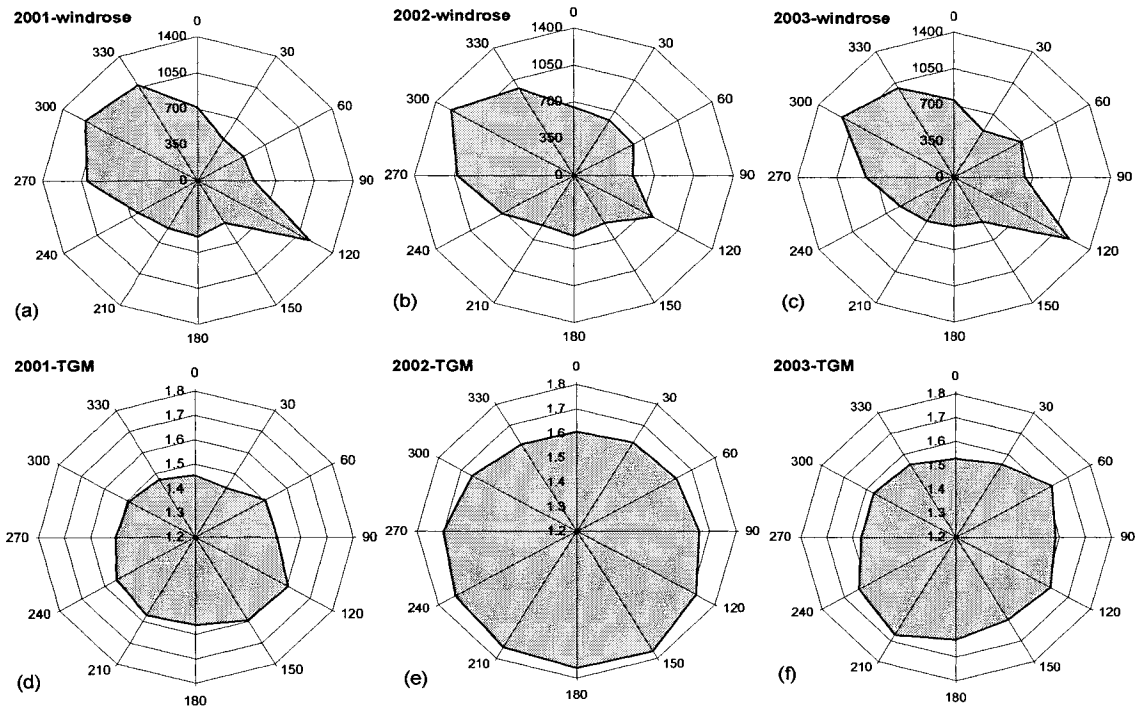


Figure 4.17 Wind rose and TGM rose at Burnt Island in 2001 to 2003. (a)-(c) Wind rose in 2001, 2002, and 2003. (d)-(f) TGM-rose in 2001, 2002, and 2003.

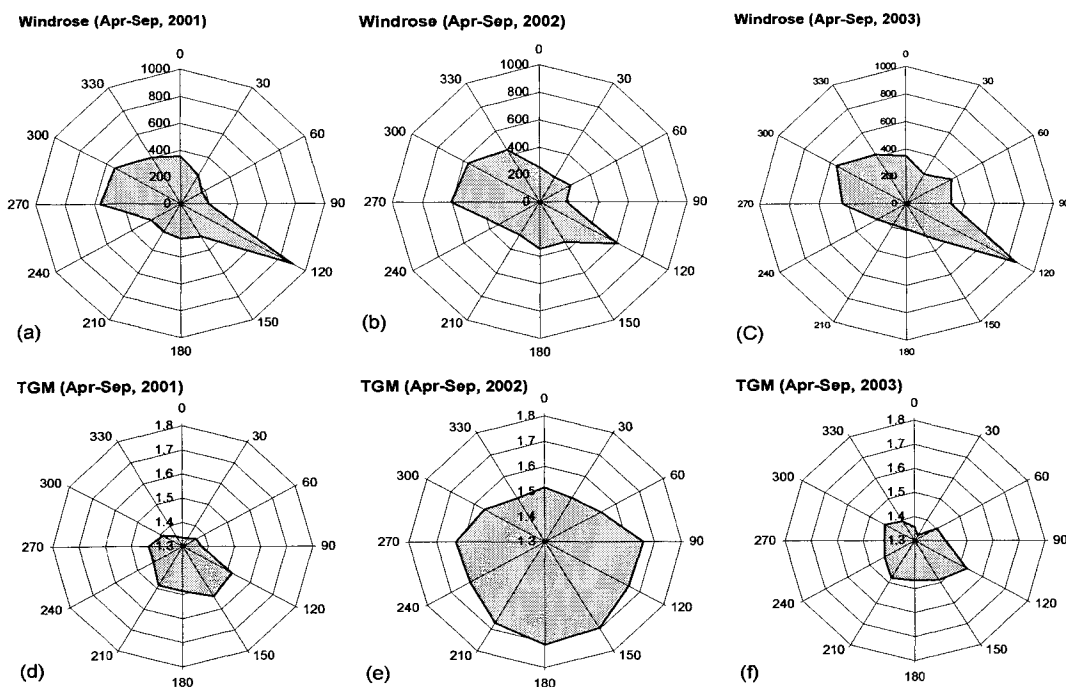


Figure 4.18 Wind rose and TGM rose at Burnt Island during April-September period of 2001 to 2003. (a)-(c) Wind rose, (d)-(f) TGM rose.

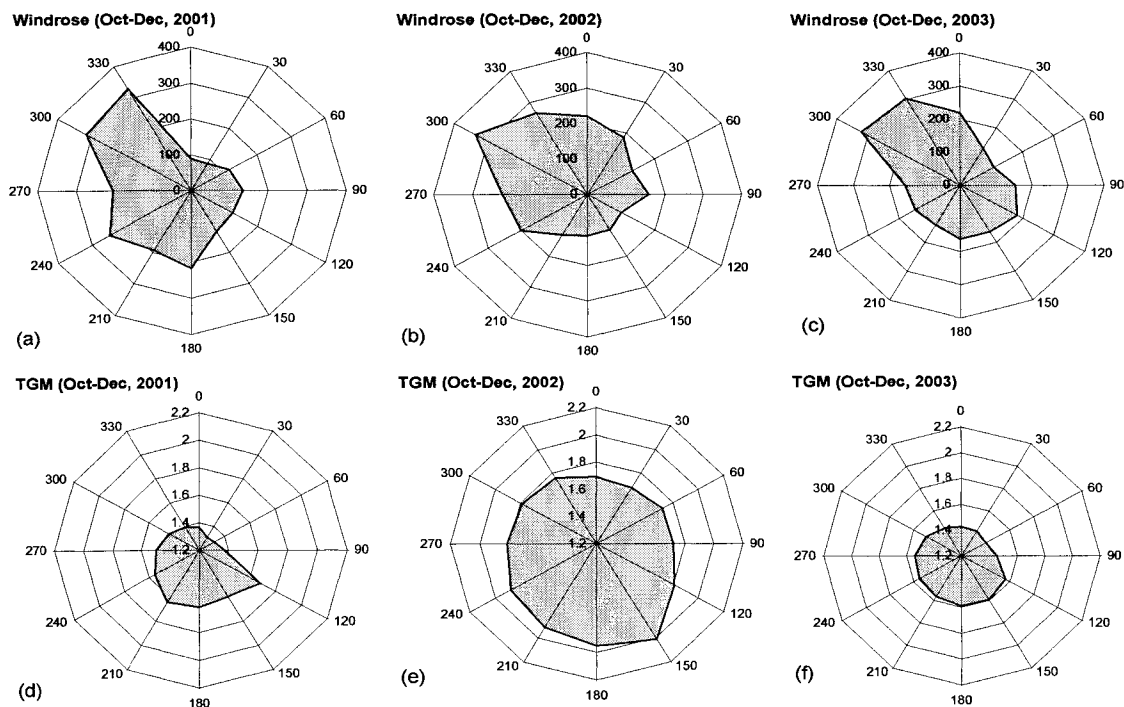


Figure 4.19 Wind rose and TGM rose at Burnt Island during October-December period in 2001 to 2003. (a)-(c) wind rose, (d)-(f) TGM rose.

Areas north/northeast of Burnt Island are a major forest area in Ontario.

According to a report by Ministry of Natural Resource (MNR, 2003), the burnt area of forest fires in Ontario in year 2002 was 173,200 hectares, compare to 26,000 hectares in 2001. During forest fire season (April to September), the ratio of TGM concentration in north (forest areas) and south in 2002 was slightly higher than that in 2001 and 2003. It suggested that forest fires might have effects on the TGM increase in 2002. However, due to lack of forest fire data, no quantitative association between forest fires and TGM concentrations could be made in this study. Detailed information of forest fires in 2002, such as time and location of fire occurrences and burnt areas may provide an explanation for this observation at Burnt Island.

4.5.2 Seven-year Trends of TGM for Egbert and Point Petre

As shown in Figures 4.20 and 4.21, no clear trend for Egbert and Point Petre was observed in the seven-year period, same as the results of the trend analysis for these two sites conducted by Blanchard et al. (2002) using the same technique and four-year data (1997 to 2000). Therefore, three years more data did not change the trend of TGM for these two sites. It is likely due to Canadian Hg emissions have remained steady somewhere around 10 ton yr⁻¹ after 1995 (Pilgrim et al., 2000).

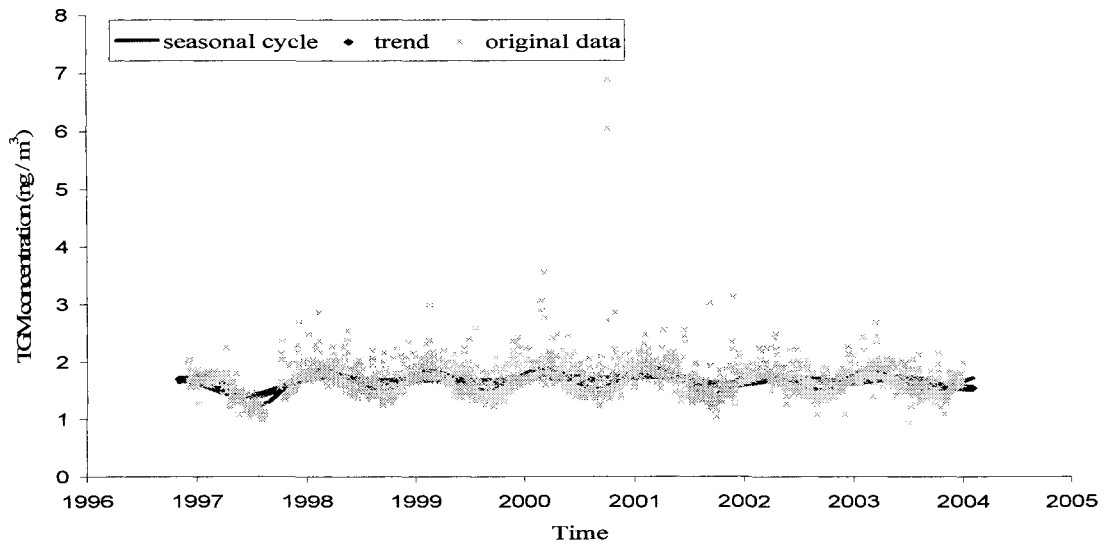


Figure 4.20 Trends and seasonal cycles of TGM concentrations for Egbert from January 1997 to December 2003

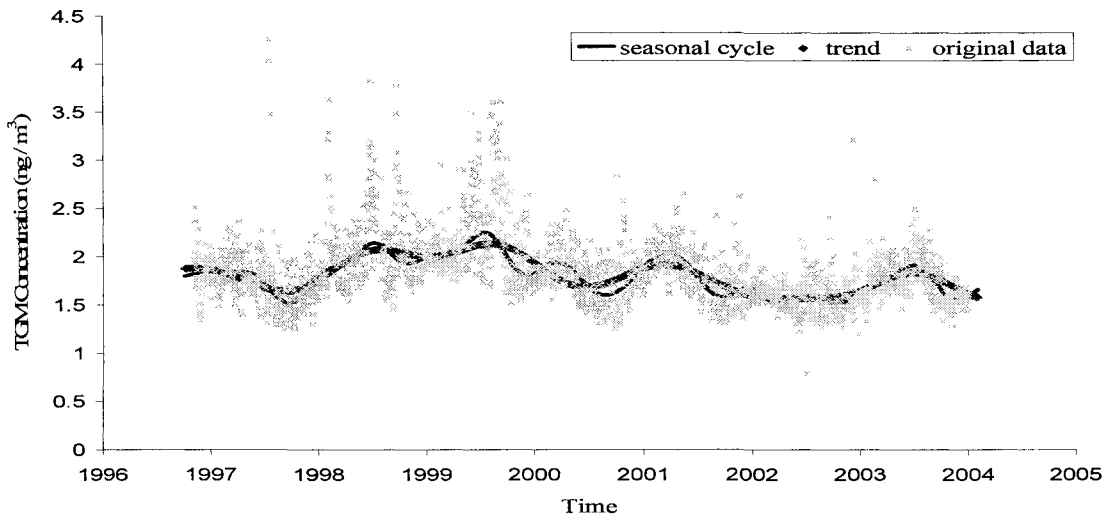


Figure 4.21 Trends and seasonal cycles of TGM concentrations for Point Petre from January 1997 to December 2003

4.6 Investigation of Source-Receptor Relationship

4.6.1 High TGM Concentration Episodes

Table 4.7 lists the high TGM concentration episodes which were identified using the statistical method discussed in Chapter 3. Briefly, the difference between monthly mean and median of TGM were calculated, then zoomed into the time series of the month contained large mean-median difference to identify the high TGM episode. No high TGM episode was found at Mingan. The outliers identified by the digital filter (Curvefit) were used as cross-references to identify high TGM concentration episodes at the three Ontario sites (Table 4.8). Point Petre has more high TGM concentration episodes than the other two Ontario sites, especially in 1998 and 1999. The total number of episodes identified by DF was more than the number identified by statistical methods. In the DF method, outliers were identified by 3 times standard errors from fitting curve, which contains the seasonal variation. On the other hand, the statistical method does not consider the seasonal variation. Therefore, the total number of high TGM episode identified by DF was more than by the statistical method. Interestingly, four consecutive low outlier of daily TGM concentration were identified by DF during September 14 to September 17, 2002 at Burnt Island, and daily TGM concentration were below 1 ng m^{-3} . Lower temperature and the occurrence of rainfall were observed during that period of time, and it may be the main reason of the low TGM concentrations.

Table 4.6 High TGM concentration episodes identified by statistical methods.

Start date, time	End date, time	Site	TGM concentration during the episodes (ng m ⁻³)		
			Max.	Min.	Mean
1999-2-1, 20:00	1999-2-2, 21:00	Burnt Island	2.66	1.74	2.2
1999-2-11, 1:00	1999-2-12, 4:00	Burnt Island	2.67	1.64	2.18
2000-2-25, 14:00	2000-2-25, 22:00	Egbert	5.41	2.27	3.77
2000-10-1, 18:00*	2000-10-2, 11:00	Egbert	25.82	1.64	10.58
1997-7-16, 6:00	1997-7-18, 23:00	Point Petre	8.5	1.41	2.32
1998-2-1, 0:00	1998-2-3, 5:00	Point Petre	4.17	2.59	3.38
1998-9-19, 2:00	1998-9-20, 23:00	Point Petre	5.67	2.58	3.65
1999-8-7, 7:00	1999-8-7, 23:00	Point Petre	3.91	1.84	3.54
2000-10-1, 4:00*	2000-10-2, 5:00	Point Petre	4.54	1.73	2.67
1999-2-15, 12:00	1999-2-16, 9:00	St. Anicet	53.08	1.6	24.35

* These two episodes have been reported by Blanchard et al. (2002).

Table 4.7 The number of high TGM concentration episodes identified by the digital filter (Curvefit).

	Total	1997	1998	1999	2000	2001	2002	2003
Burnt Island	17	N/A	5	3	5	2	1	1
Egbert	22	2	2	3	9	5	0	1
Point Petre	51	3	17	24	2	2	2	1

4.6.2 HYSPLIT Trajectory and Box Model Application

According to previous discussion, Lake Ontario may play an important role in the seasonal variation of TGM concentrations at Point Petre. One high TGM episode identified by the digital filter was used in the HYSPLIT backward trajectory and box model simulation to investigate the effects of Hg emission from Lake Ontario on TGM concentrations at Point Petre.

On August 7, 1999, the TGM concentration increased from 1.84 ng m^{-3} at 7:00 am to 3.91 ng m^{-3} at 4:00 pm at Point Petre. Trajectories showed the air mass mainly from north-northwest of Point Petre before 8:00 am, and wind direction was $330^{\circ}\sim 350^{\circ}$. After 8:00 am, wind directions changed to $190^{\circ}\sim 290^{\circ}$, i.e. the air mass travelling above the lake before arriving at Point Petre. The trajectories arrived at 8:00 am and at 4:00 pm are shown in Figure 4.22 as examples. The trajectory arrived at 8:00 am had travelled five hours over Lake Ontario before reaching Point Petre, and TGM concentration at Point Petre increased from 1.84 ng m^{-3} (7:00 am) to 2.4 ng m^{-3} (8:00 am). TGM concentration reached the maximum of 3.91 ng m^{-3} at 4:00 pm, and the trajectory arrived at 4:00 pm had travelled 16 hours above the lake before reaching the site. According to the methodology of box model application discussed in Chapter 3, five boxes were set along with the trajectory arrived at 8:00 am, and 16 boxes were set along with the trajectory arrived at 4:00pm. For other hours during the episode, boxes were set up along the corresponding trajectory based on how many hours the trajectory had travelled over the lake.

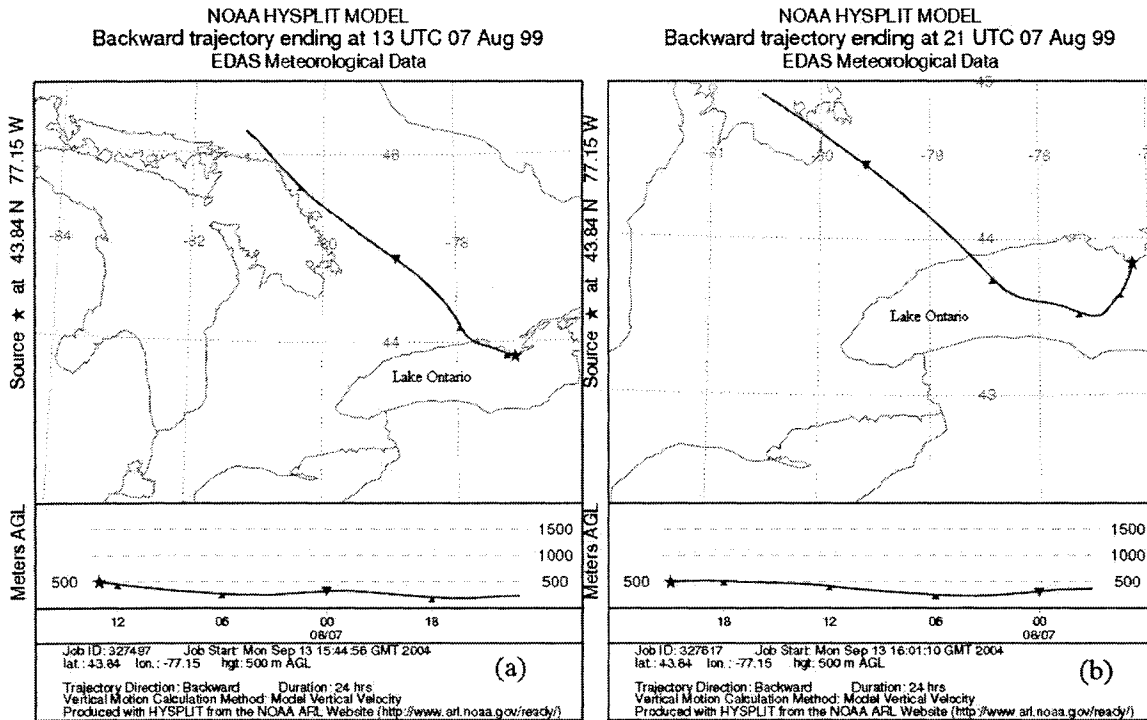


Figure 4.22 Twenty-four-hour backward trajectories at Point Petre calculated by HYSPLIT model. (a) 8:00 am, August 7, 1999; (b) 4:00 pm, August 7, 1999.

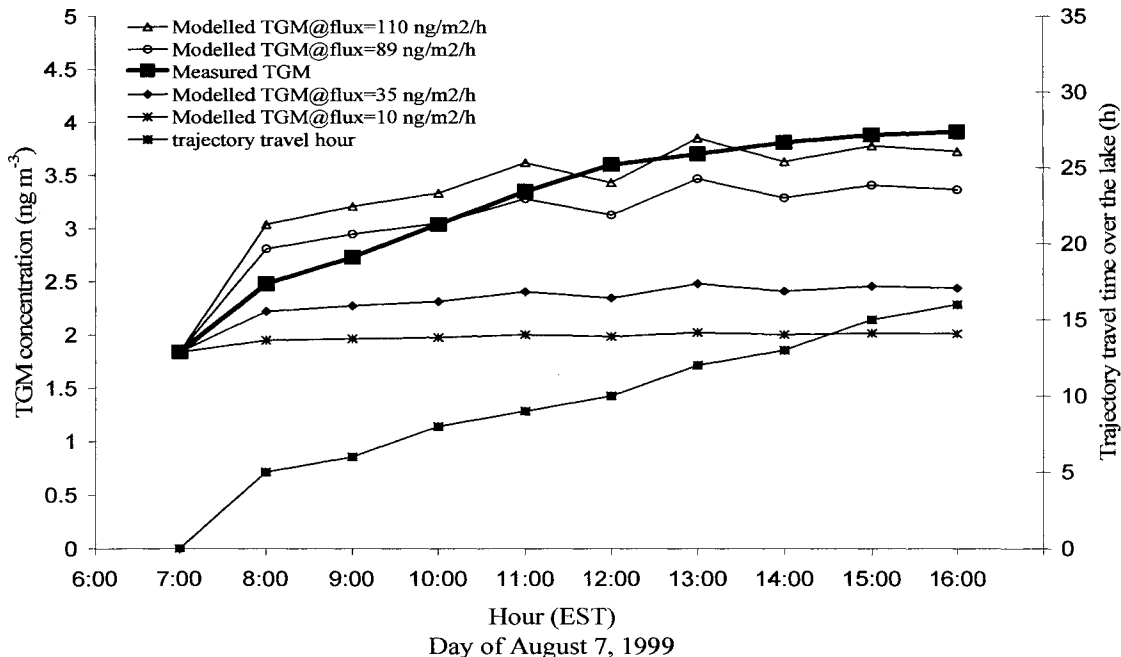


Figure 4.23 Modeled and measured TGM concentrations, along with trajectory travel time over Lake Ontario at Point Petre during the high TGM concentration episode on August 7, 1999. Estimated fluxes adopted from literatures (Table 3.3)

TGM concentration increased 2.1 ng m^{-3} during the nine-hour period of time (from 7:00 am to 4:00 pm). The simulation result of TGM concentration at Point Petre is shown in Figure 4.23. Modelled TGM concentrations apparently increased from 7:00 am to 8:00 am when winds changed from offshore to onshore. After 8:00 am, modelled TGM concentration increased gradually, suggesting the air mass picked up the Hg emission from the lake to the end point. At 12:00 pm and 2:00 pm, modelled TGM concentrations decreased likely due to the higher mixing height diluting the concentration inside the boxes.

The results also indicated that when the emission flux is $89 \text{ ng m}^{-2} \text{ h}^{-1}$ (adopted from Gardfeldt et al., 2001), modelled TGM concentration were more comparable to measured TGM concentration, compare to emission flux of 10 and $35 \text{ ng m}^{-2} \text{ h}^{-1}$ (adopted from Poissant et al., 2000 and Gardfeldt et al., 2001, respectively). Backward calculation found that when the flux is $110 \text{ ng m}^{-2} \text{ h}^{-1}$, modelled TGM concentration is most comparable to the measured TGM values. The flux of $110 \text{ ng m}^{-2} \text{ h}^{-1}$ is much higher than the maximum flux ($10 \text{ ng m}^{-2} \text{ h}^{-1}$) modelled over Lake Ontario (Poissant et al., 2000), the difference is because that Hg emission fluxes may depend on several factors such as the Hg content in water, water temperature, varied location of the lake, and different time. However, the backward calculation of flux is comparable to the maximum flux ($89 \text{ ng m}^{-2} \text{ h}^{-1}$) measured over fresh water in Europe (Gardfeldt et al., 2001). The results of modelled TGM concentration suggested that Hg emission from Lake Ontario contributed significantly to TGM concentration at Point Petre.

Simulation results indicated that the box model in this study underestimated TGM concentration at the endpoint. The possible reason for this underestimation is as follow. A

box model in a SO₂ study indicated both measured and modeled pollutant concentrations had a strong variation in vertical direction (Cheng et al., 2004). Thus, in this study, TGM concentrations in the boxes may have a vertical variation since TGM may not be mixed well in a hundreds of meters high box within one hour. In this study, TGM concentrations were measured at 3~6 m above ground, yet were modeled at hundreds of meters above ground, thus omitting vertical variation of TGM concentration in the model application likely led to this underestimation. Therefore, adding a series of boxes in vertical direction will be helpful to improve the box model application.

CHAPTER 5

CONCLUSIONS AND RECOMMENDATION

5.1 Conclusions

TGM concentrations at the five CAMNet sites during 1998 to 1999 presented a spatial variation: Burnt Island and Mingan (1.58 and 1.61 ng m^{-3}) < Egbert and St. Anicet (1.71 and 1.72 ng m^{-3}) < Point Petre (2.11 ng m^{-3}). During 1998 to 2003, the spatial variation of the three Ontario sites was observed as Burnt Island (1.59 ng m^{-3}) < Egbert (1.71 ng m^{-3}) < Point Petre (1.85 ng m^{-3}). The spatial variations indicated that TGM concentrations of rural-affected sites are significantly higher than that of rural remote sites. Point Petre has the highest TGM concentration among all five sites likely due to Hg evasion from Lake Ontario, especially in summer. Nearby anthropogenic Hg sources are likely responsible for higher TGM concentration at Egbert and St. Anicet.

Seasonal pattern of TGM concentration at all five sites showed a winter peak. Relatively lower TGM concentrations were observed in summer at most sites except for Point Petre. It suggested that coal combustion might have significant effects on the high TGM concentration in winter, while strong wet deposition and atmospheric mixing processes might lead to the lower TGM concentration in summer. High TGM concentration during summertime was observed at Point Petre, as opposed to the summer-low pattern observed at the other four sites. The Hg emission sources from

nearby industrial areas and Hg evasion from Lake Ontario are likely the primary reasons of this seasonal pattern.

At most sites except for St. Anicet, diurnal pattern of TGM concentration can be characterized as minimum TGM concentration at night/early morning and then increasing to maximum near noon. Nighttime TGM removal and daytime Hg emission from the surfaces under higher ambient temperature may lead to this diurnal pattern. Second peak of TGM concentration occurred at night at St. Anicet, for unknown reason. In all five sites, diurnal pattern in summer was more prominent than that in other seasons.

Pearson correlation analysis of TGM concentration and meteorological parameters showed that TGM has a positive correlation with ambient temperature in each season. However, an overall weak negative correlation between TGM concentration and temperature was detected likely due to the effects of non-meteorological factors such as coal combustion in winter and strong wet deposition and atmospheric mixing in summer. No straightforward correlation was found between TGM concentration and other meteorological parameters likely due to the large dataset may mask the correlations. Overall, TGM variation was not strongly associated with meteorological parameters. Weak negative correlation between TGM concentration and Hg concentration in precipitation was observed at Burnt Island, and no significant correlation was observed at other two Ontario sites. It suggested that the removal of atmospheric Hg did not significantly influence on the TGM concentration due to small quantity of RGM and Hg(p).

No clear long-term trend of TGM was found at Egbert and Point Petre. In Burnt Island, a slightly decreasing of TGM concentration was observed during 1998 to 2001. In

2002, TGM concentration increased 11% from 2001, then it was back to the average level in 2003. Higher temperature and drought condition led to TGM concentrations increasing in August and September, 2002, compared to these two months in 2001 and 2003. Wind rose and TGM rose did not indicated Hg inputs from a particular direction contributed the increase of 2002. Forest fire is suspected to be one of the contributors to this increase because of higher forest burnt area in 2002 compared to that in 2001.

HYSPLIT backward trajectory model was used to simulate the air mass pathway at Point Petre. The simulated TGM concentrations by a series of boxes with estimated Hg fluxes suggested that Hg emissions from Lake Ontario have significant effects on TGM concentrations of Point Petre.

5.2 Recommendations

In this study, the recommendations are as follows:

- 1) Meteorological parameters may not control strongly the variation of TGM concentration. Simultaneous measurements of other pollutants may be helpful to investigate the association between TGM and anthropogenic activities. For example, SO₂ may indicate coal combustions.
- 2) For the hypothesis of forest fires contributing TGM concentration increase in 2002 at Burnt Island, more detailed information of forest fire such as occurrence time, location, and burnt area will be very helpful.
- 3) In order to investigate the association between TGM concentration at Point Petre and Hg evasion from Lake Ontario, measurements of Hg

flux over the lake and adding vertical boxes in the box model will improve the model application.

- 4) Longer TGM data are needed to investigate the long term trend for the two Quebec sites.
- 5) Meteorological data will be helpful to investigate the spatial and temporal variation of TGM at the two Quebec sites.

APPENDIX A

DERIVATION OF BOX MODEL EQUATION 3.1

The concentration of the pollutant inside the box can be obtained by integrating equation (2.8) and the result is

$$C(t) = C_{in} + \frac{FL}{Hu} + (C(0) - C_{in} - \frac{FL}{Hu}) \exp(-\frac{u}{L}t) \quad (\text{A.1})$$

where $C(0)$ is the initial concentration inside the box at $t=0$; A simplified equation is obtained from equation (A.1) under the assumption that initial concentration ($C(0)$) equals the inlet concentration (C_{in}). Thus,

$$C(t) = C_{in} + \frac{FL}{Hu} (1 - \exp(-\frac{u}{L}t)) \quad (\text{A.2})$$

In the box model application, the length of the box is equal to the length of the trajectory travelling in one hour. Hence, L/u is equal to 1 hour. Therefore, concentration inside the box, i.e $C(t)$, at the end of an hour, is

$$C = C_{in} + 0.63 \frac{F}{H} \quad (\text{A.3})$$

REFERENCE

- Ames, M., Gullu, G., Olmez, I. 1998. Atmospheric mercury in the vapor phase and in fine and coarse particulate matter at Perch River, New York. *Atmospheric Environment* 32, no. 5: 865-872.
- Blanchard, P., Froude, F.A., Martin, J.B., Dryfhout-Clark, H, Woods, J.T. 2002. Four years of continuous total gaseous mercury (TGM) measurements at sites in Ontario, Canada. *Atmospheric Environment* 36: 3735-3743.
- Boudala, F. S., Folkins, I., Beauchamp, S., Tordon, R., Neima, J. 2000. Mercury Flux Measurements over Air and Water in Kejimikujik National Park, Nova Scotia. *Water, Air, and Soil Pollution* 122: 183-202.
- Brockwell, P. J. 2002. *Introduction to time series and forecasting*. New York: Springer.
- Brosset, C. 1987. The behavior of mercury in the physical environment. *Water, Air and Soil Pollution* 34: 145-166.
- Canadian Council of Ministers of the Environment, 2003. *Canada-wide standards: Mercury*. http://www.ccme.ca/initiatives/standards.html?category_id=53/ (accessed December 1st, 2003).
- Carpi, A. 1997. Mercury From Combustion Sources: A Review of The Chemical Species Emitted and Their Transport in The Atmosphere. *Water, Air and Soil Pollution* 98: 241-254.
- Chalmers, A., Mark Nilles, David Krabbenhoft, Eric Prestbo, and Mark Olson. 2003. Wet Distribution of Mercury in the Boston Metropolitan Area. In *National Atmospheric Deposition Program meeting held in Washington D.C., October 20-24, 2003*
- Cheng, S.Y., G. H. Huang, R. X. Hao, L. Liu and Z. H. Ren. 2004. A Three-dimension Multi-box Model for Air Quality Prediction. *Environmental Informatics Archives* 2: 611-627.
- Cohen, P., Cohen, J., West, S.G., Aiken, L.S. 2003. *Applied Multiple Regression/Correlation Analysis for the Behavioural Sciences*. L. Erlbaum Associates.
- Collett, R.S. and Oduyemi K. 1997. Air quality modelling: a technical review of mathematical approaches. *Meteorological Application* 4: 235-246.
- Comrey, A.L., Bott P.A., Lee, H.B. 1989. *A Problem-Solving Approach, Second Edition*. Dubuque, Iowa: WM. C. Brown Publishers.

- Draxler, R.R. 2003. Evaluation of an ensemble dispersion calculation. *Journal of Applied Meteorology* 42: 308-317.
- Draxler, R.R., Hess, G.D. 1997. *Description of the HYSPLIT_4 modeling system*. NOAA Technical Memorandum, ERL ARL-224, 24pp.
- Ebinghaus, R., Kock, H.H., Temme, C., Einax, J.W. Antarctic springtime depletion of atmospheric mercury. *Environmental Science and Technology* 36: 1238-1244.
- Environment Canada. 1999. *Canadian Environmental Protection Act*.
- Environment Canada. 2003. <http://www.ec.gc.ca/mercury/r-fa-e.html>. (accessed December 1st, 2003).
- Environment Canada. 2004. <http://www.msc.ec.gc.ca/arqp/camnet-e.cfm/> (accessed February 1st, 2004).
- European Communities. 2001. *Position Paper on Ambient air pollution by mercury (Hg)*.
- Fitzgerald, W.F. 1986. The Role of Air-Sea Exchange in Geochemical Cycling. *NATO Advance Science Institute Series, P. Buat-Menard, Ed., Dordrecht*,
- Fitzgerald, W.F. 1989. *Atmospheric and Oceanic Cycling of Mercury*. New York: Chemical Oceanography, Academic Press.
- Fitzgerald, W.F. 1995. Is mercury increasing in the atmosphere? The need for an atmospheric mercury network. *Water, Air, and Soil Pollution*, 80: 245-254.
- Friedli, Hans and Larry Radke. 2001. Wildfires and mercury pollution: A smoking gun? *Staffnotes Monthly*, July.
<http://www.ucar.edu/communications/staffnotes/0107/mercury.html>. (accessed September 1st, 2004).
- Fuentes, Mark (USEPA). 1995. *QA/QC Monitoring Manual; Appendices and Manual specific forms*.
- Gardefeldt, K., X.B. Feng, Sommar, J., and Lindqvist, O. 2000. Total gaseous mercury exchange between air and water at river and sea surfaces in Swedish coastal regions. *Atmospheric Environment* 35: 3027-3038.
- Gibbons, R.D. 2001. *Statistical methods for detection and quantification of environmental contamination*. New York: Wiley.
- Gildemeister, A.E., Keeler, G.J., Barres, J.A., Dvonch, J.T., Lyon, M.H., Malcolm, E.G., Marsik, F.J., Rea, A.W. and Vette, A.F. 2003. The Lake Superior Basin Trust Fund Study of Mercury Final Report Draft: submitted to MDEQ and the Wisconsin DNR.
- Gillis, A.A. and D.R. Miller. 2000. Some local environmental effects on mercury emission and absorption at a soil surface. *The Science of the Total Environment* 260: 191-200.

- Glass, G.E., Sorensen, J.A, Schmidt, K.W., Rapp, G.R., Jr., Yap, D. and Fraser, D. 1991. Mercury deposition and sources for the upper Great Lakes region. *Water Air and Soil Pollution* 56: 235-250.
- Gossel, T.A. and Bricker, J.D. 1990. *Principles of clinical toxicology*. 2nd edition. New York: Raven Press.
- Gustin, M.S., Biester, H. and Kim, C.S. 2002. Investigation of the light-enhanced emission of mercury from naturally enriched substrates. *Atmospheric Environment* 36: 3241-3254.
- Hall, B. 1995. The gas phase oxidation of elemental mercury by ozone. *Water Air and Soil Pollution* 80: 373 – 382.
- Hayward, J., Clevenger, K. and Crawford, T. 2003. Long-Term Atmospheric Mercury Trends for Eastern North Carolina. <http://daq.state.nc.us/toxics/studies/mercury/>.
- Hess, A., Iyer, H., Malm, W. 2001. Linear trend analysis: a comparison of methods. *Atmospheric Environment* 35: 5211-5222.
- Hirsch, R.M., Slack, J.R., and Smith, R.A. 1982. Techniques of trend analysis for monthly water quality data. *Water Resources Research* 18: 107-121.
- Hung, H., Halsall, J., Blanchard, P., Li, H.H., Fellin, P., Stern, G., and Rosenberg, B. 2002. Temporal Trends of Organochlorine Pesticides in the Canadian Arctic Atmosphere. *Environmental Science & Technology* 36: 862-868.
- Hung, H., Halsall, J., Blanchard, P., Li, H.H., Fellin, P., Stern, G., and Rosenberg, B. 2001. Are PCBs in the Canadian Arctic Atmosphere Declining? Evidence from 5 Years of Monitoring. *Environmental Science & Technology* 35: 1303-1311.
- HYSPLIT, 2004. HYbrid Single-Particle Lagrangian Integrated Trajectory, <http://www.arl.noaa.gov/ready/hysplit4.html> (accessed August 6, 2004)
- Iverfeldt, A. 1991. Mercury in forest canopy through fall water and its relation to atmospheric deposition. *Water, Air, and soil pollution* 56: 553.
- Johnson, Dale W.; Benesch, Jody A.; Gustin, Mae S.; Schorran, David S.; Lindberg, Steven E. 2003. Experimental evidence against diffusion control of Hg evasion from soils. *The Science of the Total Environment* 304: 175-184.
- Jokstad, A., Y. Thomassen, Bye E. 1992. Dental amalgam and mercury. *Pharmacol Toxicol (Copenhagen)* 70, no. 4: 308-313.
- Keeler, GJ, Hoyner ME, Lamborg CH. 1994. Measurements of atmospheric mercury in the Great Lakes basin. In *Mercury pollution integration and synthesis held in Boca Raton, Florida*: Lewis Publishers.
- Kellerhals, M., Beauchamp, S., Belzer, W., Blanchard, P., Froude, F., Harvey, B., McDonald, K., Pilote, M., Poissant, L., Puckett, K., Schroeder, B., Steffen, A., Tordon, R. 2003. Temporal and spatial variability of total gaseous mercury in

- Canada: preliminary results from the Canadian atmospheric mercury measurement network (CAMNet). *Atmospheric Environment* 37: 1003-1011.
- Kendall, M.G. 1938. A new measure of rank correlation. *Biometrika* 39: 89-93.
- Kim, K.H. and M.Y. Kim. 2001. The temporal distribution characteristics of total gaseous mercury at an urban monitoring site in Seoul during 1999-2000. *Atmospheric Environment* 35: 4253-4263.
- Kim, K.H., Lindberg, S.E. and Meyers, T.P. 1995. Meteorological measurements of mercury fluxes over background forest soils in eastern Tennessee. *Atmospheric Environment* 27: 267-282.
- Kleinbaum D.G., Kupper L.L., and Muller K.E. 1987. *Applied Regression Analysis and Other Multivariable Methods*. Duxbury Press.
- Lin, C.J., Cheng, M.D., and Schroeder, W.H. 2001. Transport patterns and potential sources of total gaseous mercury measured in Canadian high Arctic in 1995. *Atmospheric Environment* 35: 1141-1154.
- Lindberg, S.E., Meyers, T.P., Taylor, G.E., Turner, R.R., and Schroeder, W.H. 1992. Atmosphere-surface exchange of mercury in a forest: results of modeling and gradient approaches. *Journal of Geophysical Research* 97: 2519.
- Lindberg, S.E., Dong, W.J., Meyers, T.P. 2002. Transpiration of gaseous elemental mercury through vegetation in a subtropical wetland in Florida. *Atmospheric Environment* 36: 5207-5219.
- Lindqvist, O. 1994. Atmospheric Cycling of Mercury: An overview. In *Mercury Pollution – Integration and Synthesis*. Lewis Publishers.
- Lindqvist, O., Johansson K., Astrup, M., Andersson, A., Bringmark, L., Hovsenius, G., Hakanson, L., Iverfeldt, A., Meili, M., and Timm, B. 1991. Mercury in the Swedish environment – recent research on cause, consequences and corrective measures. *Water, Air, and Soil Pollution*, 56: 261.
- Lindqvist, O., Rodhe, H. 1985. Atmospheric Mercury – a review. *Tellus* 37B: 136-159.
- Liu SL, Nadim F, Perkins C, Carley RJ, Hoag GE, Lin YH, Chen LT. 2002. Atmospheric mercury monitoring survey in Beijing, China. *Chemosphere* 48: 97-107.
- Lynch, James A., Horner, Kevin S., Grimm, Jeffrey W. 2003. 2001 Mercury Report: Mercury Deposition In Pennsylvania.
http://www.dep.state.pa.us/dep/deputate/airwaste/qa/acidrain/2001rpt_hg/01_hgreport.htm.
- Malcolm, E.G. and Keeler G.J. 2002. Measurements of Mercury in Dew: Atmospheric Removal of Mercury Species to a Wetted Surface. *Environmental Science & Technology* 36:2815-2821.

- Mercury Deposition Network. 2003. <http://nadp.sws.uiuc.edu/mdn/> (accessed June 16, 2003).
- Michigan Department of Public Health. 1989. *1989 Fish Consumption Advisory*.
- Michigan. Mercury Pollution Prevention Task Force. 1996. *Mercury pollution prevention in Michigan, summary of current efforts and recommendations for future activities*.
- Microsoft Excel 2002. Microsoft, 2002.
- Minitab R14. State College, PA: Minitab Inc, 2004.
- Montgomery, D.C. 1999. *Applied statistics and probability for engineers*. : J. Wiley.
- Moore, D.S. and G.P. McCabe. 1999. *Introduction to the Practice of Statistics*. New York: W.H. Freeman and Company.
- Munthe, J. 1992. The aqueous oxidation of elemental mercury by ozone. *Atmospheric Environment* 26A: 1461 – 1468.
- Munthe, J., Wangberg, I., Pirrone, N., Iverfeldt, A., Ferrara, R. 2001. Intercomparison of methods for sampling and analysis of atmospheric mercury species. *Atmospheric Environment* 35: 3007–3017.
- Nadim, F., Perkins C., Liu, S.L., Carley R.J., Hoag, G.E. 2001. Long-term investigation of atmospheric mercury contamination in Connecticut. *Chemosphere* 45: 1033-1043.
- Nakazawa, T., Ishizawa, M., Higuchi, K., and Trivett, N. 1997. Two Curve Fitting Methods Applied to CO₂ Flask Data. *Environmetric* 8: 197-218.
- NSTC, 1999. National Science and Technology Council Committee on Environment and Natural Resources Air Quality Research Subcommittee, USA. *The Role of Monitoring Networks in the Management of the Nation's Air Quality*.
- Natural Resources Canada. 2001. *Canadian Mineral Yearbook*. : Prepared by the Minerals and Metal Sector.
- Neter, J., M.H. Kutner, W. Wasserman, C.J. Nachtsheim. 1996. *Applied Linear Statistical Models 4th Edition*. Chicago: Irwin.
- NOAA. 1999. *NOAA Technical Memorandum*.
- Nychka, D., Piergorsch, Walter W., and Cox, Lawrence H. 1998. *Case Studies in Environmental Statistics*. New York: Springer-Verlag.
- Patterson, JE, Weissberg BG, Dennison PJ. 1985. Mercury in human breathes from dental amalgams. *Bull Environ Contam Toxicol*, 34: 459-468.
- Petersen, G. Iverfeldt, and J. Munthe. 1995. Atmospheric mercury species over central and northern Europe. Model calculations and comparison with observations from

- the Nordic air and precipitation network for 1987 and 1988. *Atmospheric Environment* 29, no.1: 47-67.
- Pilgrim, W., Poissant, L., Trip, L. 2000. The Northeast States and Eastern Canadian Provinces mercury study: a framework for action: summary of the Canadian chapter. *The Science of the Total Environment* 261: 177-184.
- Pleijel, K. and J. Muthune. 1995. Modeling the Atmospheric Mercury Cycle – Chemistry in Fog Droplets. *Atmospheric Environment* 29: 1441-1457.
- Poissant, L. 1997. Field observations of total gaseous mercury behavior: interactions with ozone concentration and water vapor mixing ratio in air at a rural site. *Water, Air, and Soil Pollution* 97: 341-353.
- Poissant, L. 1999. Potential sources of atmospheric total gaseous mercury in the St. Lawrence River valley. *Atmospheric Environment* 33: 2537-2547.
- Poissant, L. 2000. Total gaseous mercury in Quebec (Canada) in 1998. *The Science of the Total Environment* 259: 192-201.
- Poissant, L. and A. Casimir. 1998. Water-air and Soil-air exchange rate of Total Gaseous Mercury at Background Sites. *Atmospheric Environment* 32: 883-893.
- Poissant, L. and A. Casimir. 1999. *Audit Protocol for Total Gaseous Mercury Measurements*: Environment Canada, Montreal.
- Poissant, L., Amyot, M., Pilote, M., and Lean, D. 2000. Mercury Water – Air Exchange over the Upper St. Lawrence River and Lake Ontario. *Environment Science & Technology* 34: 3069-3078.
- Poissant, L., Bottenheim, J.W., Roussel P., Reid N.W., Niki, H. 1996. Multivariate analysis of a 1992 SONTOS data subset. *Atmospheric Environment* 30: 2133-2144.
- RDMQ. 2003. Research Data Management and Quality Control System. http://www.msc-smc.ec.gc.ca/projects/rdmq/index_e.html. (accessed June 25, 2003).
- Schmolke, S.R., Schroeder, W.H., Kock, H.H., Schneeberger, D., Munthe, J., Ebinghaus, R. 1999. Simultaneous measurements of total gaseous mercury at four sites on a 800 km transect: spatial distribution and short-time variability of total gaseous mercury over central Europe. *Atmospheric Environment* 33: 1725-1733.
- Schroeder, W. H. and J. Markes. 1994. Measurements of atmospheric mercury concentrations in the Canadian environment near Lake Ontario. *Journal of Great Lakes Research* 20(1): 240–259.
- Schroeder, W.H. and J. Munthe. 1998. Atmospheric mercury-an overview. *Atmospheric Environment* 32, no. 5: 809-822.
- Schroeder, W.H., Anlauf, K.G., Barrie, L.A., Lu, J.Y. 1998. Arctic springtime depletion of mercury. *Nature* 394: 331-332.

- Schroeder, W.H., Yarwood, G and Niki, H. 1991. Transformation processes involving mercury species in the atmosphere – results from a literature survey. *Water Air and Soil Pollution*, 56: 653-666.
- Siegel, S. and N.J. Castellan. 1988. *nonparametric statistics for the behavioral sciences (2nd edition)*. New York: McGraw-Hill.
- Slemr, F. and E. Langer. 1992. Increase in global atmospheric concentrations of mercury inferred from measurements over the Atlantic Ocean. *Nature* 335: 434 – 437.
- Slemr, F. and H.E. Scheel. 1998. Trends in atmospheric mercury concentrations at the summit of the Wank Mountain, Southern Germany. *Atmospheric Environment* 32, no. 5: 845-853.
- Slemr, F., Schuster, G. and Seiler, W. 1985. Distribution, speciation, and budget of atmospheric mercury. *Journal of Atmospheric Chemistry*, 3: 407-434.
- Steffen, A. and W.H. Schroeder. 1999. *Standard Operating Procedures Manual Procedure for Total Gaseous Mercury Measurements—Canadian Atmospheric Mercury Measurement Network (CAMNet)*: Meteorological Service of Canada.
- Steffen, A., Schroeder, W., Bottenheim, J., Narayan, J. 2002. Atmospheric mercury concentrations: measurements and profiles near snow and ice surfaces in the Canadian Arctic during Alert 2000. *Atmospheric Environment* 36: 2653-2661.
- Stohl, A. 1998. Computation, Accuracy and Application of Trajectories – A Review and Bibliography. *Atmospheric Environment* 32: 947-966.
- Tekran Inc., Toronto, Ontario, Canada. 2003. *User manual of The Tekran Model 2537A Continuous Ultra-Trace mercury Vapor Analyzer*.
- Thiessen, H. 1997. *Measuring the real world: a textbook in applied statistical methods*. Chichester; John Wiley & Sons
- U.S. Dept. of Health and Human Services, Public Health Service. 1999. *Agency for Toxic Substances and Disease Registry, 1999, Toxicological profile for mercury*.
- U.S. Environmental Protection Agency. 1997. *Mercury Study Report to Congress*
- Vermette, S. J., S. E. Lindberg and N. S. Bloom. 1995. Field Tests for a Regional Mercury Deposition Network - Sampling Design and preliminary Test Results. *Atmospheric Environment* 29: 1247-1251.
- Wangberg, I., J. Munthe, N. Pirrone, A. Iverfeldt, E. Bahlman, P. Costa, R. Ebinghaus, X. Feng, R. Ferrara, K. Gardfeldt, H. Kock, E. Lanzillotta, Y. Mamane, F. Mas, E. Melamed, Y. Osnat, E. Prestbo, J. Sommar, S. Schmolke, G. Spain, F. Sprovieri, G. Tuncel. 2001. Atmospheric mercury distribution in Northern Europe and in the Mediterranean region. *Atmospheric Environment* 35: 3019-3025.

- Watras, C.J. and Huckabee, J.W., Eds. 1994. Sources and fates of mercury and methylmercury in Wisconsin lakes. In *Mercury Pollution: Integration and Synthesis*. Chelsea, MI: Lewis Publisher.
- Worthy, D.E.J., Levin, I., Trivett, N.B.A., Kuhlmann, A.J., Hopper, J.F., and Ernst M. K. 1998. Seven years of continuous methane observations at a remote boreal site in Ontario, Canada. *Journal of Geophysical Research* 103: 15995-16007.
- Xu, X.H., Yang, X.S., Miller, D, Helble, J.J., Carley, R.J. 1999. Formulation of bi-directional atmosphere-surface exchanges of elemental mercury. *Atmospheric Environment* 33: 4345-4355
- Zhang, H.; Lindberg, S. E.; Marsik, F. J.; Keeler, G. J. 2001. Mercury Air/Surface Exchange Kinetics of Background Soils of the Tahquamenon River Watershed in the Michigan Upper Peninsula. *Water, Air, and Soil Pollution* 126: 151-169.

VITA AUCTORIS

NAME: Hongyu You

PLACE OF BIRTH People's Republic of China

YEAR OF BIRTH 1970

EDUCATION TianJin Institute of Urban Construction, TianJin, China
1988 – 1992, Bachelor of Engineer in Environmental
Engineering

University of Windsor, Windsor, Ontario, Canada
2001-2002, Bachelor of Science in Computer Science

University of Windsor, Windsor, Ontario, Canada
2003-2004, Master of Applied Science in Environmental
Engineering